Innovative analytical tools in the biopharmaceutical development

Applying SPR/Biacore, calorimetry and light scattering methods to the study of interactions between anticancer antibodies and the EGFR

Dissertation

zur Erlangung des Doktorgrades (Dr. rer. nat.)

der Mathematisch-Naturwissenschaftlichen Fakultät

der Rheinischen Friedrich-Wilhelms-Universität Bonn

vorgelegt von

Maria Leonor Mendes Godinho de Alvarenga

aus Lissabon (Portugal)

Bonn 2010

Angefertigt mit Genehmigung der
Mathematisch-Naturwissenschaftlichen Fakultät
der Rheinischen Friedrich-Wilhelms-Universität Bonn

Diese Dissertation ist auf dem Hochschulschriftenserver der
ULB Bonn http://hss.ulb.uni-bonn.de/diss_online elektronisch publiziert.

Erscheinungsjahr 2010

Erstgutachter	Prof. Dr. Klaus-Jürgen Steffens
Zweitgutachter	Prof. Dr. Alf Lamprecht
Tag der Promotion	27.09.2010

Auszüge dieser Arbeit wurden an folgender Stelle vorab veröffentlicht:

Alvarenga, M.L., Schmiedel, J., Hannewald, J., Metzger, A.U., Bomke, J., Wegener, A., Krah, A.

“Biophysical characterization of EGFR interactions with therapeutic antibodies”

Poster, MipTec 2009, Basel, Switzerland, October 13-15, 2009

Acknowledgment

Zu allererst möchte ich Alexander Krah der Firma Merck Serono für die Betreuung dieser Doktorarbeit sehr herzlich danken. Das Vertrauen und die erforderliche wissenschaftliche Freiheit die Du mir gelassen hast haben diese Arbeit erst ermöglicht. Sehr dankbar bin ich auch für die Möglichkeit meiner Promotion bei Merck Serono anfertigen zu dürfen, in ein industrielles vielfältiges Umfeld wo die Anregungen groß und verschieden waren, und für die Teilnahme an einigen Kongressen und Veranstalgungen außerhalb Mercks. Ich habe die Zeit als Doktorandin sehr genossen.

Herrn Prof. Klaus-Jürgen Steffens des Pharmazeutischen Instituts der Universität Bonn danke ich für die Bereitschaft, die Betreuung von der Universitätsseite zu übernehmen und für das immerwährende Interesse am Gelingen dieser Arbeit. Danke auch für die Möglichkeit bei der Vortragsrunde in Bonn teilzunehmen. Ein weiteres Dankeschön an die Doktoranden des Instituts, die mich so herzlich aufgenommen haben; es war eine schöne Zeit mit Euch in Wasserburg am Inn. Herrn Prof. Alf Lamprecht danke ich auch für die Unterstützung und für das Gutachten meiner Arbeit.

Ansgar Wegener und Jörg Bomke danke ich für das enthusiastische Interesse an meinem Projekt und für die strukturierte wissenschaftliche Vorgehensweise, bzw. Die Wichtigkeit von Kontrollversuchen und kein zu frühes Verwerfen von Hypothesen. Darüber hinaus waren die unendlichen wissenschaftlichen Diskussionen ein sehr kreativer Motor für meine Arbeit. Ansgar und natürlich auch Eva-Maria Leibrock und Gerlinde Boenisch danke ich außerdem für die jeder Zeit sehr offene Art, mich zu empfangen und für die vielen ITC-Versuche die ich bei Euch machen durfte. Jens Hannewald danke ich für die große Hilfe und Unterstützung bei den vielen Lichtstreuungsversuchen.

Meiner Gruppe in der ehemaligen Abteilung Biotech Product Development danke ich für die Unterstützung jeglicher Art und zu jeder Zeit. Allen Doktoranden, die mit mir diese Zeit bei Merck geteilt haben, danke ich sehr herzlich für die offenen Diskussionen, die Hilfsbereitschaft und die freundliche Art. Ich danke insbesondere ganz herzlich Judith Schmiedel für den wichtigen Input für meine Arbeit und viele aufregende Diskussionen.

Meine Freunde und Freundinnen in Darmstadt, Nona, Laure, Murat und Laura in Zurich danke ich für die Freundschaft und das Teilen guten und schweren Momenten in den letzen Jahren. Danke auch an die Truppe der Viktoriastraße, Steffen und die Hochmaus-roqueiras; Ihr habt außerdem dafür gesorgt dass ich einen freien Kopf behielt, auch in Zeiten höchster Anstrengung. Insbesondere danke ich Christian für die liebevolle Unterstützung.

Aos meus irmaos Ocas, Cachana, Farrica, Joana, Luisa, Bartolomeu e Carlota, por todo o apoio e compreensão, pela enorme amizade e pela alegria! Obrigada por me terem transmitido sempre o amor e os valores dos Pais, principalmente através dos vossos exemplos.

“Ithaca has given you the beautiful voyage.
Without her you would have never taken the road.”

in Ithaca, by Kavafis

Abstract

Targeting of the epidermal growth factor receptor (EGFR) has become an established antitumor strategy with anti-EGFR antibodies approved for clinical use or in late stages of development. Postulation of antibody effector mechanisms has been based on in vivo or cell studies. These need to be complemented by an understanding of antibody/EGFR interactions on the molecular level. Thereon, crystal structures of the Fab fragments from different inhibitory antibodies in complex with the extracellular regions of EGFR have enlightened the molecular basis behind antibody-mediated EGFR inhibition. This study was focused on the further in vitro characterization of antibody/EGFR complexes in terms of stoichiometry, kinetics and thermodynamics of binding. Surface plasmon resonance (SPR)/Biacore, isothermal titration calorimetry (ITC) and static light scattering (SLS) were the tools employed to characterize the interactions between anticancer monoclonal antibodies and the epidermal growth factor receptor (EGFR). Clear stoichiometric evidence is provided for the binding of the monoclonal antibodies matuzumab, cetuximab and panitumumab to EGFR. These three antibodies are able to bind two EGFR molecules simultaneously, thus forming heterotrimer complexes. Independency of the two simultaneous EGFR binding events to one antibody molecule was confirmed with both kinetic and thermodynamic evidence. Unexpected stoichiometry results obtained for the nimotuzumab/EGFR interaction strongly indicate partial inactivity of the binding sites of this marketed antibody solution. Kinetically, the strong affinities of cetuximab and panitumumab could be related, respectively, to fast association and slow dissociation rates for the interactions of these two antibodies with EGFR. Similarly, the lower affinity of matuzumab could be assigned to a very fast dissociation of the matuzumab/EGFR complex. As for nimotuzumab, the lower affinity was mainly the result of a slower association rate to EGFR. Thermodynamically, the lower affinity known for matuzumab could be assigned to a higher entropic penalty upon binding. Interestingly, similar strong affinities of cetuximab and panitumumab were resolved to somewhat different thermodynamic profiles. Respectively, cetuximab interaction involves a higher enthalpy change compensated by an entropic penalty, while panitumumab interaction involves the lower enthalpy contribution of all four antibodies and an entropy change close to zero. All antibody/EGFR interactions were enthalpy-driven with either an entropy penalty or an entropy change close to zero. In contrast, interactions of the agonistic ligands EGF and TGF-α with EGFR were entropy driven and enthalpy penalised. Such different

thermodynamic profiles are indicative of different binding processes for inhibitory antibodies and agonistic ligands.

Motivated by reports on synergetic effects of the combined use of different EGFR-targeting antibodies, studies of the interdependent binding of antibody combinations to EGFR delivered insights into allosterism and relative epitope mapping. Results presented strongly corroborate the simultaneous binding of the antibody combinations matuzumab/cetuximab and matuzumab/nimotuzumab to EGFR. Concerning the binding of the combinations matuzumab/panitumumab, nimotuzumab/cetuximab and nimotuzumab/panitumumab to EGFR, displacement of the first antibody present upon binding of the second was observed. SPR results indicate that displacement of the first antibody could be caused by small conformational shifts upon binding of the second antibody.

The applicability of the biophysical methods used for the generation of meaningful quantitative data on binding interactions is demonstrated. Furthermore, a comparative assessment of the biophysical tools SPR, ITC and SLS to the study of protein-protein interactions is presented. The possibility of real time monitoring of the interactions was a special feature of SPR that enabled determination of the binding kinetics. Since SPR analysis involves immobilization of one interactant, it is not necessarily representative of what happens in solution. However, thermodynamic characterization of antibody interactions with EGFR performed with SPR delivered enthalpy and entropy changes that correlate well with ITC results. In fact, EGFR being a membrane protein, the adequacy of a solution method such as ITC to be more representative of the in vivo situation than a surface method such as SPR could be contested. The results presented rather demonstrate the combined utilities and corroborative use of SPR and ITC, with SLS providing an additional qualitative confirmation of the assembly states.

Table of Contents

List of Figures

List of Tables

List of abbreviations

ΔC_P	heat capacity change
ΔG	Gibbs free energy change
ΔH	enthalpy change
ΔS	entropy change
ADCC	antibody dependent cellular cytotoxicity
CDC	complement dependent cytotoxicity
CDR	complementarity determining regions
cet	cetuximab
cetuxi	cetuximab
Da	Dalton (1 Da = 1 g/mol)
DNA	deoxyribonucleic acid
EDC	*N*-ethyl-*N'*-(dimethylaminopropyl)-carbodiimide hydrochloride
EDTA	ethylenediaminetetraacetic acid
EGF	epidermal growth factor
EGFR	epidermal growth factor receptor
EGFRvIII	epidermal growth factor receptor – variant III
ErbB	human epidermal growth factor receptor
Fab	fragment antigen-binding
Fc	fragment crystallisable region
FDA	US American Food and Drug administration
Fig.	figure
HER	human epidermal growth factor receptor
HER2	human epidermal growth factor receptor 2
HB-EGF	heparin binding EGF-like growth factor
HPLC	high performance liquid chromatography
ITC	isothermal titration calorimetry
k_a	rate constant of association
k_d	rate constant of dissociation
K_A	equilibrium association constant
K_D	equilibrium dissociation constant
LS	light scattering
mAb	monoclonal antibody

MALS	multi-angle light scattering
mat	matuzumab
matuzu	matuzumab
NaCl	sodium chloride
N	stoichiometry
NHS	*N*-Hydroxysuccinimide
nim	nimotuzumab
nimotuzu	nimotuzumab
NRG	neuregulin
panitumu	panitumumab
pan	panitumumab
PBS	phosphate buffered saline
PBS-EP+	phosphate buffered saline with addition of EDTA and Tween
R^2	coefficient of determination
Rec	receptor
RI	refractive index
R_{max}	maximum response
RU	response /resonance units
SDS-PAGE	sodium dodecyl sulfate polyacrylamide gel electrophoresis
SEC	size exclusion chromatography
SLS	static light scattering
SPR	surface plasmon resonance
t	time
T	temperature
TGF-α	transforming growth factor α
UV	ultra-violet

1 AIM OF THE THESIS

Cancer patients often suffer from serious side effects of chemo- and radiotherapy treatment to combat the uncontrolled proliferation in malignant tumors. Targeted therapy, such as therapeutic antibodies directed against specific cancer related cell surface proteins, might offer a more efficient treatment. One of these cancer related cell surface proteins is the epidermal growth factor receptor (EGFR). EGFR is aberrantly activated in a variety of epithelial tumors – colon, breast, lung, pancreas, head and neck – and is a target in anti-cancer therapy. In 2004, Erbitux/cetuximab (Merck KGaA) was the first FDA-approved anti-EGFR monoclonal antibody. Cetuximab is a chimera, i.e., a hybrid structure made by the fusion of murine variable regions and human conserved regions of the antibody structure. The antibody technology production has evolved very fast in the past years in the direction of reducing the percentage of murine sequence, which may lead to immunogenicity. Vectibix/panitumumab (Amgen) is an anti-EGFR fully human antibody, the second to be approved by the FDA in 2006. Theracim/nimotuzumab (YM Biosciences) is a humanized antibody approved in several countries in the world with reported exemplary low side effects occurrence. Apart from these three marketed antibodies, many others are in advanced stages of pharmaceutical development.

Despite the fast growing clinical use of monoclonal antibodies in the oncology field, their mechanisms of tumor inhibition are often not yet fully understood. It is known that anti-EGFR antibodies interact with the extracellular region of the receptor, thereby interfering with the EGFR-dependent signalling that is involved in cellular processes crucial for growth and differentiation. Postulation of mAbs effector mechanisms has been based on in vivo or cell studies. These need to be complemented by an understanding of mAb/EGFR interactions on the molecular level. Thereon, crystal structures have delivered valuable information about the molecular interfaces formed between mAbs and their EGFR epitopes. Studies of the kinetics and thermodynamics of binding can provide a more complete understanding of the forces that lead to complex formation and the dynamics of the interaction.

Surface plasmon resonance, isothermal titration calorimetry and static light scattering were the biophysical tools employed to study the biomolecular interactions of EGFR with four therapeutic monoclonal antibodies and two natural ligands. The applicability of the innovative biophysical methods used for the generation of meaningful quantitative data about binding interactions is demonstrated. The high quality data generated provided quantitative evidence to answer the following questions related to antibody/EGFR interaction:

- How many EGFR molecules can one antibody bind simultaneously?
- How fast do the molecules bind?
- How long does the complex last?
- How strong is the interaction?
- Why does it take place, what are the thermodynamic reasons that drive the interaction?

Answers to those questions were generated and provided highly resolved definition of the macromolecular interactions studied in terms of assembly state, affinity, kinetics and thermodynamics of complex formation. Added to this, studies of binding interdependence of antibody combinations to EGFR delivered insights into epitope and allostery mapping with interesting application for combination therapeutic strategies. Cell surface assays and clinical investigations were beyond the scope of this thesis and results are discussed based on literature.

2 BIOPHARMACEUTICALS

2.1 Introduction

Biopharmaceuticals are proteins, peptides, viruses and DNA-based products used for therapeutic or diagnostic use (Wu-Pong and Rojanasakul, 2008). They can be, and usually are, obtained by biotechnology. Biotechnology as an industry emerged in the 1970s, based largely in the discovery of recombinant DNA technology by Cohen and Boyer (Cohen *et al.*, 1973). One of the biggest breakthroughs in biotechnology happened in the manufacture of recombinant human insulin (Sun, 1980; Johnson, 1983). In 1982, insulin became the first medicine made via recombinant DNA technology to be approved by the FDA. When compared to animal purified insulin, recombinant human insulin had advantages in terms of costs, safety and supply. Its successful establishment as routine diabetes therapy was a milestone that contributed to the acceptance of recombinant DNA technology. As a matter of fact, since then biotechnology has created more than 200 new therapies and vaccines based on recombinant DNA, and other 400 are currently in clinical trials (Biotechnology Industry Organization, 2008). Target diseases include cancer, Alzheimer's disease and autoimmune and inflammatory disorders.

The first protein biopharmaceuticals were already existing human proteins, whose shortage in the body was responsible for disease. These included insulin as well as human growth hormone, and erythropoietin. In the era of the human genome project, with the emergency of the fields of genomics and proteomics, scientists could identify genes implicated in disease. Novel-designed drugs, like monoclonal antibodies, could thus be developed against specific disease-related targets. Monoclonal antibodies are genetically engineered and thus unique and novel to the cell. However, they are still basically the same in structure as other human antibodies. The next step was the development of completely novel scaffolds, bearing less and less resemblance to existing human proteins (Projan *et al.*, 2004). Examples of these new scaffolds are immunoglobulin-type molecules developed on the basis of modular construction of single variable domain antibodies (Gill and Damle, 2006). Evolution in the field of biotechnology has thus shaped the design and development of novel biopharmaceuticals. In

the future, biotechnology is expected to play a more and more important role in healthcare, if individualized disease prevention and treatment come true (Biotechnology Industry Organization, 2008; Wu-Pong and Rojanasakul, 2008). Genetic analysis will enable drugs to be designed specifically for groups of people with similar genetic profiles. The breast cancer drug Herceptin (trastuzumab) is an example of a pharmacogenomic drug. Initially approved in 1998, Herceptin targets and blocks the HER2 protein receptor, which is overexpressed in some aggressive cases of breast cancer. A test can identify which patients are overexpressing the receptor and can benefit from the drug. In 2005, FDA approved for the first time a drug for a specific race: BiDil treats congestive heart failure in self-identified black patients.

2.2 Monoclonal antibodies

One of the fastest growing biopharmaceuticals is the monoclonal antibody, which is now used to treat diseases mainly in oncology and auto-immune and infectious diseases segments. Antibodies are bifunctional molecules (Congy-Jolivet *et al.*, 2007; Peipp *et al.*, 2008). On one hand, they recognize their antigen through the variable regions of the antigen binding portion (Fab). As a result, they may interfere with one or several functions of this antigen, leading to the therapeutic effect. On the other hand, through the constant regions (Fc) they may interact with Fc-binding molecules and recruit patient immune effector functions to destroy the marked target. The antibody dependent cellular cytotoxicity (ADCC) is triggered by an interaction between the Fc region of an antibody bound to, for example, a tumor cell and the Fcγ receptors on immune effector cells, leading to elimination of the tumor cell by phagocytosis or lysis, depending on the type of mediating effector cell. Complement dependent cytotoxicity (CDC) is initiated by complement component C1q binding to the Fc region of the antibody, triggering activation of the complement that leads to cell death by phagocytosis, lysis or disruption of the cell membrane. The recruitment of these patient immune effector functions is thought to be essential in the therapeutic effect of several recombinant mAbs used in oncology; the binding of recombinant mAb to the antigen is a necessary but not always sufficient condition for therapeutic effect. Fc-dependent effector mechanisms are best achieved with antibodies of the IgG1 subclass. Monoclonal antibody can also be coupled to a chemotherapy agent or a radioactive isotope and so selectively deliver chemo- or radiotherapy to a cancer cell while avoiding healthy cells (Nieri *et al.*, 2009).

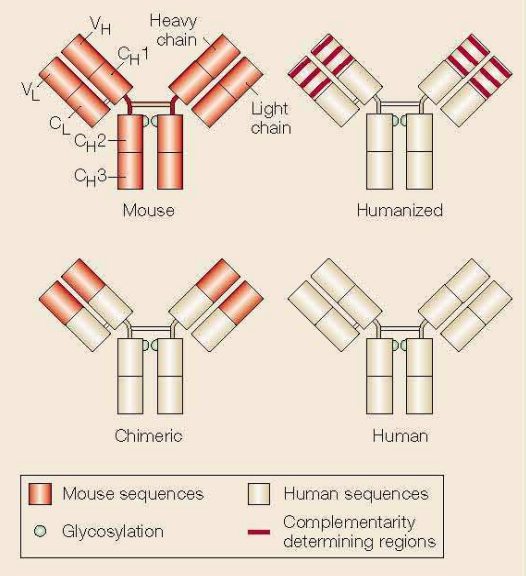

Fig. 1: Engineering of monoclonal antibodies.
Schematic representation of mouse, chimeric, humanized and human IgG monoclonal antibodies. Figure reproduced (Carter, 2001).

Production of monoclonal antibodies was enabled by the hybridoma technology developed by Köhler and Milstein in 1975 (Kohler and Milstein, 2005). They fused a human myeloma cell (a cancerous immune B cell) that can no longer secrete antibodies to a normal B cell from a mouse that has been immunized to secrete a particular antibody. The result of this fusion is called hybridoma and it has the properties of multiplying indefinitely and producing one single type – thus monoclonal – of antibody. The first mAbs obtained by hybridoma technology turned out to have safety and efficacy problems (Carter, 2001). Due to their mouse origin, these mAbs are immunogenic to humans, have short *in vivo* half-lives and generally do not kill target cells efficiently because they fail to trigger the immune effector functions of antibody dependent cellular cytotoxicity (ADCC) and complement dependent cytotoxicity (CDC). The realization of the great therapeutic potential of monoclonal antibodies was only made possible by the advent of technologies designed to overcome the limitations of the first mouse monoclonal antibodies – Fig. 1. These technologies are, in historical order of development, the chimerization and humanization of murine antibodies, and direct routes to high-affinity human antibodies using phage display libraries or transgenic mice (Carter, 2001; Waldmann, 2003). Chimerization consists on joining the antigen binding variable domains of a mouse mAb to human constant domains (Morrison *et al.*, 1984). Humanization implies grafting the appropriate complementarity-determining regions (CDRs) (responsible for the desired binding properties) into a human antibody framework (Jones *et al.*, 1986). Human monoclonal antibodies can either be obtained from very large, single chain variable fragments or Fab phage display libraries (de Haard *et al.*, 1999) or from hybridoma technology using

transgenic mice with human immunoglobulin genes (Lonberg, 2005). Chimeric, humanized and human antibodies have reduced immunogenicity resulting in improved pharmacokinetics and since the Fc regions can be recognized by the patient's immune system, they are efficacious on recruiting effector functions to kill target cells.

The generation of more specific and higher affinity mAbs with reduced immunogenicity have enabled antibody therapeutics to become a major weapon in the treatment of leukemia and lymphoma. The first anticancer mAb, Rituxan/rituximab, was approved in 1997 for the treatment of non-Hodgkin's lymphoma. From the nine commercially available therapeutic mAbs approved by the FDA, five are being used for treatment of hematological malignancies and the other four for solid tumors (Table 1).

Table 1: Antibodies approved by the FDA for cancer treatment.

Antibody /Product name	Target	Type	Indications
Rituximab /Rituxan	CD20	Chimeric	B-cell lymphoma
Trastuzumab /Herceptin	HER2	Humanized	Breast cancer
Gemtuzumab /Mylotarg	CD33	Humanized; toxin-conjugate	Acute myeloid leukemia
Alemtuzumab /Campath	CD52	Humanized	Chronic lymphatic leukemia.
^{90}Y-ibritumomab /Zevalin	CD20	Murine; radionuclide-conjugate	B-cell lymphoma
^{131}I-tositumomab /Bexxar	CD20	Murine; radionuclide-conjugate	B-cell lymphoma
Bevacizumab /Avastin	VEGF	Humanized	Colorectal, breast and lung cancer
Cetuximab /Erbitux	EGFR	Chimeric	Colorectal and head and neck cancer
Panitumumab /Vectibix	EGFR	Entirely human	Colorectal cancer

Sources: (Zhang *et al.*, 2007b; Biotechnology Industry Organization, 2008)

3 EGFR-TARGETED ANTICANCER THERAPY

3.1 Introduction

Classical anticancer therapy has been based on cytotoxic agents with steep dose-toxicity relationships that limited clinical dose and efficacy. In the last decade, exponential growth in knowledge about cancer has led to the development of agents targeted against the inherent basis of cancer. It is hoped that such therapeutics will result in greater specificity, less toxicity and higher therapeutic indices (Rowinsky *et al.*, 2007). In order to develop such agents it is necessary to identify and understand the aberrant biochemical and molecular pathways that distinguish malignant from non-malignant cells. Cancer research of the past decades has provided definitive evidence that cancer is a genetic disease (Park and Vogelstein, 2003). The current view is that cancers arise through a multistage process in which inherited and somatic mutations of genes lead to selection of variant progeny with the most robust and aggressive growth properties. Two classes of genes, proto-oncogenes and tumor suppressor genes, have been identified as mutation targets. In general, proto-oncogenes have critical roles in growth regulatory pathways and mutation leads to an increased activation (Pierotti *et al.*, 2003). Tumor suppressor genes, on the contrary, are defined by their inactivation in cancer (Park and Vogelstein, 2003). The epidermal growth factor receptor is one proto-oncogene; mutation or abnormal expression can convert it into an oncogene and may lead to oncogenic transformation of the cell.

3.2 The epidermal growth factor receptor

The Epidermal Growth Factor Receptor (EGFR) is one of a family of four receptor tyrosine kinases known as the ErbB or HER receptors involved in critical cellular processes such as proliferation, differentiation and apoptosis (Schlessinger, 2000; Holbro and Hynes, 2004; Hubbard and Miller, 2007). The mature EGFR contains an extracellular ligand binding region, a transmembrane domain and an intracellular tyrosine kinase domain similar to other receptors from the ErbB family (Burgess *et al.*, 2003). EGFR is regulated by at least seven distinct peptide ligands (Harris *et al.*, 2003), including EGF, transforming growth factor-α

(TGF-α), amphiregulin, betacellulin, epigen, epiregulin, and heparin binding EGF-like growth factor (HB-EGF). It is widely accepted that ligand binding to EGFR shifts a monomer-dimer equilibrium favouring receptor dimerization (Zhang *et al.*, 2006; Lemmon, 2009). Receptor dimerization brings the intracellular tyrosine kinase domains into close proximity resulting in activation of the kinase domain through an allosteric mechanism. Intracellular kinase activation involves auto-transphosphorylation, which promotes the recruitment of downstream signalling proteins and subsequent modulation of a complex intracellular signalling network (Oda *et al.*, 2005). It is also thought that EGFR can form an array of heterodimers with other ErbB receptors, thus increasing the complexity of signalling by this family (Yarden and Sliwkowski, 2001).

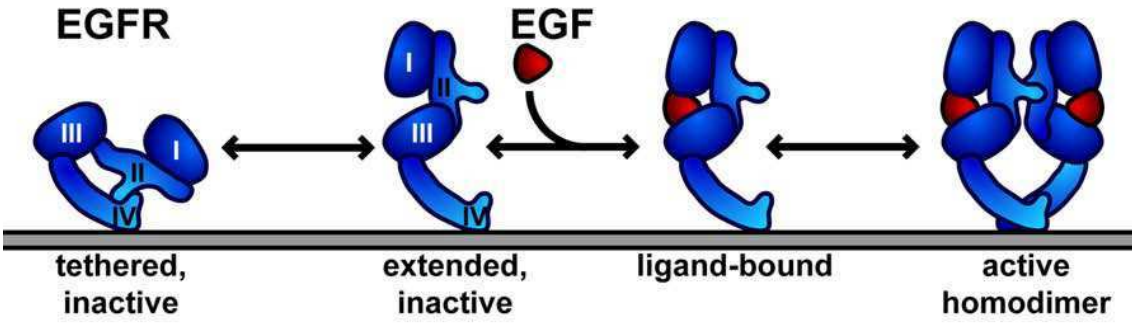

Fig. 2: Cartoon representation of EGF-induced dimerization of the EGFR extracellular region.
The unliganded state of the EGFR extracellular region adopts a tethered configuration (left). EGF binding to this structure is accompanied by a conformational change that can be modelled approximately by a 130° rotation of the domain I/II fragment about the axis between domains II and III (Burgess *et al.*, 2003). This change causes EGFR to adopt an extended conformation, in which EGF binding to both domains I and III is allowed and the dimerization arm in domain II is exposed. The extended EGFR molecule dimerizes through domain II-mediated interactions, with possible additional contributions from domain IV. Conceptual structural intermediates are shown: (i) an extended, unliganded monomer and (ii) an extended ligand-bound monomer. Crystal structures have been observed of the tethered monomer (Ferguson *et al.*, 2003) and ligand-induced dimers (Ogiso *et al.*, 2002; Garrett *et al.*, 2002). Figure reproduced and adapted (Schmitz and Ferguson, 2009).

Based on x-ray crystal structures solved for EGFR extracellular regions in the absence (Ferguson *et al.*, 2003) and presence (Ogiso *et al.*, 2002; Garrett *et al.*, 2002) of ligand, a model for ligand dependent dimerization and activation of EGFR has been proposed (Burgess *et al.*, 2003) (Fig. 2). In the unliganded state the receptor adopts a tethered conformation characterized by an intramolecular interaction between domain II and domain IV (Ferguson *et al.*, 2003) (left hand in Fig. 2). This conformation is thought to be autoinhibited (Burgess *et al.*, 2003). Ligand binding to both domains I and III stabilizes an extended conformation of EGFR where dimerization interfaces on domain II and IV are exposed. Ligand binding is thus linked to a dramatic conformational change that is involved in receptor dimerization. In contrast to other receptor tyrosine kinases, EGFR dimerization is entirely receptor mediated

(Ogiso *et al.*, 2002; Garrett *et al.*, 2002). The majority of interactions in the dimer of the EGFR extracellular domains is contributed by a region in domain II that has been called 'dimerization arm' (Ogiso *et al.*, 2002). Further interactions in the extracellular EGFR dimer are contributed by parts of domain IV that are close to or contacting each other as suggested by modeled structures (Ferguson *et al.*, 2003) and biochemical and biophysical data (Berezov *et al.*, 2002; Dawson *et al.*, 2007).

The model for ligand-dependent EGFR dimerization presented in Fig. 2 is a simplification of a complex equilibrium of EGF binding to EGFR and receptor homo- and hetero-dimerization on the cell surface (Lemmon, 2009). Various reports have suggested negative cooperativity in EGF binding to EGFR and the existence of pre-formed EGFR dimers (Wofsy *et al.*, 1992; Macdonald and Pike, 2008). Furthermore, it is thought that the transmembrane and intracellular domains also contribute to trigger dimerization and could be crucial for regulating the association of two EGFR.

3.3 EGFR and cancer

EGFR has been an oncology target for over 20 years. It was the first cell-surface receptor to be linked directly to cancer, as described in fibroblasts infected with oncogenic viruses (De Larco and Todaro, 1987). This report followed seminal observations about growth factors (De Larco and Todaro, 1978) and the elaboration of the theory of autocrine secretion (Sporn and Roberts, 1985): cancer cells generally exhibit a reduced requirement for exogenously supplied growth factors to maintain a high rate of proliferation. EGFR signalling can activate proliferation, protection from apoptosis, loss of differentiation, migration and invasion – all known hallmarks of cancer. It is now known that EGFR is aberrantly activated in a variety of epithelial tumors (Mendelsohn and Baselga, 2006). Mechanisms leading to aberrant receptor activation include receptor overexpression, gene amplification, activating mutations, overexpression of associated ligands and/or loss of negative regulatory controls (Mendelsohn and Baselga, 2006; West *et al.*, 2008). Moreover, increased EGFR expression has been correlated to poorer clinical outcome for patients (Normanno *et al.*, 2006). The type III EGFR mutation (EGFRvIII) is the most common EGFR mutation and clinically connected with cancer. It is a truncated version of the wild type EGFR showing constitutive signaling activity and impaired down-regulation (Pedersen et al., 2001). Structurally, EGFRvIII is characterized

by unaltered domains III and IV while nearly the whole of domains I and II are missing in comparison to full length EGFR.

There are two classes of therapeutics targeting EGFR: low molecular weight tyrosine kinase inhibitors and monoclonal antibodies. Tyrosine kinase inhibitors act on the protein kinase domain of the receptor by either competing with ATP or modifying the ATP binding pocket so that receptor phosphorylation is inhibited. They are somewhat promiscuous in their specificity for the target and usually inhibit other tyrosine kinases to varying degrees. Although in general a disadvantage, such low specificity can be of clinical benefit, as tumor cells usually contain several ErbB family members and heterodimerization occurs routinely (Zhang *et al.*, 2007a).

Table 2: EGFR overexpression in tumors.

Tumor type	Percentage of tumors overexpressing EGFR
Colon	25-77%
Head and neck	80-100%
Pancreatic	30-50%
Non-small cell lung	40-80%
Breast	14-91%

Source: (Herbst and Shin, 2002)

3.4 Anti-EGFR monoclonal antibodies

Effective inhibition of EGFR signalling by mAbs has been related to several modes of action: direct steric blockage of ligand binding or receptor dimerization, stabilization of the tethered conformation, block of the domain rearrangement required for receptor dimerization, antibody-dependent cellular cytotoxicity (ADCC) and complement dependent cytotoxicity (CDC), antibody-mediated receptor down-regulation and augmentation of the antitumor effects of chemo- and radiotherapy (Mendelsohn and Baselga, 2006; Leahy, 2008; Schmitz and Ferguson, 2009).

Examples of anti-EGFR monoclonal antibodies already approved or that have made it all the way to clinical trials are given below.

Cetuximab/Erbitux. A chimeric modification of the antibody 225, the latter originally obtained by inoculation of mice with EGFR and hybridoma technology by Prof. Mendelsohn (University of Texas M.D. Anderson Cancer Center) (Sato *et al.*, 1983). The chimeric version was developed by ImClone Systems and has been approved by the FDA (2004), the EU (2004) and Japan (2008) for treatment of patients with colorectal and head and neck cancer. The approval covers the application in combination with chemo- or radiotherapy or as a single agent in patients who have failed those therapies. Erbitux is manufactured and distributed by ImClone and Bristol-Myers Squibb in North America and by Merck KGaA in the rest of the world.

Panitumumab/Vectibix. A fully human antibody of the IgG2 type derived from the immunization of transgenic mice that express fully human antibodies (Yang *et al.*, 2001). Initially developed by Abgenix, it is nowadays developed and commercialized by Amgen. It has been approved by the FDA (2006) and EU (2007) for the treatment of patients with colorectal cancer in combination with chemotherapy or as monotherapy after failure of chemotherapy regimens.

Nimotuzumab/Theracim. A humanized antibody developed at the Centre of Molecular Immunology in Havana (Fernandez *et al.*, 1992; Mateo *et al.*, 1997). It has limited nation approval for the treatment of head and neck cancer and glyoma and is commercialized by YM Biosciences and its licensees.

Zalutumumab. A fully human monoclonal antibody developed by GenMab using transgenic mice (Bleeker *et al.*, 2004). It is in advanced clinical testing.

Matuzumab/EMD72000. The humanized form of the murine mAb 425 developed at the Wistar Institute, in Philadelphia (Murthy *et al.*, 1987). Development is driven by Merck KGaA and Phase I data is available.

IMC-11F8. A fully human antibody constructed using an isolate from a non-immunized human Fab display library (Lu *et al.*, 2004). Development is driven by Imclone and Phase I data is available.

c806. A chimeric version of mAb 806, derived from mice immunized with fibroblasts expressing EGFR variant III, but also binds to overexpressed wild-type EGFR (Mishima *et al.*, 2001). EGFRvIII is the most common gene disruption of the extracellular region of EGFR, and is found in about 25% of glioblastomas, as well as in a number of solid tumors (Kuan *et al.*, 2001). c806 is in Phase I trials.

Anti-EGFR mAbs interact with the extracellular region of EGFR and interfere with EGFR signalling by different mechanisms, as revealed by structural studies (Peipp *et al.*, 2008). Mechanisms of EGFR antagonist by mAbs include i) stabilization of tethered conformation, ii) block of domain rearrangement required to attain the extended state, iii) direct block of ligand binding and iv) direct block of receptor dimerization.

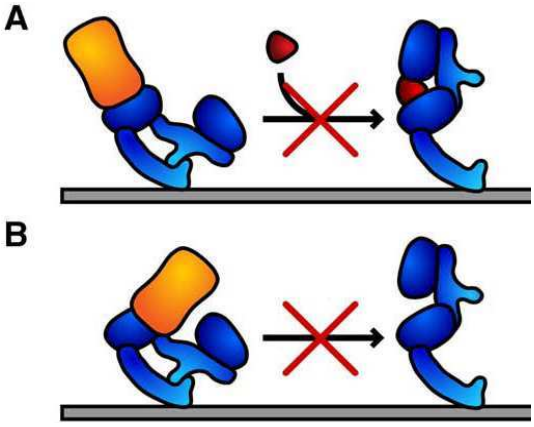

Fig. 3: EGFR inhibition by antibodies.
(A) Antibody binding directly occludes the ligand-binding site – this mode of inhibition is important for cetuximab, IMC-11F8, panitumumab and zalutumumab (Rich and Myszka, 2007b; Rich and Myszka, 2008). **(B)** Antibody sterically prevents the receptor from adopting the conformation required for high affinity ligand binding and dimerization, without directly occluding a ligand-binding site. This mode is observed for matuzumab. Figure reproduced and adapted (Schmitz and Ferguson, 2009).

Cetuximab (Fan *et al.*, 1994; Li *et al.*, 2005), panitumumab (Freeman *et al.*, 2008), zalutumumab (Lammerts van Bueren *et al.*, 2008) and IMC-11F8 (Li *et al.*, 2008) interact with epitopes on domain III of EGFR that overlap with the EGF binding site on that domain, thus competing with EGF binding to the receptor). These antibodies inhibit EGFR primarily by directly blocking the ligand-binding site (Fig. 3A). Additionally, they sterically prevent the receptor from adopting the extended dimerization-capable conformation and they eventually stabilize the tethered conformation. Nimotuzumab also binds to an epitope situated in domain III, overlapping with the ligand binding site, thus blocking ligand binding. However, differently from the other mAbs, nimotuzumab binding to EGFR seems to be compatible with the active extended receptor conformation (Talavera *et al.*, 2009). Matuzumab interacts with an epitope situated on domain III of EGFR, not overlapping with the ligand-binding site. Ligand binding is not directly blocked (Fig. 3B); instead matuzumab sterically prevents the receptor from adopting the conformation required for high affinity ligand binding and

receptor dimerization (Schmiedel *et al.*, 2008). An altogether different inhibition mechanism is followed by c806, which binds to an epitope in domain II near the dimerization domain that does not seem to be available in either tethered or extended conformation (Johns *et al.*, 2004; Sivasubramanian *et al.*, 2006). Thus, it is believed that c806 binds to an intermediary EGFR conformation, directly blocking receptor dimerization.

4 BIOPHYSICAL CHARACTERIZATION OF ANTIBODY-RECEPTOR INTERACTIONS

4.1 Introduction

Binding specificities of monoclonal antibodies against virtually any antigen can be generated whether by conventional hybridoma technology or with antibody libraries displayed on filamentous phage or other display systems. The determination of antibody-antigen interaction properties is key to understand antibody performance in therapeutic applications. Scientists aim to understand the mechanisms of antibody-antigen interactions, their energetic and dynamic properties as well as structure-function relationships. Biophysical tools help providing a quantitative basis together with a highly resolved definition in terms of assembly state, epitope and/or allostery mapping, affinity, kinetics and thermodynamics of complex formation (Bergethon, 1998). Focus of this thesis was the biophysical characterization of the interactions between EGFR and four therapeutic monoclonal antibodies. Interactions of the receptor with two natural agonists were also studied. In this chapter, an introduction to the physical properties that characterize an interaction and the innovative biophysical tools used – surface plasmon resonance, isothermal titration calorimetry and static light scattering – will be given.

4.2 Physical properties of molecular interactions

One of the most fundamental ways to quantitatively characterize the interaction between antibody (mAb) and receptor (Rec) as defined in Eq. 1 is to determine the binding affinity, or equilibrium dissociation constant (K_D). K_D is defined as the ratio of the rate constants (kinetic) or the ratio of concentrations at equilibrium, when k_a is equal to k_d, for a two-phase reversible interaction as defined in Eq. 2.

$$\mathrm{mAb} + \mathrm{Rec} \underset{k_d\ (s^{-1})}{\overset{k_a\ (M^{-1}s^{-1})}{\rightleftharpoons}} \mathrm{mAb \cdot Rec} \qquad \textbf{Eq. 1}$$

$$K_D = \frac{[mAb][Rec]}{[mAb \cdot Rec]} \text{ or } K_D = \frac{k_d}{k_a} \qquad \textbf{Eq. 2}$$

Affinity measurements give quantitative meaning to phrases such as tight binding and weak interaction, and refer to the stability of the bimolecular complex. Most often, bimolecular interactions are dynamic processes that occur in solution and include multiple association and dissociation phases. The smaller the dissociation constant, the more tightly bound the complex $mAb \cdot Rec$ is, i.e. the higher the affinity of the complex. The dissociation constant is also of great practical utility for determining the protein concentration at which a complex might be formed.

The study of protein-protein interactions in terms of the rates of association and dissociation is called kinetics. For the above given example, the rate at which the complex is formed is given by the product of the molar concentrations of mAb and Rec and the association rate constant, k_a (Eq. 3). The association rate is a measure of the speed of recognition of two interactants in solution. It is thus dependent on the concentration of the interactants. Similarly, the rate at which the complex dissociates is the product of the molar concentration of complex $mAb \cdot Rec$ and the dissociation rate constant, k_d (Eq. 4). The dissociation rate is a measure of the instability of a complex; the higher the dissociation rate, the less stable is the complex. It is independent from the interactants concentration in solution.

$$forward \frac{d[mAb \cdot Rec]}{dt} = k_a[mAb][Rec] \qquad \textbf{Eq. 3}$$

$$reverse \frac{d[mAb \cdot Rec]}{dt} = k_d[mAb \cdot Rec] \qquad \textbf{Eq. 4}$$

The rate constants k_a and k_d are physical parameters that are fixed for a given pair of interactants under given conditions of temperature and solution environment - they are characteristics of the interaction process. Association and dissociation rates of antibody interaction vary by several orders of magnitude. Kinetics of antibody-antigen is commonly temperature dependent, which may be indicative of the structural plasticity involved in antigen binding – not rigid body-like. This plasticity is more common for small antigens.

Thermodynamically, the affinity is defined by the free energy difference between the associated and dissociated states of the proteins and surrounding solvent. At equilibrium, the Gibbs free energy change, ΔG, relates with the equilibrium dissociation constant (K_D) by Eq. 5, where *R* is the gas constant and *T* is the absolute temperature.

$$\Delta G = RT \ln K_D \qquad \textbf{Eq. 5}$$

However, the free energy change of complex formation is only one part of the thermodynamics. Dissection of binding forces into enthalpic (ΔH) and entropic (ΔS) contributions provide useful information about the importance of various factors involved in the association and complements structure and kinetic information by providing a more complete understanding of the forces that lead to complex formation (Jelesarov *et al.*, 1996; Jelesarov and Bosshard, 1999; Perozzo *et al.*, 2004). The enthalpy and entropy change relate to the Gibbs free energy change by the Gibbs equation shown in Eq. 6 (Williams *et al.*, 2004).

$$\Delta G = \Delta H - T\Delta S \qquad \textbf{Eq. 6}$$

The Gibbs equation states that ΔG is negative for a spontaneous change. The enthalpy term is related to the strength of polar interactions (H-bonds, van der Waals) that take place in the complex and in the interactants alone. ΔH magnitude is related to geometry and strength of protein-protein and/or protein-solvent polar interactions; ΔH signal depends upon whether there is a net gain (negative) or loss (positive) of polar interactions (Velazquez-Campoy *et al.*, 2001; Holdgate, 2001). ΔH is negative if the process is exothermic and is positive if the process is endothermic. The entropy term is related to conformational and dynamic phenomena involving the proteins and the solvent. Favourable (positive) entropy changes are often associated with the release of water molecules from a binding interface whereas unfavourable (negative) entropy values are often linked to conformational or dynamic restrictions (Ward and Holdgate, 2001; Kwong *et al.*, 2002).

The ΔH of a reaction can, in general, be determined in one of two ways; it can be determined directly using calorimetry of indirectly by measuring the temperature dependence of the equilibrium constant. The latter is known as the van't Hoff method. Substituting Eq. 5 in Eq. 6 gives the van't Hoff relation in Eq. 7.

$$RT\ln K_D = \Delta H - T\Delta S \quad \text{or} \quad \ln K_D = \frac{\Delta H}{R}\cdot\frac{1}{T} - \frac{\Delta S}{R} \qquad \textbf{Eq. 7}$$

The plot of ln K_D against 1/T is a straight line, with slope $\Delta H/R$ and intercept on the y-axis $\Delta S/R$. This simplified relationship does not hold if the heat capacities of reagents and products differ, i.e. if ΔH and ΔS are not constant with the temperature. In such cases, the plot of ln K_D against 1/T is not linear and the relationship becomes

$$RT\ln K_D = \Delta H_{T_0} - T\Delta S_{T_0} + \Delta C_P\left(T - T_0\right) - T\Delta C_P \ln\left(\frac{T}{T_0}\right) \qquad \textbf{Eq. 8}$$

where T_0 is the reference temperature (25°C for standard conditions). A non-linear fitting of the data to this extended equation yields in addition to ΔH and ΔS a value for the standard heat capacity change ΔC_P, that stands for the temperature dependence of the enthalpy change.

4.3 Surface plasmon resonance

The use of surface plasmon resonance for biosensing purposes was first demonstrated by Liedberg in 1983 (Liedberg *et al.*, 1983), making use of the Kretschmann method for excitation of surface plasmons (Kretschmann, 1971). In 1990, Pharmacia Biosensor launched Biacore (Liedberg *et al.*, 1995), the first and until today most commonly used SPR-based technology for characterization of real-time biomolecular interactions (Ernst *et al.*, 2009). SPR detection allows direct measure of the binding of a molecule in solution to a surface immobilized binding partner and determine both the kinetics of that interaction, association (k_a) and dissociation rates (k_d), and the affinity (equilibrium dissociation constant, K_D). SPR-based biosensors are nowadays an established method for the real-time label-free analysis of molecular interactions (Morton and Myszka, 1998; Rich and Myszka, 2006; Rich and Myszka, 2007b; Rich and Myszka, 2008)). The advantages of these technologies include no labelling of the molecules and small sample volumes. The majority of the work published in the antibody field originates from real time binding analysis based on biosensor instruments produced by Biacore (GE Healthcare), although several other instrumentation manufacturers have entered the field (Rich and Myszka, 2007a).

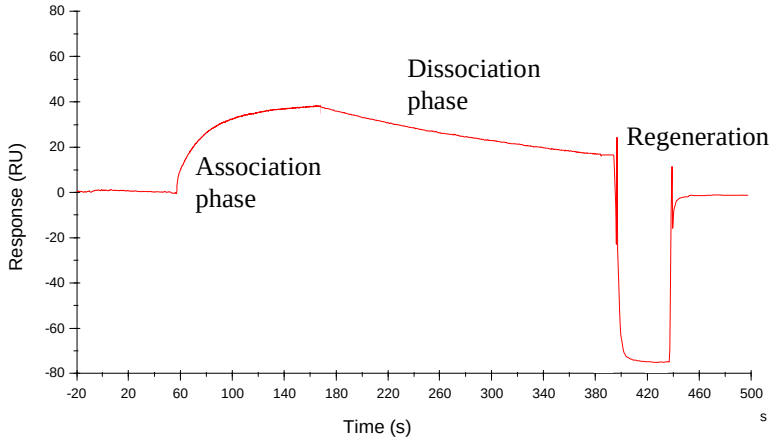

Fig. 4: An example of a sensorgram.
Real time information about the antibody antigen interaction is observed. The association and dissociation phases are measured in resonance or response units (RU) as a function of time.

The basic diagram of biosensor output is called sensorgram (Fig. 4). The change in the detected SPR signal is expressed as resonance/response units, or RU, and is followed as a function of time. The response detected has been shown to be proportional to the mass bound or deposited at the surface (Stenberg *et al.*, 1991). The sensorgram in Fig. 4 outlines the five basic phases during the binding of an antigen to an immobilized antibody or vice-versa. The first phase is the baseline signal or the pre-injection phase of buffer only, which is followed by the injection of analyte and consequent association phase. Once the injection is stopped, the association phase ends. Then, the analyte solution is replaced with buffer and the dissociation phase begins, which monitors the dissociation of the analyte from the immobilized ligand or the dissociation of the complex over time. The final phases are for the regeneration of the sensor surface, to remove all bound analyte using predetermined regeneration reagents and conditions, followed by a stabilization phase where only buffer is flowing and maintaining the surface in preparation for the next round of analyte injection. In a typical kinetic experiment, a set of varying concentrations of one binding partner is injected sequentially onto the surface where the other binding partner has been immobilized. The kinetic data analysis is done by curve fitting calculations. The simplest model for kinetic evaluation is the 1:1 binding model, describing a binary interaction, where one analyte species interacts with one ligand at a single uniquely defined site. This model is recommended for data treatment as default unless there is good experimental reason to choose a different model. Other more complicated binding models include heterogeneous ligand model, where bound interactant may be present in multiple forms, bivalent and heterogeneous analyte models (Karlsson *et al.*, 1994; Karlsson and Falt, 1997; Alfthan, 1998). The use of these alternative models requires previous knowledge of such interactions that deviate from 1:1 interaction.

Surface plasmon resonance biosensing is based on measures of refractive index change occurring as molecules adsorb to or dissipate from a sensor surface during reaction (Huber and Mueller, 2006). If light of an appropriate wavelength is directed upon the metal/prism interface at an incident angle within certain narrow limits, the delocalised surface electrons of the metal at the metal/external medium interface are resonantly excited into a collective motion, termed a 'plasmon'. Energy is thus transferred from the light beam to the surface electrons, resulting in a decrease in the intensity of the reflected beam (Liedberg *et al.*, 1995). The angle at which incident light excites the surface plasmon is extremely sensitive to the refractive index of the medium adjacent to the metal surface. Thus, either the binding or dissociation of proteins to the surface perturbs the local refractive index and produces a change in the angle at which incident light must strike the interface to produce a minimum in the intensity of the measured reflected light (Fig. 5). The energy that is transferred from the light beam to the surface electrons has been called evanescent wave. Intensity of the optical fields in this surface wave decays exponentially with distance from the surface over about 100 nm, and the value of the SPR angle is therefore very sensitive to the refractive index of the medium adjacent to the surface.

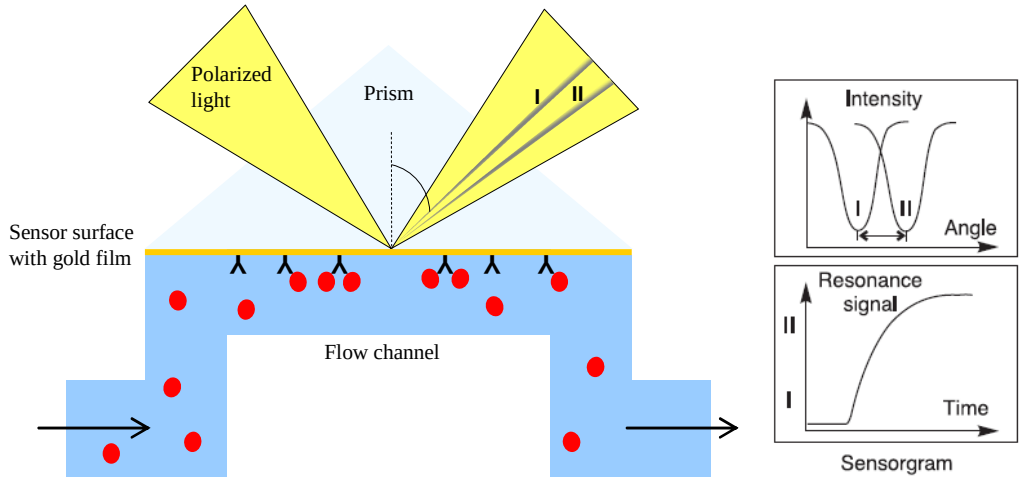

Fig. 5: The surface plasmon resonance detection.
In Biacore systems, the incident p-polarized light is focused into a wedge-shaped beam providing simultaneously a continuous interval of light wavevectors k_x. This range covers the working range for the plasmon wavevector k_{sp} during biomolecular interaction analysis. An increased sample concentration in the surface coating of the sensor chip causes a corresponding increase in refractive index which alters the angle of incidence required to create the SPR phenomenon (the SPR angle). This SPR angle is monitored as a change in the detector position for the reflected intensity dip (from I to II). By monitoring the SPR-angle as a function of time the kinetic events in the surface are displayed in a sensorgram. (Biacore, 1998)

Biacore systems typically use a carboxymethylated dextran layer on the surface of a gold chip for biomolecular interactions. The dextran layer, about 100 nm thick, utilizes the evanescent

field in an efficient way and provides for a hydrophilic and freely mobile environment for the interaction to take place, as it contains 97 to 98% water. Furthermore, it provides the surface with the carboxyl groups to which biomolecules can be coupled using known techniques (Jonsson *et al.*, 1991). Immobilization of biomolecules to the sensor chip surface can be done by covalent immobilization, high affinity capture or hydrophobic adsorption. Immobilization via amine groups is the most popular method used for surface immobilization. The coupling normally occurs between the primary amine group of lysine residues at the surface of the protein and the free carboxylic acid groups on the surface of the sensor chip which are generated by treatment with 1-ethyl-3-(3-dimethylaminopropyl) carbodiimide (EDC) and N-hydroxysuccinimide (NHS). The preparation of a surface that can be regenerated for multiple cycles of analysis is crucial for kinetic analysis using a series of analyte concentrations (Biacore, 2008).

The establishment of commercial biosensors and concretely Biacore technology was due to the development of automated liquid handling capacity with the integrated fluid control unit (Liedberg *et al.*, 1995). The integrated microfluidic cartridge contains sample and buffer loops and provides for very efficient and accurate sample delivery that is important for assay reproducibility and provides the controlled conditions necessary for kinetic studies (Sjolander and Urbaniczky, 1991). The microfluidic cartridge is pressed against the sensor chip to form the flow cells, where the interaction takes place.

4.4 Isothermal titration calorimetry

Isothermal titration calorimetry (ITC) is the only technique that directly measures the enthalpy change upon binding (Holdgate and Ward, 2005). The technology is well established in drug discovery and has proven applicability for the study of antibody-receptor interactions (Jelesarov *et al.*, 1996). ITC analysis is based on the direct measurement of the heat absorbed or released upon interaction. Most ITC instruments operate a differential cell feedback system (Pierce *et al.*, 1999; Holdgate and Ward, 2005), as shown in Fig. 6. A pair of identical coin shaped cells is enclosed in an adiabatic outer shield: a reference cell, filled with water or buffer; and a sample cell containing a solution of one interactant. Injection of the other interactant into the sample cell produces heat effects that arise from three sources: the binding interaction, dilution of the interactants and mixing. The heat changes arising in the sample cell cause a temperature difference between the two cells, which is detected by the calorimeter and

triggers a change in the feedback power applied to maintain temperature equilibrium. A reaction which results in the evolution of heat within the sample cell (exothermic) causes a negative change in the feedback power since the heat evolved chemically provides heat that the feedback power is no longer required to provide (see example titration in Fig. 6). The opposite is true for endothermic reactions.

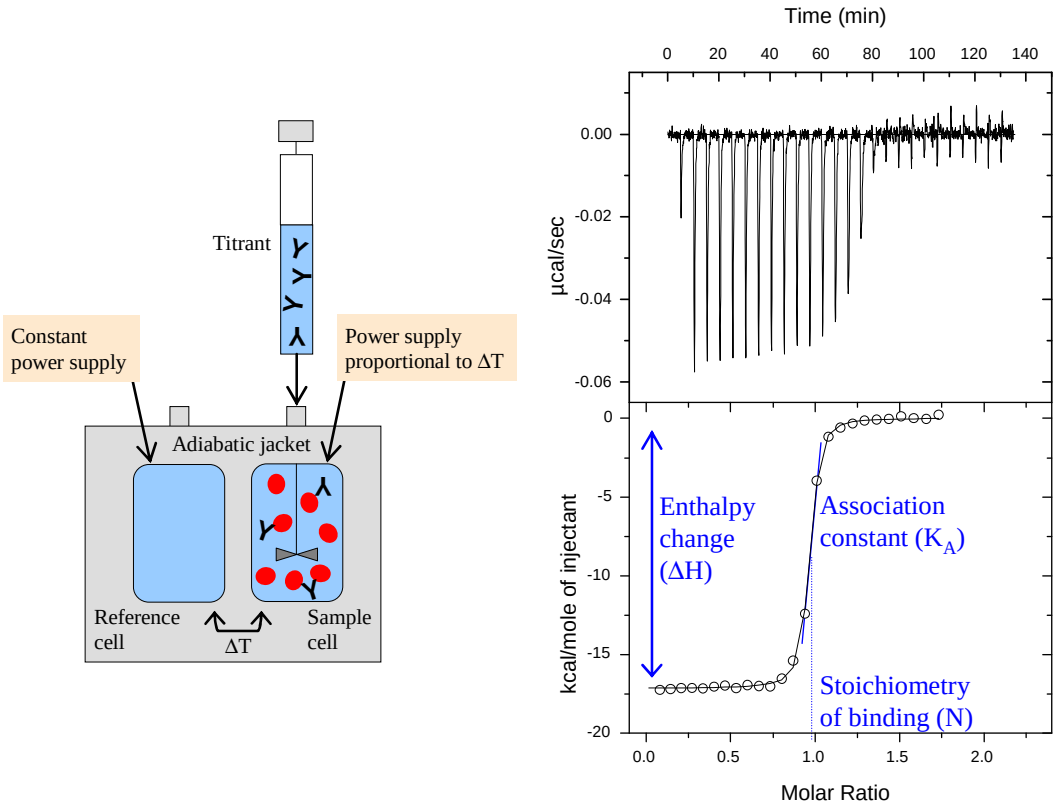

Fig. 6: Typical isothermal titration calorimetry instrument and data.

In Fig. 6 is shown a schematic illustration of an example ITC experiment where antibody is titrated to receptor. On the right side of the picture, the raw data resulting from the titration and the typical titration sigmoidal curve resulting from integration of the raw data are presented. Each peak in µcal/sec vs. time corresponds to the heat released on addition of an aliquot of antibody to the receptor. Integration of the differential power signal with respect to time yields the apparent heat change between two consecutive antibody additions, that corresponds to the area of the peak. If the association constant ($K_A=1/K_D$) is large and the molar ratio of antibody to receptor at the beginning of the titration is low, then virtually all the antibody is bound to the receptor and the peak areas are similar, giving a measure of the binding enthalpy (ΔH). As the fractional saturation increases, the apparent heat change gradually decreases. This part of the titration allows estimation of the association constant (K_A) and stoichiometry (N) of the binding. Eventually, all receptor sites are saturated. Small

heat changes registered after full saturation are caused by the heat of antibody dilution or by other non-specific effects. A non-linear regression to the procedure yields stoichiometry, association constant and binding enthalpy from one single titration experiment.

The enthalpy change measured by ITC is a global property of the system. It is the total heat released or absorbed in the calorimetric cell on each addition of the antibody. The total heat contains contributions arising from non-specific effects, such as dilution, mixing of buffers with slightly different compositions or incomplete match of the temperatures of the solutions in the cell and at the injection syringe. Unspecific contributions to the enthalpy of binding arising from unmatched buffer compositions in the cell and in the syringe can be avoided through dialysis of samples in the same buffer.

Modern ITC instruments allow to precisely measure enthalpies in a wide temperature range and from the temperature dependence of enthalpy, the heat capacity change (ΔC_P) can be calculated.

4.5 Static light scattering

When light impinges on a macromolecule, the oscillating electric field of the light induces an oscillating dipole within the molecule. Light is thus re-radiated with an intensity that depends on the magnitude of the dipole induced within the macromolecule. The more polarizable the macromolecule is, the larger the induced dipole, and hence, the greater the intensity of the scattered light. Analysis of the intensity of light scattered by a solution can provide information about the native molecular weight, oligomeric composition and conformation of the molecules present in solution. The theory of light scattering was developed by some of the greatest scientists of the twentieth century; among them Einstein, Lord Rayleigh, Raman and Debye. Although the theory of light scattering dates back to the nineteenth century, routine use of light scattering techniques was linked to the commercial availability of stable lasers as light sources (Demeester *et al.*, 2005).

Static light scattering is based on the principle of analyzing the time-averaged intensity of light scattered by a solution. Static light scattering methods are based on the Debye-Zimm equation, shown in Eq. 9 (Harding and Jumel, 2001).

$$\frac{Kc}{R_\theta} = \frac{1}{MP(\theta)}(1 + A_2 c + ...) \qquad \textbf{Eq. 9}$$

Where A_2 is the thermodynamic nonideality coefficient, R_θ is the Rayleigh excess ratio (the ratio of the intensity of excess light scattered compared to pure solvent) at a scattering angle θ, K is an experimental constant dependent on the square of the solvent refractive index, the square of the refractive index increment (dn/dc) and the inverse fourth power of the incident wavelength, M is the molecular weight, c is the solute concentration and P(θ) is the form factor.

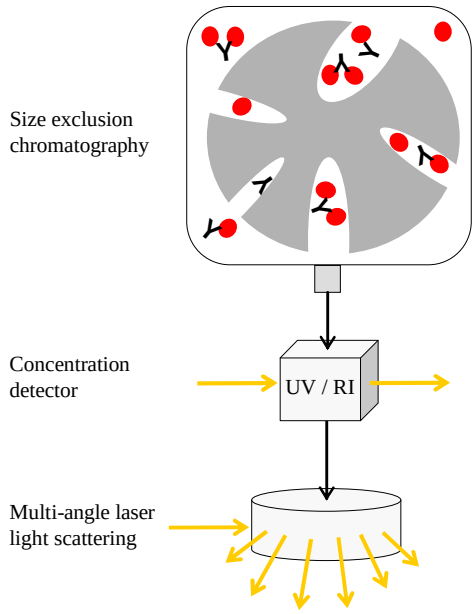

Fig. 7: Schematic representation of typical light scattering method for analysis of antibody-receptor interactions.

In this study, a multi-angle light scattering detector was employed, in combination with size exclusion chromatography and a refractive index detector – Fig. 7. Multi-angle light scattering (MALS) analysis involves performing light scattering measurements at different angles with the advantage of higher precision in the determination of molecular weights in comparison to single angle methods (Harding and Jumel, 2001). The coupling of MALS photometers to size exclusion chromatography systems has been a revolutionary development since it allowed fractionation of polydisperse materials prior to scattering analysis (Wyatt, 1993). MALS analysis of the chromatographically separated fractions provides information on the molecular weight distribution of proteins or protein complexes provided an additional concentration detector is present. Typically, a refractive index (RI) or UV detector is employed. An important feature of the RI detector is that it requires no knowledge of the

extinction coefficient of the proteins for data analysis. For a protein, or protein complex, that does not contain carbohydrates, the refractive index increment, dn/dc – where n is the refractive index and c is the protein concentration – is constant and nearly independent of its amino acid composition. Combining protein concentration from RI (or UV) detection with light scattering at different angles (normalized to the calibrated 90° detector), absolute measurement of molecular weight of proteins eluting from SEC can be performed. This technology has already been applied for the analysis of antibody-antigen mixtures in stoichiometry studies (Qian *et al.*, 1997; Arakawa and Wen, 2001; Rehder *et al.*, 2008).

5 MATERIALS AND METHODS

5.1 Buffer

The buffer PBS with 3mM EDTA, 0.05% (v/v) Tween 20 pH 7.4 will be further referred to as PBS-EP+.

5.2 Proteins

EGFR

A truncated soluble form of EGFR, excreted by A431 cells and consisting in almost the entire external domain was used for this work (Weber *et al.*, 1984; Ullrich *et al.*, 1984). It was obtained from PD Dr. Wolfgang Weber (UKE, Hamburg, Germany). EGFR stock solution was 2mg/ml and it was stored in aliquots at -70°C.

The deletion mutant EGFR variant III (EGFRvIII) was a most kind donation from Dr. Judith Schmiedel (Merck KGaA).

Anti-EGFR antibodies

The antibodies matuzumab and cetuximab were provided by Merck KGaA. The antibodies panitumumab and nimotuzumab are commercially available. An independent nimotuzumab vial was a very kind donation from Christof Reusch (Merck KGaA). Antibody solutions were 5 to 20 mg/ml and were stored at 4°C.

Fab fragments preparation

The antibodies matuzumab were enzymatically cleaved by papain digestion to generate Fab fragments. The Fab fragments were further purified by protein A affinity chromatography. The Pierce Fab Preparation Kit from Thermo Scientific (Rockford, IL, USA) was used according to the manufacturer's instructions. Antibody formulations of 7.5 mg yielded about 2 mg pure Fab fragments. These purified Fab fragments were stored at 1 mg/ml at 4°C in PBS-EP+.

EGFR ligands

EGF was from US Biological (Swampscott, MS, USA). It was reconstituted in water to a concentration of 1 mg/ml in PBS and stored at -20°C. TGF-α was from Chemicon /Millipore (Billerica, MA, USA). It was directly reconstituted in PBS-EP+ to a concentration of 1 mg/ml and stored at -20°C.

Other proteins

Protein A and Human Fab Binder for surface plasmon resonance biosensor immobilization were obtained from GE Healthcare Biosciences AB (Uppsala, Sweden).

5.3 Surface plasmon resonance

SPR studies were carried using a Biacore T100 from GE Healthcare (Uppsala, Sweden) (Biacore, 2005; Biacore, 2006). All experiments were done using PBS-EP+ as running and sample buffer. Biacore data was collected with Biacore T100 Control Software and analyzed using Biacore T100 Evaluation Software, both delivered with the instrument.

5.3.1 Protein immobilization and regeneration conditions

All proteins were immobilized onto Biacore CM5-chips from GE Healthcare (Uppsala, Sweden) as follows: the CM-dextran matrix was activated with *N*-ethyl-*N'*-(dimethylaminopropyl)-carbodiimide hydrochloride (EDC) and *N*-hydroxysuccinimide (NHS). After protein immobilization the remaining reactive sites were blocked with 1 M ethanolamine-HCl (pH 8.5). Immobilization, capture and regeneration were performed at a flow rate of 10 µl/min.

Protein A surface

Protein A (100 µg/ml) was immobilized in 10 mM sodium acetate (pH 4.5) for 7 min with a final immobilization level of 4800 response units (RU). Antibodies matuzumab, cetuximab and panitumumab (0.5 µg/ml) were captured onto protein A surface for 30 s with capture levels of 60 RU. Nimotuzumab (0.5 µg/ml) was captured for 60 s with a capture level of 60 RU. Protein A surfaces were regenerated with a 30 s pulse of 10 mM glycine (pH 1.7).

Human Fab Binder surface

The Biacore Human Fab Capture Kit from GE Healthcare (Rockford, IL, USA) was used according to the manufacturer's instructions. Human Fab binder (20 µg/ml) was immobilized for 7 min with a final immobilization level of 14000 RU. Fab fragments of the antibodies matuzumab, and nimotuzumab (0.5 µg/ml) were captured onto Human Fab Binder surface for 30 s with capture levels of 30 RU. Fab fragments of panitumumab was captured for 42 s with capture levels of 30 RU. Human Fab Binder surfaces were regenerated with a 60 s pulse of 10 mM glycine (pH 2.1).

Antibody/Fab fragment surface

For kinetic studies, all four mAbs (1 µg/ml) were immobilized in 10 mM sodium acetate (pH 5.0). Matuzumab was immobilized for 100 s with a bound immobilization of 280 RU. Cetuximab was immobilized for 80 s with a bound immobilization of 180 RU. Panitumumab was immobilized for 80 s with a bound immobilization of 140 RU. Nimotuzumab was immobilized for 120 s with a bound immobilization of 380 RU. Fab fragments were immobilized in 10 mM sodium acetate (pH 5.0). Matuzumab, cetuximab and panitumumab Fab fragments (1µg/ml) were immobilized for 120 s with a bound immobilization of 250 RU, 40 RU and 30 RU respectively. Nimotuzumab Fab fragment (8µg/ml) was immobilized for 120 s with a bound immobilization of 860 RU.

For studies of interdependence of antibody binding, the flow rate and immobilization buffer were maintained but concentration and contact time were increased to 25 µg/ml and 7 min respectively. Matuzumab, cetuximab, panitumumab and nimotuzumab yielded final immobilization levels of 17,500, 15,000, 12,000 and 18,000 RU, respectively. EGFR (3µg/ml) was then captured by these surfaces through 40 s – in matuzumab or nimotuzumab – or 60 s injections – in cetuximab or panitumumab surfaces. EGFR capture levels were 360, 820, 700, 300 RU, for matuzumab, cetuximab, panitumumab and nimotuzumab respectively.

Antibody and Fab fragment surfaces were regenerated with a 15 s pulse of 10 mM NaOH and 1 M NaCl.

mAb-EGFR crosslinked surface

Matuzumab, cetuximab, panitumumab and nimotuzumab were immobilized as described above for studies of interdependence of antibody binding. Subsequently, EGFR (100 µg/ml)

was injected for 120 s onto matuzumab, cetuximab and panitumumab surfaces. As for nimotuzumab surface, EGFR (33 µg/ml) was injected for 120 s. EGFR capture was followed by a 120 s long injection of EDC/NHS and a 120 s long injection of ethanolamine for crosslinking of EGFR to the immobilized mAbs. Crosslinked EGFR yielded 750, 4000, 4700 and 600 RU for matuzumab, cetuximab and panitumumab surfaces respectively.

EGFR surface

For EGF/TGF-α titrations, EGFR (5 µg/ml) was immobilized in 10 mM sodium acetate (pH 5.0) for 6.7 min with a final immobilization level of 3000 RU. For Fab fragment titrations, EGFR (1.7 µg/ml) was immobilized in 10 mM sodium acetate (pH 5.0) for 6.7 min with a final immobilization level of 470 RU. EGFR surfaces were regenerated with a 15 s pulse of 10 mM NaOH and 1 M NaCl.

EGF surface

EGF (50µg/ml) was immobilized in 10 mM sodium acetate (pH 4.0) for 40 s with a final immobilization level of 100 RU. EGF surface were regenerated with a 15 s pulse of 10mM NaOH and 1M NaCl.

5.3.2 Titration and competition experiments

For antibody/EGFR kinetic studies, EGFR was flown as twofold serial dilutions covering a concentration range 1.6 - 800 nM over the matuzumab, cetuximab, panitumumab and nimotuzumab antibodies either captured by protein A or directly immobilized. For Fab fragments/EGFR kinetic studies, the same EGFR concentrations were flown over directly immobilized Fab fragments. Alternatively, the Fab fragments were flown as twofold serial dilutions covering a concentration range 1.6 - 800 nM over directly immobilized EGFR. Nimotuzumab mAb/Fab kinetic experiments included one higher concentration point, 1600 nM. For EGFRvIII binding studies, EGFRvIII was flown as twofold serial dilutions covering a concentration range 1.6 - 800 nM over cetuximab, panitumumab and nimotuzumab antibodies captured by protein A. All kinetic studies were performed at 40 µl/min with an association time of 100 s and a dissociation time of 200 s. 1:1 interaction models were fitted to binding curves.

For ligand/EGFR affinity experiments, EGF and TGF-α were flown as twofold serial dilutions covering concentration ranges 3.9 - 2000 nM and 7.8 - 4000 nM, respectively. These were injected at 30 µl/min for 30 s over EGFR surface. The dissociation time was 60 s. Steady state analysis was performed to the experimental results.

Competition experiments were carried out with a constant concentration of the receptor protein (800 nM). The binding to a ligand surface was monitored while increasing amounts of antibodies ranging from 0-15 µM were added to the receptor sample.

5.3.3 Van't Hoff analysis

Van't Hoff analysis was performed for matuzumab, cetuximab, panitumumab, nimotuzumab, EGF and TGF-α. EGFR was titrated onto antibody that has been captured by protein A. Other conditions used were the same as described in 5.3.2 and the analysis was repeated twice at 15, 19, 22, 25, 31 37 and 40°C. Kinetic-originated antibody affinities and steady state-analysis ligand affinities were plotted ln K_D vs. 1/T. The plots were all fitted with linear regression.

5.3.4 Analysis of maximal EGFR binding capacity on antibody surfaces

Row-diluted concentrations 400, 800, 1600, and 3200 nM EGFR were titrated onto matuzumab and cetuximab mAbs. Row-diluted concentrations 400, 800, 1600, 3200 and 6400 nM EGFR were titrated onto matuzumab and cetuximab Fab fragments. Row-diluted concentrations 400, 800, 1600, 3200, 6400 and 12800 nM EGFR were titrated onto nimotuzumab mAb and Fab fragments. mAbs were immobilized by protein A capture and Fabs were immobilized by Humab Fab binder capture. All experiments were repeated twice.

5.3.5 Binding interdependence of antibody combinations to EGFR

Row-diluted concentrations 1.5, 3, 6, 12, 25, 50, 100, 200, 400, 800, 1600 and 3200 nM of antibodies matuzumab, cetuximab, panitumumab and nimotuzumab were titrated onto EGFR captured by immobilized antibodies or to EGFR crosslinked to immobilized antibodies.

5.4 Isothermal titration calorimetry

All ITC measurements were performed with a VP-ITC microcalorimeter from Microcal, LLC (Northampton, MA, USA). Analysis buffer was PBS with 3 mM EDTA, 0.05% (v/v) Tween 20 pH 7.4 and samples were previously dialysed at 4°C overnight against it. Data analysis was done using Origin 7 calorimetry software (MicroCal LLC). mAbs results were normalized to concentration of binding site.

Simple titrations were performed as follows: Fab fragment (20 µM) or whole antibody (10 µM) solutions were injected in 11 µl steps into the sample cell containing 2 ml EGFR (2 µM). Binding interdependence titrations were performed as follows: whole antibody (10 µM) solutions were injected in 11 µl steps into the sample cell containing 2 ml EGFR (2 µM) and a saturation concentration (such as 2 µM) of a second antibody.

All binding experiments were carried out at 25°C with a spacing time between the injections of 320 s.

Matuzumab/EGFR and cetuximab/EGFR titrations were repeated at 20°C and 33°C.

Temperature dependence titration

To study the temperature dependence of the binding enthalpy, an alternative method was developed that allowed for maximal sample savings. Antibody (10 µM) solutions were injected in 11 µl steps into the sample cell containing 2 ml EGFR (2 µM) in a temperature-changing titration that was executed as follows: the titration was started at 20°C, 3 to 5 titrant injections were performed at this temperature; afterwards, the titration was paused and the temperature was changed to 25°C and after temperature stabilization another 2 to 4 injections were performed; this process was repeated at 29 and at 33°C. Binding enthalpies were determined by averaging the peak areas determined for the multiple peaks. The titration was designed in such a way that the inflection of the curve took place at 33°C. After the inflection point, the peaks obtained enabled correction of the enthalpy values obtained.

5.5 Static light scattering

Analytical SEC/static light scattering (SLS) studies were performed to determine the size of complexes formed in EGFR/mAb and EGFR/Fab samples. An Agilent 1200 HPLC system from Agilent (Böblingen, Germany) was used. Light scattering data for protein eluting from the SEC column were collected using a multi-angle light scattering detector DAWN-HELEOS-II from Wyatt Technologies (Dernbach, Germany). A refractive index detector Optilab rEX, also from Wyatt Technologies was used as concentration detector. The data were analyzed using the Astra V software (Wyatt Technologies).

Studies of EGFR mixtures with matuzumab and cetuximab Fab fragments were done at a flow rate of 0.3 ml/min by injecting 20 µl protein solution onto a Superdex 200 GL analytical SEC column (GE Healthcare) equilibrated in PBS buffer, pH 7.4. Studies of EGFR mixtures with panitumumab and nimotuzumab Fabs, whole antibodies and antibody combinations were done at a flow rate of 0.05 ml/min by injecting 20 µl protein solution onto a Superose 6 PC 3.2/30 analytical SEC column (GE Healthcare) equilibrated in PBS buffer, pH 7.4.

6 RESULTS

6.1 Characterization of EGFR interactions with surface plasmon resonance

6.1.1 Kinetics of antibody and Fab fragments binding EGFR

The binding kinetics of EGFR/mAb or EGFR/Fab was determined by surface plasmon resonance (SPR) /Biacore. Representative results of different assay configurations used are shown in Fig. 8. A closer look at the binding curves in Fig. 8 shows that the kinetic profile of the antibodies studied is conserved like a fingerprint in all tested assay design alternatives. Matuzumab is characterized by a very fast dissociation of the complex. In the other extreme is panitumumab that, among the mAbs studied, forms the most stable complex with EGFR. Cetuximab has a very similar kinetic profile to panitumumab, although the dissociation is somewhat faster for panitumumab-EGFR complex. Nimotuzumab is characterized by the slowest association rate, as observed by a longer association phase that takes longer to reach equilibrium.

Best fit values of 1:1 binding model to the experimental data delivered the association rate (k_a) and dissociation rate (k_d) constants presented in Fig. 8 for each assay design used. The equilibrium dissociation constant (K_D) was calculated from the rate constants ratio.

Good overall consistency was observed between kinetic results obtained by the protein A /mAb assay (first row of Fig. 8) and by the immobilized EGFR /Fab assay (fourth row of Fig. 8). Obtaining comparable results from such distinct assays shows robustness of the kinetic determination. Moreover, agreement of antibody and Fab fragment results indicates independence of both antibody arms binding to EGFR. The direct immobilization of mAbs (second row) or Fab fragments (third row) delivered lower association rate constant values although dissociation rates are consistent with those obtained by protein A or EGFR immobilization.

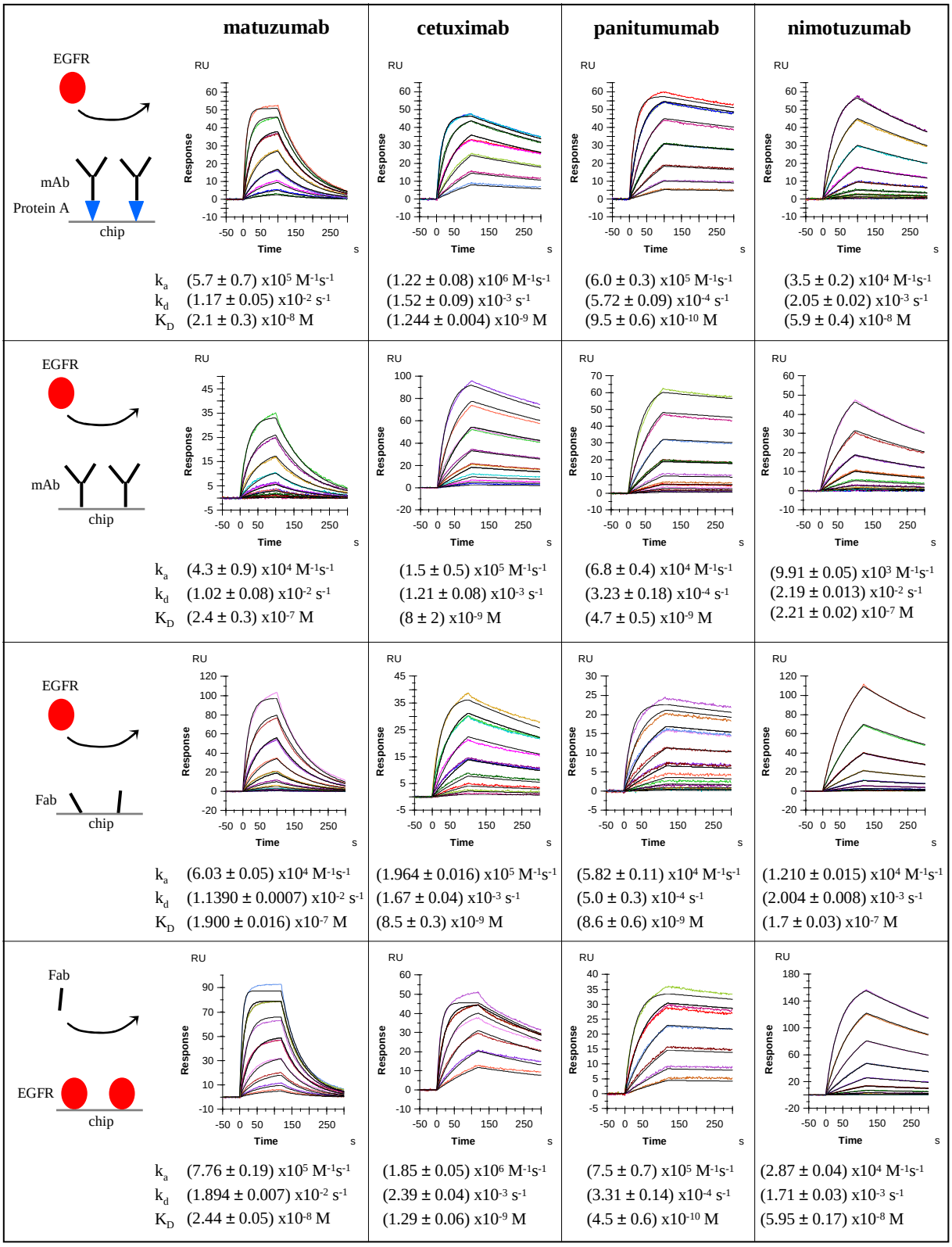

Fig. 8: Kinetics and affinity of antibodies and Fab fragments binding to EGFR.

SPR analysis of mAb binding was performed with capture of mAb on protein A that had been directly amine coupled to the biosensor chip **(first row)** or with direct amine coupling of the mAb itself **(second row)**. In both cases, EGFR was passed over the surface as analyte. Analysis of Fab fragments was performed with direct amine coupling of the Fab to the biosensor surface **(third row)** and EGFR as analyte. Alternatively, EGFR was amine coupled to the biosensor surface and solutions Fab fragments were titrated as analyte **(fourth row)**. Twofold serial dilutions of analyte covered a concentration range 1.5 - 800 nM. 1:1 binding model was fit to all experiments. For the model fitting not all concentrations were used, the higher concentrations were left out in some cases due to insufficient fitting. Values presented are the average of two independent determinations.

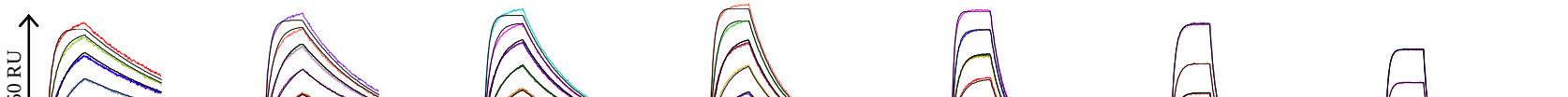

	15°C	19°C	22°C	25°C	31°C	37°C	40°C
matuzumab							
k_a	(3.8 ± 0.2) x10^{5} M^{-1}s^{-1}	(4.29 ± 0.12) x10^{5} M^{-1}s^{-1}	(4.80 ± 0.18) x10^{5} M^{-1}s^{-1}	(5.7 ± 0.7) x10^{5} M^{-1}s^{-1}	(6.71 ± 0.18) x10^{5} M^{-1}s^{-1}	(9 ± 3) x10^{5} M^{-1}s^{-1}	(1.1 ± 0.5) x10^{6} M^{-1}s^{-1}
k_d	(3.11 ± 0.03) x10^{-3} s^{-1}	(5.25 ± 0.03) x10^{-3} s^{-1}	(7.76 ± 0.17) x10^{-3} s^{-1}	(1.17 ± 0.05) x10^{-2} s^{-1}	(2.94 ± 0.06) x10^{-2} s^{-1}	(6.7 ± 0.9) x10^{-2} s^{-1}	0.105 ± 0.014 s^{-1}
K_D	(8.2 ± 0.5) x10^{-9} M	(1.22 ± 0.04) x10^{-8} M	(1.62 ± 0.09) x10^{-8} M	(2.1 ± 0.3) x10^{-8} M	(4.37 ± 0.03) x10^{-8} M	(7.8 ± 1.3) x10^{-8} M	(1.0 ± 0.3) x10^{-7} M
cetuximab							
k_a	(9.0 ± 0.9) x10^{5} M^{-1}s^{-1}	(9.9 ± 0.2) x10^{5} M^{-1}s^{-1}	(1.14 ± 0.09) x10^{6} M^{-1}s^{-1}	(1.22 ± 0.08) x10^{6} M^{-1}s^{-1}	(1.46 ± 0.04) x10^{6} M^{-1}s^{-1}	(1.81 ± 0.04) x10^{6} M^{-1}s^{-1}	(1.96 ± 0.15) x10^{6} M^{-1}s^{-1}
k_d	(4.8 ± 0.9) x10^{-4} s^{-1}	(7.8 ± 0.9) x10^{-4} s^{-1}	(1.08 ± 0.10) x10^{-3} s^{-1}	(1.52 ± 0.09) x10^{-3} s^{-1}	(3.21 ± 0.17) x10^{-3} s^{-1}	(6.9 ± 0.4) x10^{-3} s^{-1}	(1.08 ± 0.07) x10^{-2} s^{-1}
K_D	(5.4 ± 0.4) x10^{-10} M	(7.9 ± 0.8) x10^{-10} M	(9.53 ± 0.09) x10^{-10} M	(1.244 ± 0.004) x10^{-9} M	(2.19 ± 0.06) x10^{-9} M	(3.81 ± 0.15) x10^{-9} M	(5.52 ± 0.05) x10^{-9} M
panitumumab							
k_a	(4.1 ± 0.3) x10^{5} M^{-1}s^{-1}	(4.9 ± 0.3) x10^{5} M^{-1}s^{-1}	(5.4 ± 0.3) x10^{5} M^{-1}s^{-1}	(6.0 ± 0.3) x10^{5} M^{-1}s^{-1}	(7.4 ± 0.3) x10^{5} M^{-1}s^{-1}	(9.28 ± 0.11) x10^{5} M^{-1}s^{-1}	(1.13 ± 0.06) x10^{6} M^{-1}s^{-1}
k_d	(2.03 ± 0.07) x10^{-4} s^{-1}	(2.78 ± 0.12) x10^{-4} s^{-1}	(4.05 ± 0.04) x10^{-4} s^{-1}	(5.72 ± 0.09) x10^{-4} s^{-1}	(1.06 ± 0.09) x10^{-3} s^{-1}	(1.90 ± 0.19) x10^{-3} s^{-1}	(3.1 ± 0.8) x10^{-3} s^{-1}
K_D	(5.0 ± 0.5) x10^{-10} M	(5.8 ± 0.6) x10^{-10} M	(7.5 ± 0.5) x10^{-10} M	(9.5 ± 0.6) x10^{-10} M	(1.44 ± 0.18) x10^{-9} M	(2.1 ± 0.2) x10^{-9} M	(2.8 ± 0.5) x10^{-9} M
nimotuzumab							
k_a	(2.33 ± 0.11) x10^{4} M^{-1}s^{-1}	(2.7 ± 0.2) x10^{4} M^{-1}s^{-1}	(3.11 ± 0.16) x10^{4} M^{-1}s^{-1}	(3.5 ± 0.2) x10^{4} M^{-1}s^{-1}	(4.4± 0.3) x10^{4} M^{-1}s^{-1}	(5.5 ± 0.4) x10^{4} M^{-1}s^{-1}	(5.9 ± 0.4) x10^{4} M^{-1}s^{-1}
k_d	(4.50 ± 0.14) x10^{-4} s^{-1}	(8.0 ± 0.3) x10^{-4} s^{-1}	(1.29 ± 0.011) x10^{-3} s^{-1}	(2.05 ± 0.02) x10^{-3} s^{-1}	(5.58 ± 0.09) x10^{-3} s^{-1}	(1.67 ± 0.003) x10^{-2} s^{-1}	(2.93 ± 0.006) x10^{-2} s^{-1}
K_D	(1.94 ± 0.15) x10^{-8} M	(3.0 ± 0.3) x10^{-8} M	(4.15 ± 0.18) x10^{-8} M	(5.9 ± 0.4) x10^{-8} M	(1.26 ± 0.06) x10^{-7} M	(3.1 ± 0.2) x10^{-7} M	(5.0 ± 0.4) x10^{-7} M

Fig. 9: Temperature dependence of antibody/EGFR kinetics and affinity.

EGFR twofold serial dilutions covering a concentration range 1.5 - 800 nM were passed over each antibody captured on protein A surface. 1:1 Interaction model was fitted to all the experiments. For the model fitting not all concentrations were used, the higher concentrations were left out in some cases due to insufficient fitting. Values presented are the average of two independent determinations.

6.1.2 Temperature dependence of antibody/EGFR kinetics

The temperature dependence of the EGFR/mAbs binding kinetics EGFR is shown in Fig. 9. Global fitting of binding data to 1:1 binding models yielded temperature-dependent rate constants and equilibrium constants also summarized in Fig. 9. The affinity weakened with increasing temperature from 15°C to 40°C for all four mAbs tested. In every case, the temperature dependence of K_D is due to an increase in the dissociation rate constant, which can also be observed from the binding curves shown in Fig. 9. A slight increase in the association rate is also observed.

6.1.3 Temperature dependence of ligand/EGFR affinity

Interactions between EGFR and two natural ligands, EGF and TGF-α, were studied with SPR at different temperatures. The results are shown in Fig. 10. The binding curves of EGF and TGF-α binding to immobilized EGFR were evaluated by steady state analysis, yielding the equilibrium dissociation constants K_D summarized in Fig. 10.

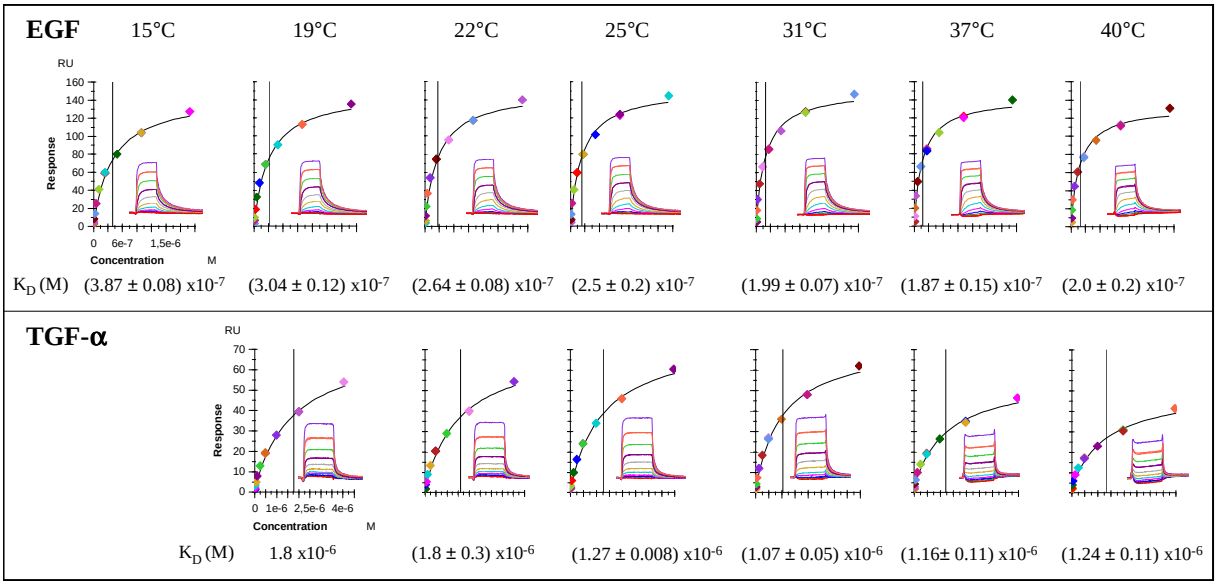

Fig. 10: Temperature dependence of ligand/EGFR kinetics and affinity.

EGF and TGF-α twofold serial dilutions covering concentration ranges 3.9 - 2000 nM and 7.8 - 4000 nM, respectively, were passed over EGFR surface. The binding curves were evaluated with steady state analysis to yield K_D. Values presented are the average of two independent determinations.

6.1.4 Van't Hoff analysis

The temperature dependent equilibrium constants of EGFR/mAb and EGFR/ligand binding determined by SPR analysis (see Fig. 9 and Fig. 10) were used to estimate binding enthalpies and entropies by plotting ln(K_D) versus 1/T. The resulting van't Hoff plots are shown for antibodies and ligands in Fig. 11. Linear fitting yielded the regression lines and the resulting thermodynamic properties also presented in Fig. 11.

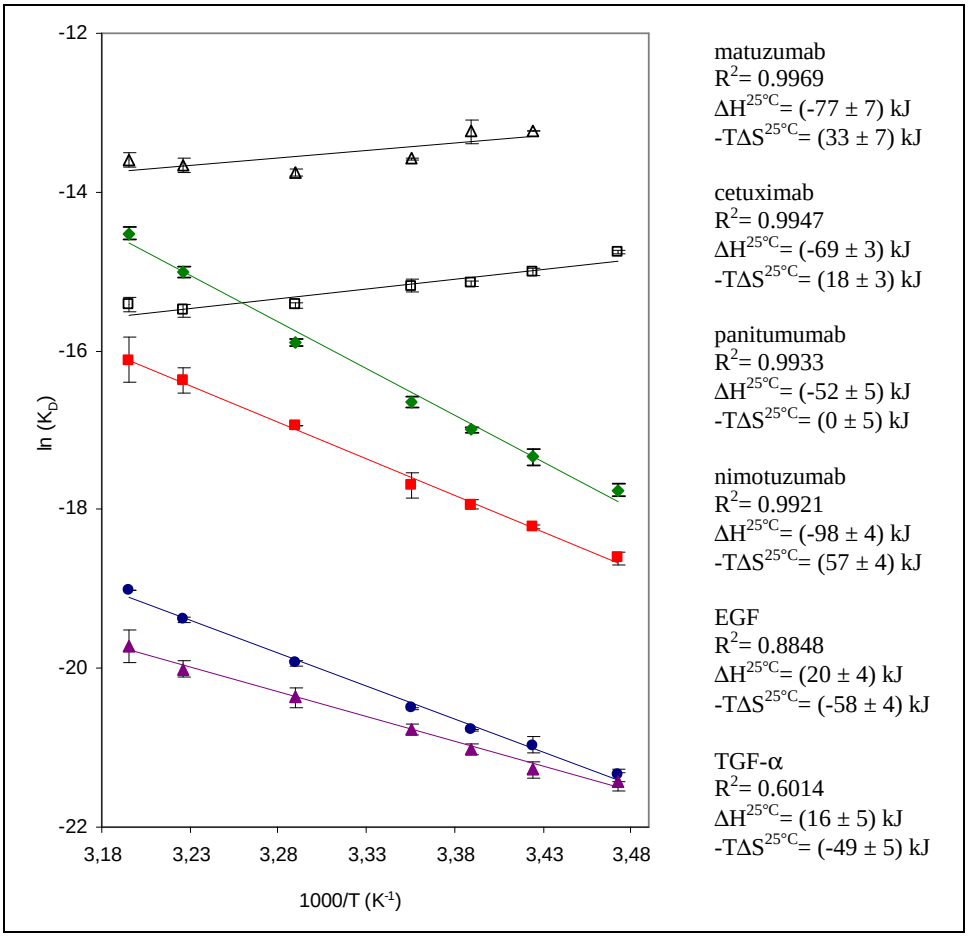

Fig. 11: Van't Hoff analysis of antibody/EGFR and ligand/EGFR affinity results.

Antibody K_D values were kinetically determined by SPR while ligand K_D values were determined by steady state analysis of SPR binding curves. Error bars indicate the standard deviation on two independent measurements – see Fig. 9 and Fig. 10. Linear regressions were fitted to the van't Hoff values; Coefficient of determination (R^2) and thermodynamic results are presented on the right. Legend: □ EGF; Δ TGF-α; ■ matuzumab; ● cetuximab; ▲ panitumumab; ◆ nimotuzumab.

6.1.5 Analysis of maximal EGFR binding capacity on antibody surfaces

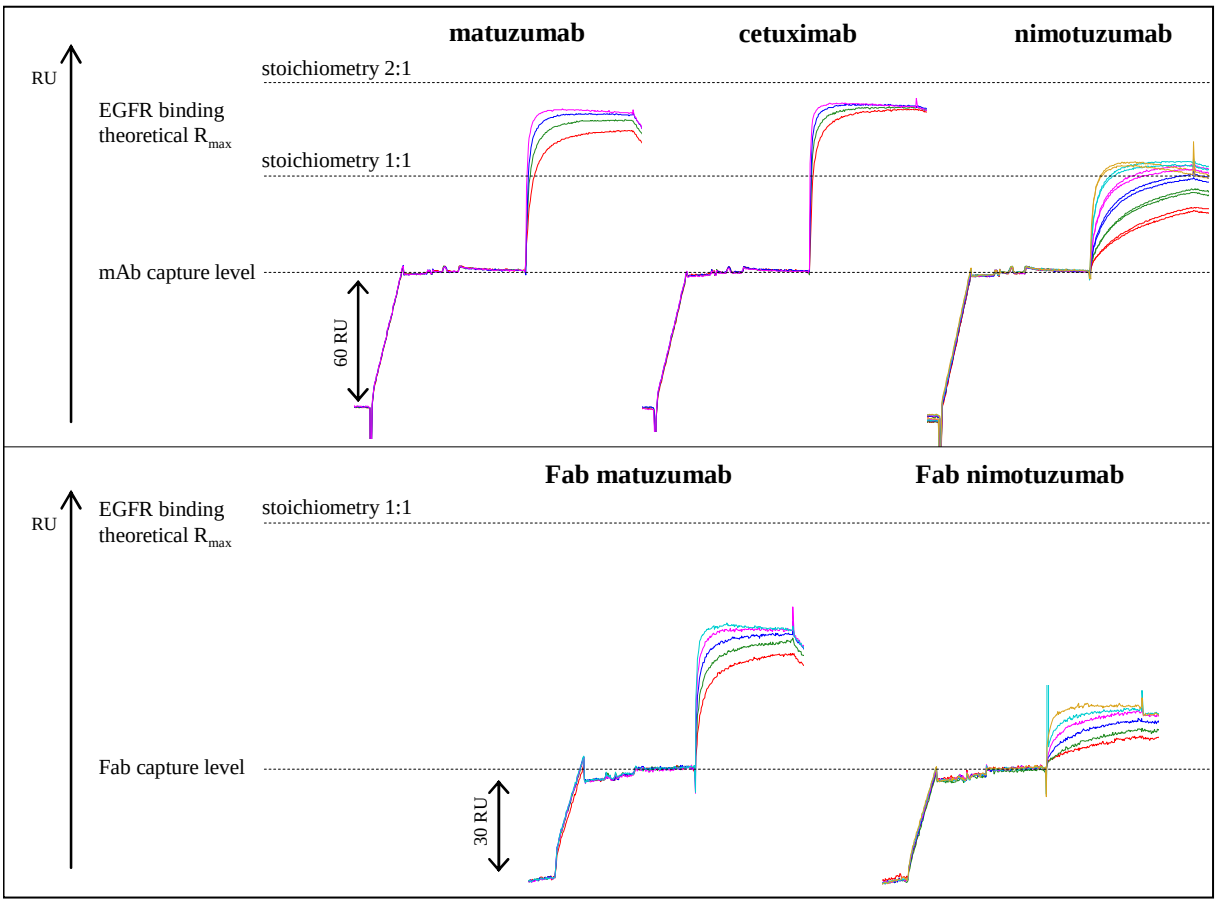

Fig. 12: SPR saturation studies of EGFR on oriented mAb (upper) and Fab (down) surfaces.
Upper: matuzumab, cetuximab and nimotuzumab were captured by protein A surface; **Lower:** Fab fragments of matuzumab and nimotuzumab were captured by Biacore human Fab binder. Levels of theoretical R_{max} were calculated with the capture level and the molecular weights of mAbs/Fabs and EGFR. Two independent batches of nimotuzumab were analyzed. Titrated concentrations of EGFR were 400, 800, 1600 and 3200 nM for mAbs matuzumab and cetuximab; 400, 800, 1600, 3200 and 6400 nM for Fab matuzumab and 400, 800, 1600, 3200, 6400 and 12800 nM for mAb and Fab nimotuzumab. Panitumumab was not measured. Note: The results are from single experiments.

With the objective of corroborating stoichiometric evidence provided by ITC and SLS with an orthogonal method, SPR saturation studies of EGFR in antibody surfaces were performed. The resulting sensorgrams are shown in Fig. 12 for whole antibodies (upper) and Fab fragments (lower). The antibodies were captured in a controlled manner by protein A directly immobilized on the biosensor surface. With the capture level and the molecular weights of EGFR and mAbs, the theoretical saturation level (R_{max}) was calculated and is represented in Fig. 12 (upper) for the hypothetical binding stoichiometries EGFR:mAb 1:1 and 2:1. The obtained R_{max} for EGFR binding to matuzumab and cetuximab surfaces is comparable and lays between the theoretical R_{max} calculated for the two considered stoichiometries. This result is in accordance with a 2:1 stoichiometry of these antibodies. The R_{max} observed for

EGFR on nimotuzumab surface was well below the other two antibodies but slightly above the theoretical R_{max} calculated for stoichiometry 1:1. This shows a different stoichiometric profile of nimotuzumab when compared with the other antibodies and is coherent with the lower extent of bivalent binding observed for nimotuzumab in ITC and SLS analyses (Fig. 16 and 20).

The Fab fragments of matuzumab and nimotuzumab were captured by Biacore human Fab binder that had been directly immobilized on the biosensor surface (Fig. 12 lower). The values of R_{max} obtained for EGFR binding to captured matuzumab and nimotuzumab Fab fragments lay below the theoretical R_{max} calculated for a stoichiometry 1:1. For comparable capture levels of Fab fragments, nimotuzumab Fab fragment offered lower EGFR binding capacity. This result is coherent with ITC analysis of Fab fragments (Fig. 17).

6.1.6 Ligand competition analysis of antibodies

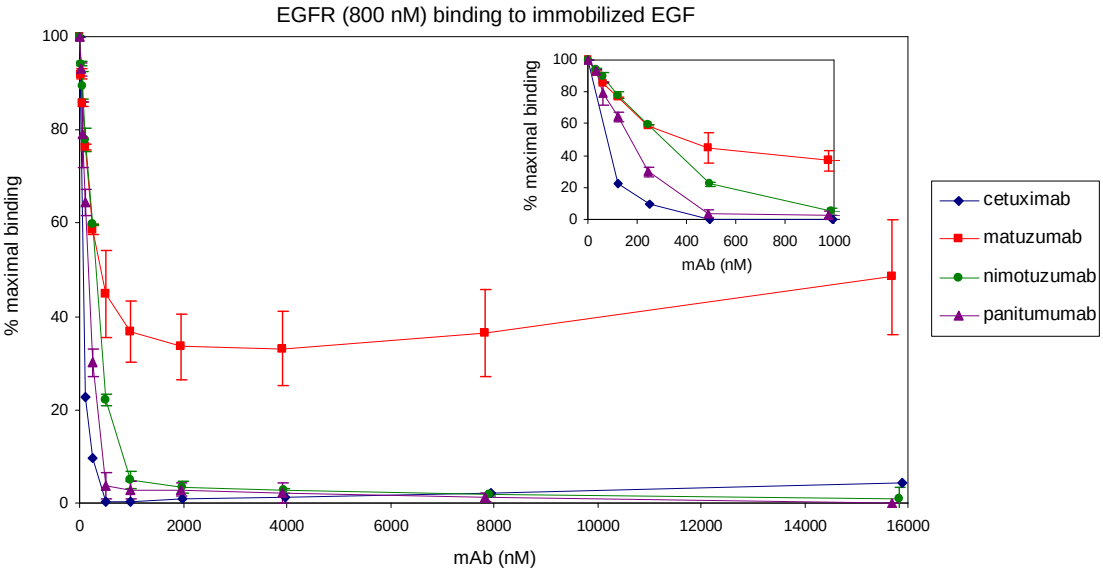

Fig. 13: Ligand competition properties of anti-EGFR antibodies.
Competition experiments showing the effect of addition of anti-EGFR mAbs upon the binding of 800 nM EGFR to immobilized EGF. Mixtures of 800 nM EGFR plus the indicated concentrations of mAbs were passed over a biosensor surface to which EGF had been amine coupled. The equilibrium SPR responses for each mixture is shown, normalized to the response obtained with no added mAb. Error bars indicate the standard deviation on two independent measurements. The line simply connects the data points.

Competition assays were carried out to investigate the ability of the anti-EGFR mAbs in study to compete with ligand binding to EGFR. The binding of EGFR to immobilized EGF at different concentrations of anti-EGFR mAbs was tested. The results are shown in Fig. 13. For antibodies cetuximab, panitumumab and nimotuzumab, at a molar ratio above 1:1 of

EGFR:mAb, SPR response is below 10 % of that obtained with no added mAb (see close up). In the case of matuzumab, there is an initial decrease in the equilibrium SPR response as increasing mAb is added. At a 1:1 molar ratio of EGFR:matuzumab the SPR response is about 40 % of that obtained with no added mAb. Addition of increasing excesses of matuzumab does not further reduce this binding level.

6.1.7 Antibodies binding to EGFRvIII

The variant III mutation of EGFR (EGFRvIII) is an EGFR mutant where nearly the whole of domains I and II are missing, while domains III and IV are unaltered. Thus, analysis of the binding to this mutant allows considerations about epitope positioning relating to EGFR extracellular domains to be done. Surface plasmon resonance (SPR)/Biacore experiments were carried out to characterize the binding kinetics of cetuximab, panitumumab and nimotuzumab binding to EGFRvIII. Solutions with different concentrations of EGFRvIII were titrated to protein A captured mAbs. For comparison purposes, wild type EGFR (EGFRwt) was titrated in the same assay construction. The kinetic results are summarized in Table 3. Matuzumab was not included in the analysis.

Table 3: SPR results of binding kinetics and affinity of mAbs binding to EGFR wild type (EGFRwt) and variant III (EGFRvIII).

Interaction	k_a ($M^{-1}s^{-1}$)	k_d (s^{-1})	K_D (M)
Cetuximab – EGFRwt	9.7×10^{5}	0.0015	1.5×10^{-9}
Cetuximab – EGFRvIII	2.5×10^{6}	0.0011	4.5×10^{-10}
Panitumumab – EGFRwt	4.6×10^{5}	6.7×10^{-4}	1.5×10^{-9}
Panitumumab – EGFRvIII	1.3×10^{6}	5.0×10^{-4}	3.8×10^{-10}
Nimotuzumab – EGFRwt	8.9×10^{4}	0.0012	1.3×10^{-8}
Nimotuzumab – EGFRvIII	4.8×10^{5}	7.8×10^{-4}	1.6×10^{-9}

Note: The results with EGFRvIII are single measurements; the results with EGFRwt are the average of two independent measurements.

6.1.8 Binding interdependence of antibody combinations to EGFR

SPR was applied to study how the anti-EGFR mAbs in study influence each other upon binding to EGFR. Two experimental setups were developed. The first was a sandwich setup where a second mAb was titrated to a controlled density of EGFR previously captured by directly immobilized mAb – Fig. 14. This assay setup provided real time monitoring of mAb binding to “un-crosslinked” EGFR. However, the rapid dissociation of EGFR from the surface, especially in the case of immobilized matuzumab, hindered observation of the

binding curves of the second antibody. A second setup was developed with crosslinking of EGFR to the first antibody, thus disabling the dissociation of EGFR from the immobilized antibody – Fig. 15. The second assay setup could thus be used as control to the results obtained with the first setup. However, binding may be influenced by EGFR crosslinkage. Moreover it should be tested if the crosslinkage itself happens in an oriented way to assure that simultaneous binding of mAbs is actually observed. Positive and negative control experiments were included to check the activity of EGFR molecules and that (epitope, steric, allosteric) interdependence was conserved after crosslinkage. For both SPR setups, negative controls were provided by the titration of the same mAbs as the immobilized ones. For the second SPR setup, the pair cetuximab/panitumumab provided a further negative control, since these antibodies cross-blocked each other in the first setup. Positive control for the second SPR setup was provided by the pairs that showed simultaneous binding in the first setup: matuzumab/cetuximab and matuzumab/nimotuzumab. These controls showed that EGFR remains active after crosslinking. However, steady state analysis of the binding curves obtained for the simultaneous binding of these pairs with crosslinked EGFR showed that mAb/EGFR affinity could be 100 times weaker after crossblocking (Table 4) and therefore the results obtained from the second setup remain qualitative.

Both assay orientations of the matuzumab/cetuximab pair yield SPR concentration-dependent binding curves – Fig. 14. The same effect is observed for the pair matuzumab/nimotuzumab. Steady state analysis of cetuximab and nimotuzumab binding to matuzumab-complexed EGFR yielded affinity values comparable to free EGFR affinity – Table 4. Matuzumab binding curves to cetuximab- or nimotuzumab-complexed EGFR yielded stronger affinity values than to free EGFR – Table 4. The matuzumab/EGFR binding is stronger in the presence of one other antibody binding simultaneously to EGFR. One probable explanation for this is the slower dissociation rate observed for the matuzumab/EGFR complex when cetuximab or nimotuzumab simultaneously bind EGFR, as observed in Fig. 14 in comparison to Fig. 8. The simultaneous binding of matuzumab/cetuximab and matuzumab/nimotuzumab to EGFR was confirmed by the second SPR setup, involving EGFR crosslinkage – Fig. 15. Both orientations of the cetuximab/panitumumab sandwich assay configuration showed no binding detectable upon titration of the second antibody, indicating that these antibodies crossblock each other upon EGFR binding – Fig. 14 and Fig. 15. The titrations cetuximab to nimotuzumab-bound EGFR and panitumumab to matuzumab- or nimotuzumab-bound EGFR yielded negative binding curves that follow a concentration dependency – Fig. 14.

Matuzumab titrated to panitumumab-bound EGFR delivers initially positive concentration-dependent binding curves that after a few seconds result in negative response. Reverse titrations delivered a similar but weaker effect, indicating asymmetry of the phenomenon. Analysis of the antibody combinations cetuximab/nimotuzumab, panitumumab/matuzumab, and panitumumab/nimotuzumab with the second SPR experimental setup involving EGFR crosslinking showed simultaneous binding of the two antibodies to EGFR – Fig. 15.

Table 4: Comparison of mAbs affinity to free, mAb-captured and mAb-crosslinked EGFR (SPR results).

mAb	…binding to EGFR	K_D (M)
Matuzumab	free	2×10^{-8}
	captured by cetuximab	8×10^{-9}
	captured by nimotuzumab	4×10^{-9}
	crosslinked to cetuximab (control)	5×10^{-8}
	crosslinked to nimotuzumab (control)	4×10^{-8}
	crosslinked to panitumumab	2×10^{-6}
Cetuximab	free	1×10^{-9}
	captured by matuzumab	4×10^{-9}
	crosslinked to matuzumab (control)	1×10^{-7}
	crosslinked to nimotuzumab	2×10^{-7}
Panitumumab	free	1×10^{-9}
	crosslinked to matuzumab	6×10^{-7}
	crosslinked to nimotuzumab	8×10^{-7}
Nimotuzumab	free	6×10^{-8}
	captured by matuzumab	9×10^{-8}
	crosslinked to matuzumab (control)	6×10^{-7}
	crosslinked to cetuximab	-
	crosslinked to panitumumab	-

Note: The results are from single experiments.

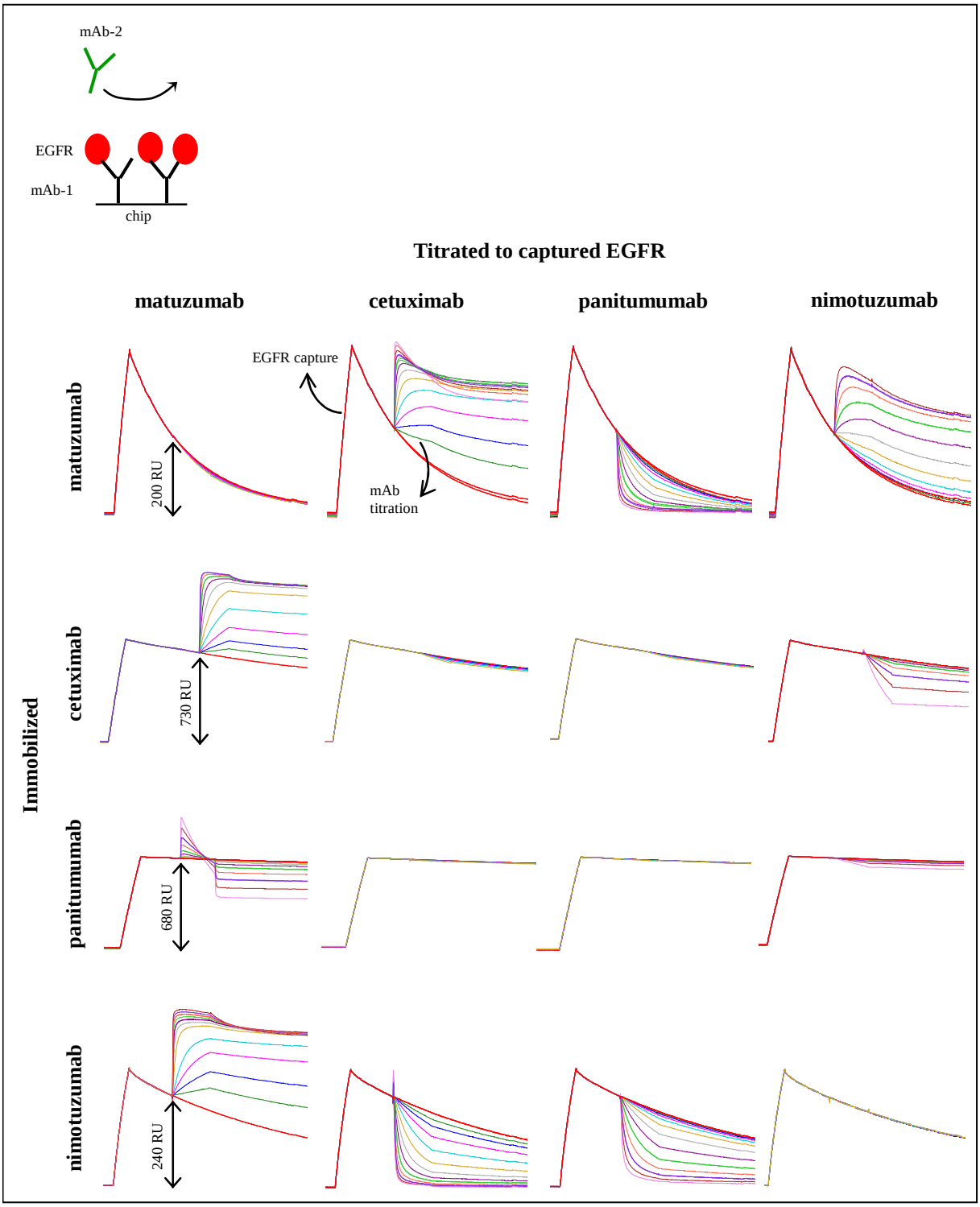

Fig. 14: SPR analysis of antibodies binding interdependence with transiently captured EGFR.

Each of the four anti-EGFR mAbs in study **(columns)** was titrated to biosensor surfaces where EGFR had been captured by each of the amine coupled mAbs **(rows)**. The sensorgrams shown have been subtracted by reference surfaces with the same level of immobilized mAb where EGFR has not been passed over. The level of EGFR capture in each mAb surface is shown in the figure. Concentrations of mAb solutions titrated were 1.5, 3, 6, 12, 25, 50, 100, 200, 400, 800, 1600 and 3200 nM. Shown results are representative of two independent measurements.

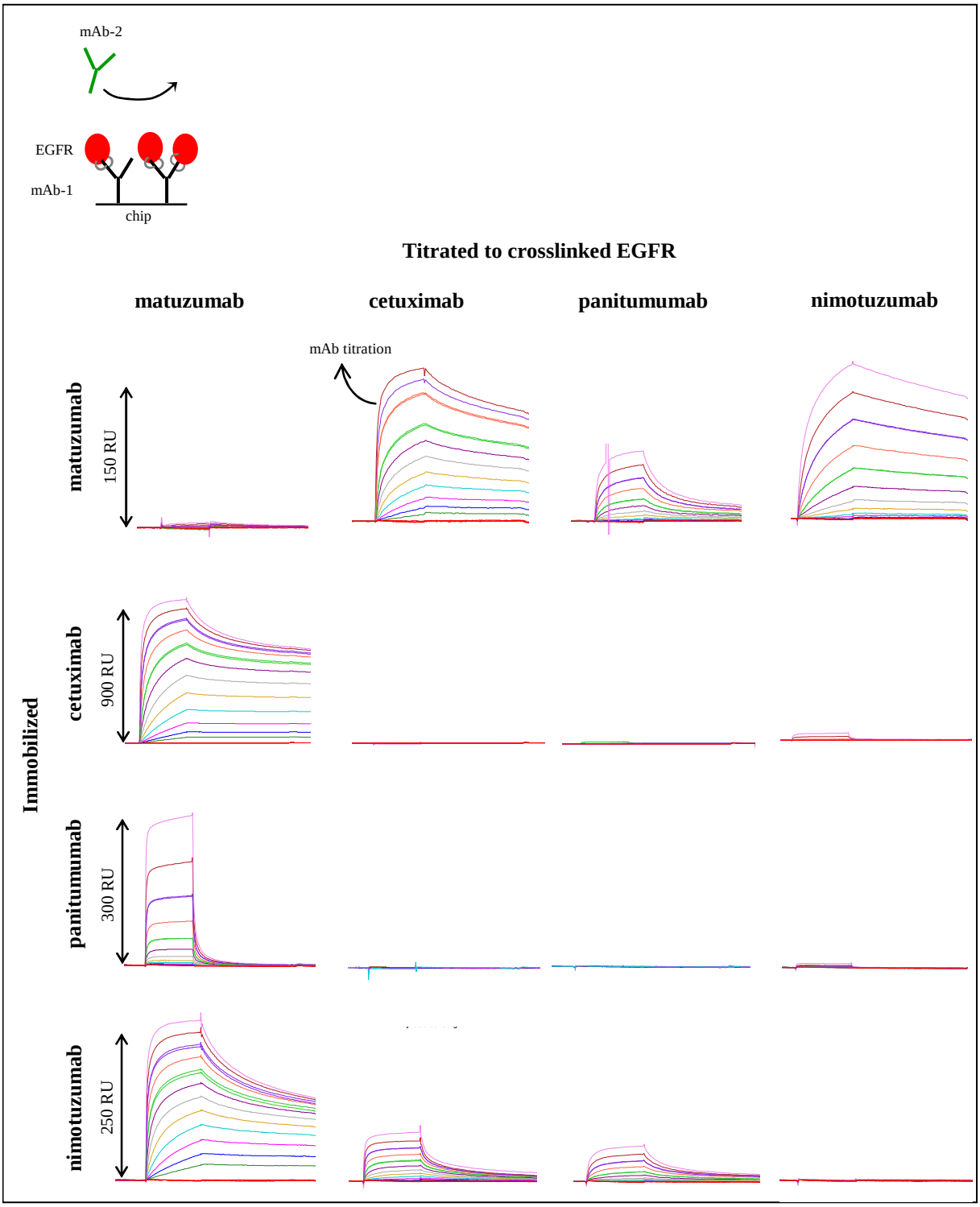

Fig. 15: SPR analysis of antibodies binding interdependence with covalently crosslinked EGFR.

Each of the four anti-EGFR mAbs in study **(columns)** was titrated to biosensor surfaces where EGFR had been crosslinked to each of the amine coupled mAbs **(rows)**. The sensorgrams shown have been subtracted by reference surfaces with the same level of immobilized mAb where EGFR has not been passed over. The level of mAb binding in each surface is shown in the figure. Concentrations of mAb solutions titrated were 1.5, 3, 6, 12, 25, 50, 100, 200, 400, 800, 1600 and 3200 nM. Shown results are representative of two independent measurements.

6.2 Characterization of EGFR interactions with isothermal titration calorimetry

6.2.1 Ligand and antibody titrations to EGFR

ITC analyses were performed by titrating (injecting) ligands or antibodies to the EGFR solution placed in the calorimeter cell. The differential power signals recorded (raw data), and the data integration points fitted to single-site binding isotherms are presented in Fig. 16. Titrations of ligands EGF and TGF-α into EGFR result in positive differential power signal, indicating that the reaction is endothermic (Fig. 16). The opposite is true for titrations of antibodies; here, negative differential power signal are indicative of exothermic reactions.

Isothermal titration calorimetry analysis delivers direct measurements of stoichiometry (N), equilibrium association constant and enthalpy of binding (ΔH). The results of single-site binding isotherms fitted to the data integrated points are presented in Fig. 16 to the respective ITC experiments. For comparison purposes with SPR results and since it is the most commonly used affinity measure, the equilibrium association constant was converted into equilibrium dissociation constant (K_D). Analyses have been normalized for binding sites to enable direct comparison between mAb (two binding sites), ligands (one binding site) and Fab fragments (one binding site) – see Fig. 17.

Stoichiometry results of ligands/EGFR were approx. 1 mol ligand /mol EGFR. The interactions of mAbs matuzumab, cetuximab and panitumumab yielded approx. 1 mol mAb binding sites /mol EGFR. Since antibody molecule has two binding sites, 1 mol mAb binding sites / mol EGFR translates to one mAb molecule binding two EGFR. The stoichiometry of nimotuzumab/EGFR interaction was atypical 1.4 mol mAb binding sites /mol EGFR, which translates into one mAb molecule binding between one and two EGFR.

The ligand EGF binds EGFR with stronger affinity than does TGF-α, although less enthalpy is absorbed by the system upon binding of TGF-α. Both ligands show weaker EGFR affinity than the four antibodies studied. Affinities of the strong binders cetuximab and panitumumab could not be delivered since the titration curves are too steep for reliable determination. All four mAbs/Fabs mean relatively similar enthalpy changes upon EGFR binding. The largest binding enthalpy is released upon EGFR interaction with matuzumab. Panitumumab

interaction, on the other hand, involves the smallest enthalpy release of the four antibodies studied.

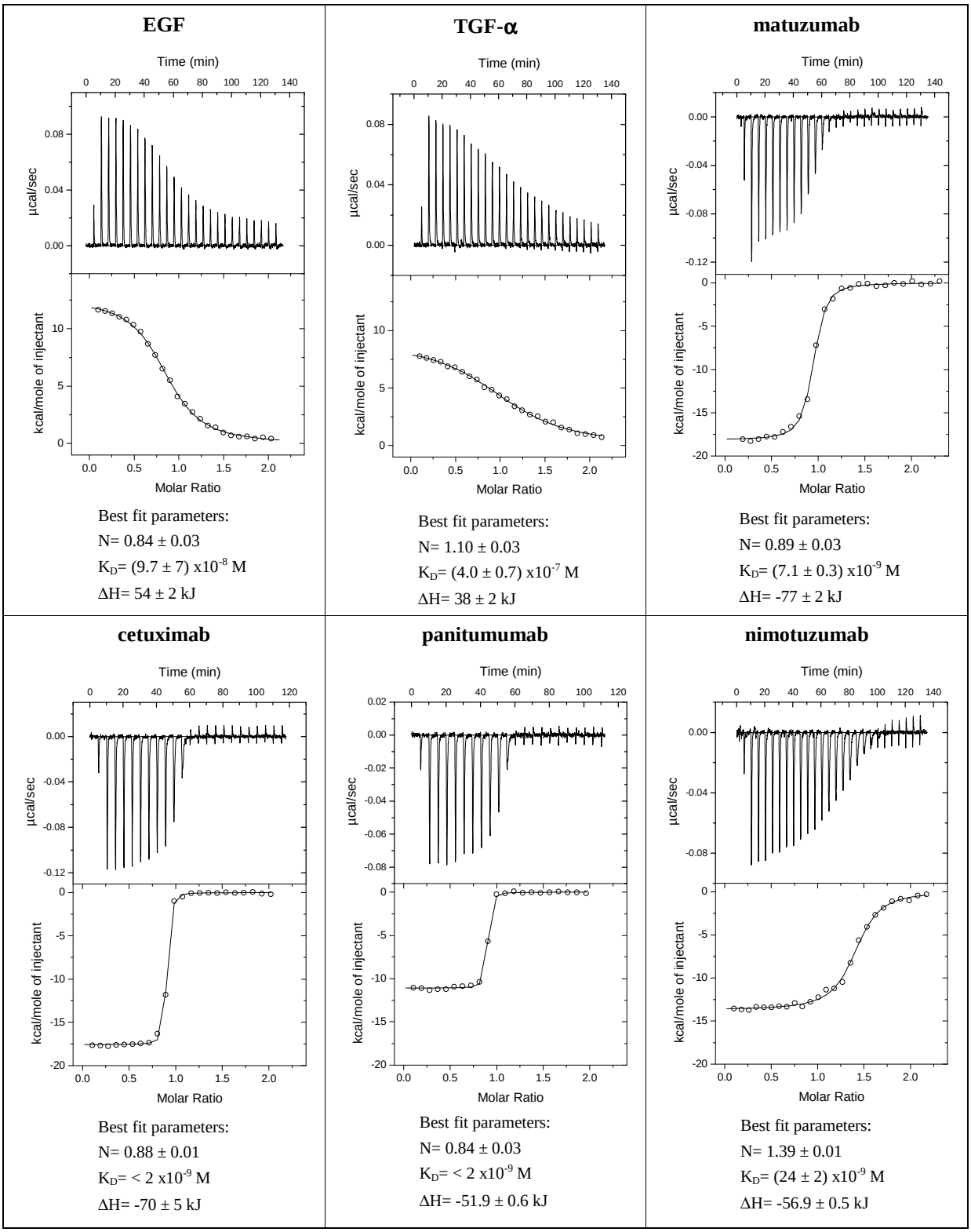

Fig. 16: ITC analysis of antibody/EGFR and ligand/EGFR interactions.

For each ligand and antibody studied, the ITC results shown are representative of two independent measurements at 25°C and the best fit parameters are the average of the two measurements. The **upper plot** represents the raw data or heat of binding following each injection; the **lower plot** shows the integrated results, where each point represents the normalized heat change for each injection.

6.2.2 Antibody Fab fragment titrations to EGFR

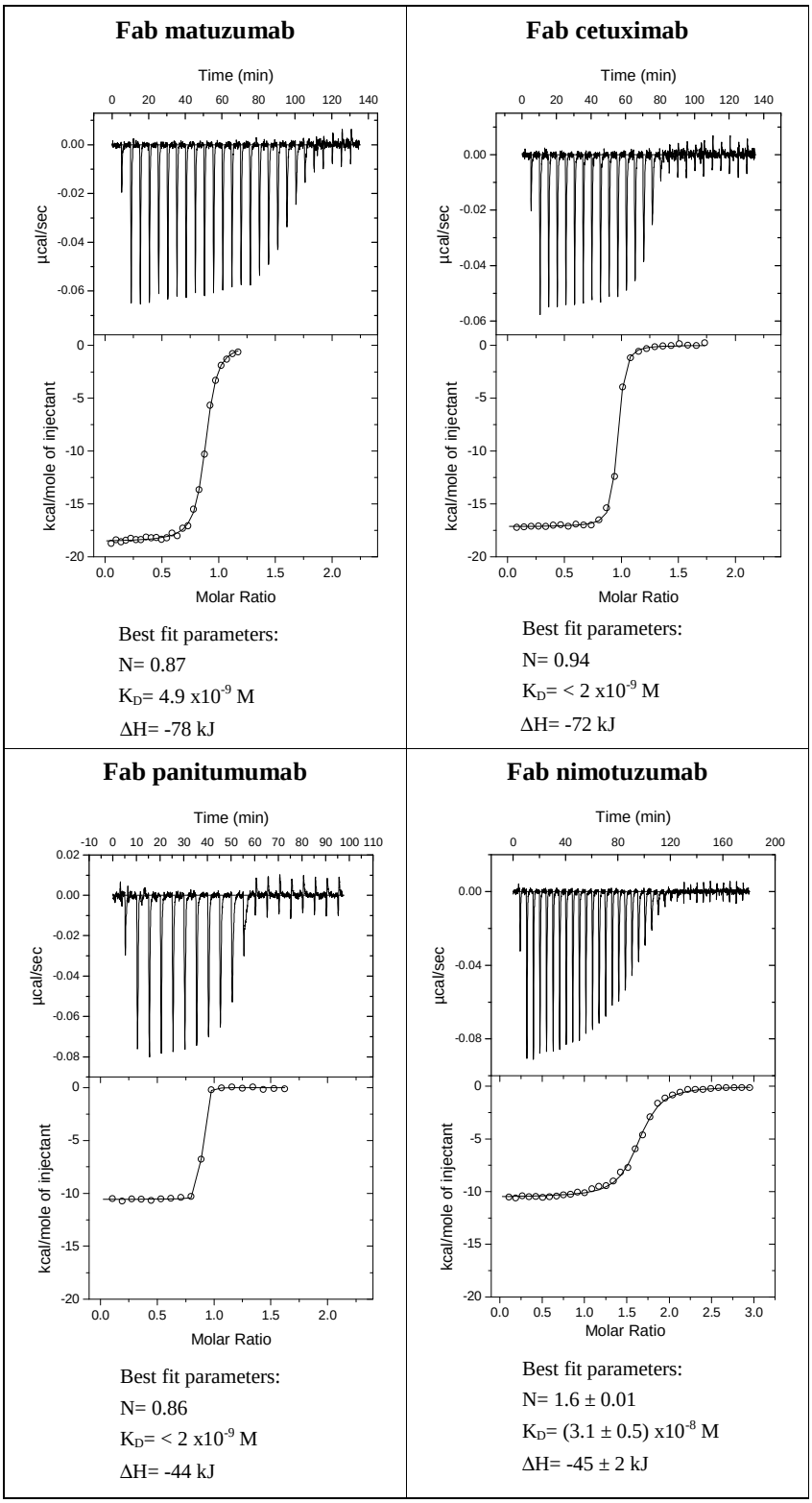

Fig. 17: ITC analysis of antibody Fab fragments/EGFR interactions.

For Fab matuzumab, Fab cetuximab and Fab panitumumab, the ITC results shown are single measurements at 25°C. For Fab nimotuzumab, the result is representative of two independent measurements at 25°C and the best fit parameters are the average of the two measurements. The **upper plot** represents the raw data or heat of binding following each injection; the **lower plot** shows the integrated results, where each point represents the normalized heat change for each injection.

Calorimetric analyses were performed by titrating (injecting) antibody Fab fragments to the EGFR solution placed in the calorimeter cell. Results are shown in Fig. 17. Affinity and enthalpy results are comparable to the ones obtained for the whole antibodies, thus indicating that the two antibody binding sites bind to EGFR independently. The interactions with matuzumab, cetuximab and panitumumab Fab fragments delivered consistent stoichiometric results of approx. 1 mol Fab /mol EGFR. Nimotuzumab Fab stoichiometric result was atypical 1.6 mol Fab /mol EGFR, which is coherent with the results obtained for the antibody – see Fig. 16.

6.2.3 Temperature dependence of antibody/EGFR binding enthalpy

A method was developed that involved aliquot injection at different temperatures in the same titration, with temperature stabilization time before sample injections (Fig. 18). This allowed important material savings, since binding enthalpy was obtained for four different temperatures (20°C, 25°C, 29°C and 33°C) with the material needed for one titration. Binding enthalpies determined at each of the temperatures are represented by open circles (○) in the plots ΔH versus T in Fig. 18. Full titrations were performed for matuzumab and cetuximab at 20°C, 25°C and 33°C. The binding enthalpies obtained from full titrations are represented by closed circles (●) in the plots ΔH versus T in Fig. 18. As can be seen for matuzumab and cetuximab, the enthalpy values obtained by the temperature change titration correlate well with the values obtained from full titrations. As seen in Fig. 18, matuzumab, panitumumab and nimotuzumab interactions to EGFR are associated with a negative dependence of enthalpy with the temperature. The change in heat capacity $\Delta Cp° = \delta(\Delta H)/\delta T$ is obtained from the slopes of plots ΔH versus T. Results of linear regression to the data shown in Fig. 18 are summarized in Table 5. A negative change in heat capacity was determined for matuzumab, panitumumab and nimotuzumab respectively. As for cetuximab, no clear temperature dependence of binding enthalpy could be established, due to high scattering of the data points.

Table 5: Heat capacity change of antibody/EGFR binding.

Antibody	Regression R^2	ΔCp° (kJ/mol/K)
Matuzumab	0.9757; 0.9877	-1.7 ± 0.3
Cetuximab	0.8537; 0.0637	-0.3 ± 0.5
Panitumumab	0.946	-0.83 ± 0.14
Nimotuzumab	0.6887	-1.3 ± 0.6

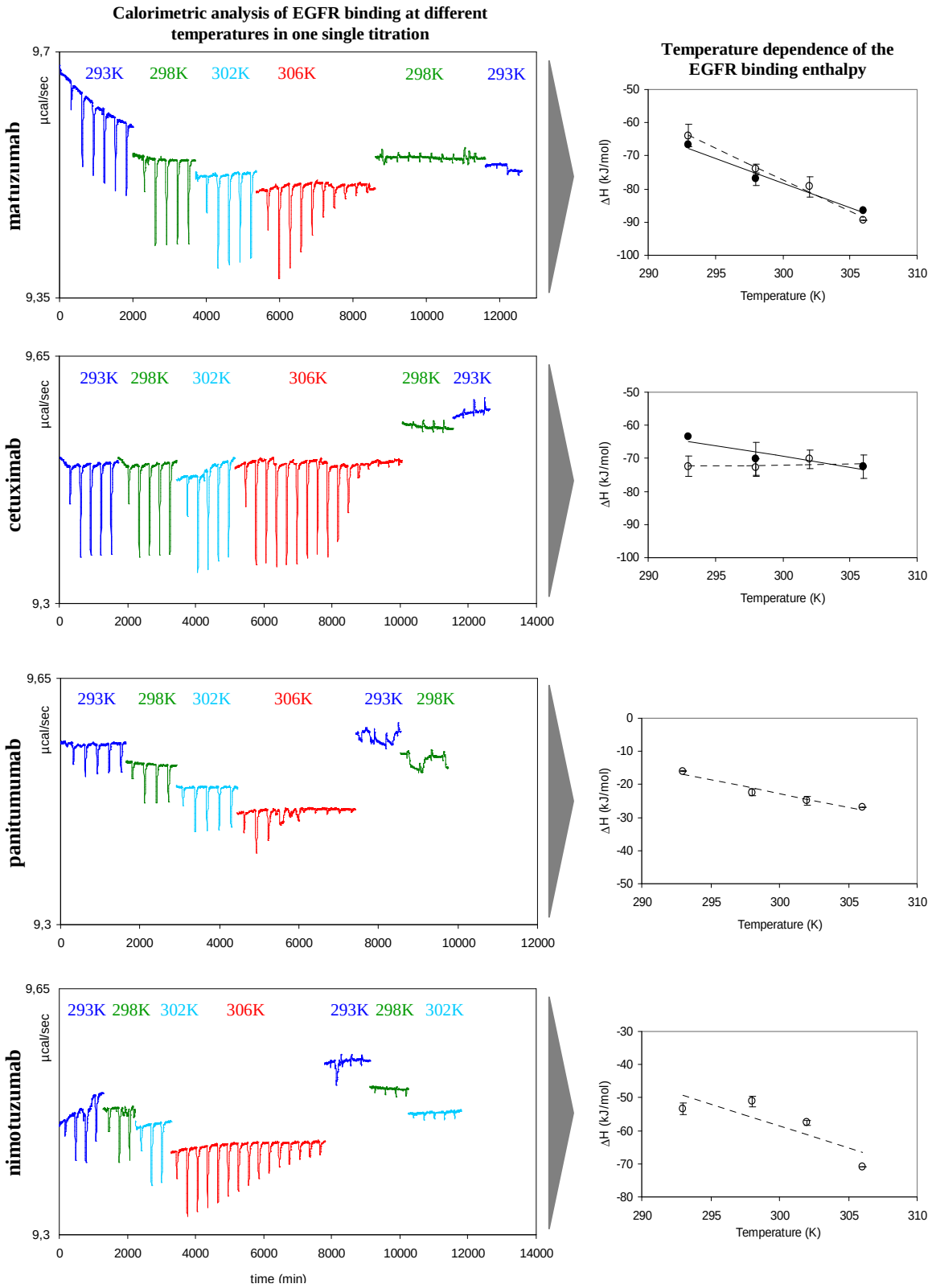

Fig. 18: Temperature dependence of antibody/EGFR binding enthalpy.

Binding enthalpy at different temperatures was measured in one single calorimetric titration **(left hand plots)** and is represented in plots of ΔH vs. Temperature by ○ **(right hand plots)**. Error bars indicate the standard deviation on at least two ITC injections. For matuzumab and cetuximab, full titrations were also done at 20°C and 33°C (293K and 306K); these are represented on the right hand plots by ●.

6.2.4 Binding interdependence of antibody combinations to EGFR

To investigate the interdependence of antibody combinations binding to EGFR, antibodies were titrated to EGFR solutions containing saturating molar amounts of another antibody. Calorimetric titrations of antibodies to different mAb combinations are shown in Fig. 19. Raw data were left out for simplification and the fitted models of titrations to mAb-saturated EGFR were overlapped with titrations to free EGFR. A closer look to Fig. 19 shows unchanged stoichiometry (molar ratio in the titration inflection point) observed for titrations to bound EGFR of mAb combinations matuzumab/cetuximab (first row) and matuzumab/nimotuzumab (second row). This means that interaction of one of these antibodies with mAb-complexed EGFR is thermodynamically identical to interaction with free EGFR. The affinity (slope in the titration inflection point) calculated in experiments of simultaneous binding is comparable, or enhanced in case of matuzumab, to the affinity of free EGFR binding. The calculated binding enthalpy (titration curve amplitude) of matuzumab or cetuximab titrated to bound EGFR is somewhat lower than to free EGFR. However, this is compensated by a lower entropic penalty resulting in overall comparable binding strength. Additionally, the titration of a matuzumab/cetuximab antibody mixture to free EGFR (Fig. 19) resulted in a stoichiometry of two mAb binding sites per EGFR molecule, in accordance with the simultaneous binding of matuzumab and cetuximab to EGFR. Here again, a lower enthalpic contribution seems to be compensated by a lower entropic penalty, resulting in comparable average mAb/EGFR affinity. ITC titrations of panitumumab to matuzumab- (third row) or nimotuzumab-saturated EGFR (fourth row in Fig. 19) resulted in the detection of positive enthalpy changes. Overlay of the binding isotherms obtained from titrations of mAbs to free EGFR shows that the positive enthalpy change measured corresponds to the difference between the negative enthalpy changes of matuzumab and panitumumab upon EGFR binding. This suggests that upon addition of panitumumab, matuzumab or nimotuzumab molecules previously bound to EGFR are substituted by panitumumab molecules. No measurable ITC signal was detected upon interdependence titrations of the antibody combinations cetuximab/nimotuzumab and panitumumab/cetuximab (fifth row).

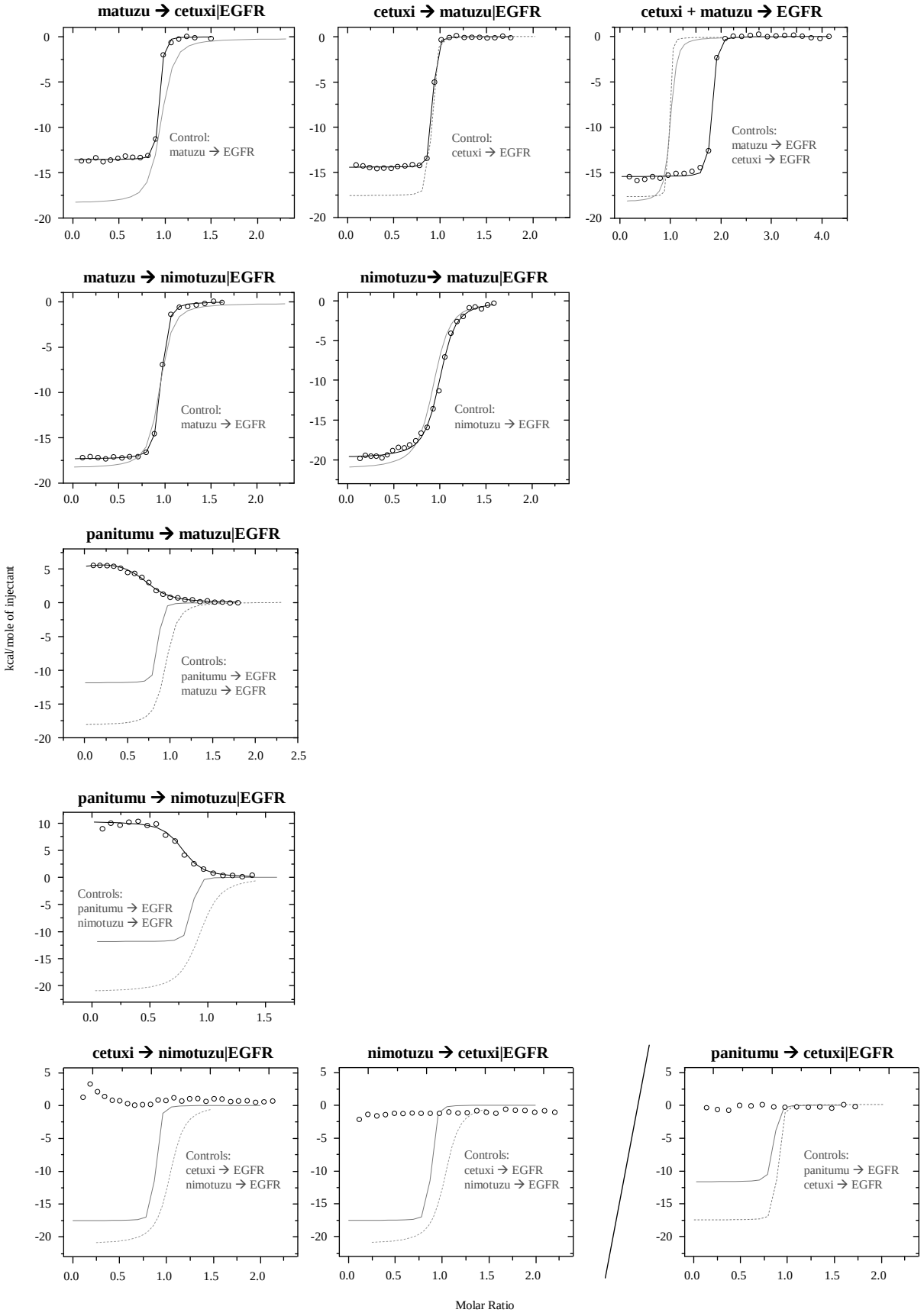

Fig. 19: ITC analysis of antibodies binding interdependence.

Binding to EGFR was tested for the different combinations of therapeutic antibodies. Over each plot is described the respective experiment, e.g. matuzu → cetuxi|EGFR means matuzumab titrated to cetuximab-saturated EGFR. Raw data were left out for simplification. Isotherms of ITC analysis to free EGFR are shown in overlay. The one-sites model was fitted to all titrations shown except for the titrations panitumu → matuzu|EGFR and panitumu → nimotuzu|EGFR, where competition model was fitted. The results are from single experiments.

6.3 Characterization of EGFR interactions with static light scattering

6.3.1 Size of complexes formed in antibody/EGFR mixtures

Static light scattering was used to determine the size of complexes formed in mixtures of EGFR with anti-EGFR antibodies matuzumab, cetuximab, nimotuzumab and panitumumab. Samples of EGFR and mAb controls as well as EGFR/mAb mixtures with different molar ratios were injected into the SEC-LS/UV/RI system separately. Representative chromatograms of EGFR/mAb mixtures and respective controls are shown in Fig. 20. The red line in the chromatograms represents the average molecular weight detection of eluting molecules, calculated by static light scattering analysis. The black line is the refractive index detection, directly proportional to protein concentration. Molecular weight results are summarized in Table 6. In a first approach, the molecules used were characterized. Apparent molecular weights of 97,000, 160,000, 162,000, 154,000 and 154,000 Da were measured for EGFR, matuzumab, cetuximab, panitumumab and nimotuzumab, respectively. The molecular weight obtained for EGFR indicates that the receptor exists as a monomer in solution under the conditions used. Primary structure information reveals a predicted protein molecular weight of approx. 70,000 for EGFR and a total molecular weight, including glycosylation of 105,000 (Weber *et al.*, 1984; Ullrich *et al.*, 1984; Stroop *et al.*, 2000). Molecular weights obtained for the mAbs are in agreement with typical sizes for antibodies of the IgG type (Stanfield and Wilson, 2009). The molecular weight distribution of peaks in control chromatograms is horizontal (Fig. 20) indicating size monodispersity of the eluting molecules. The calculated molecular weights of EGFR and mAb controls are all in agreement with predicted and published results, showing validity of the results and applicability of the method.

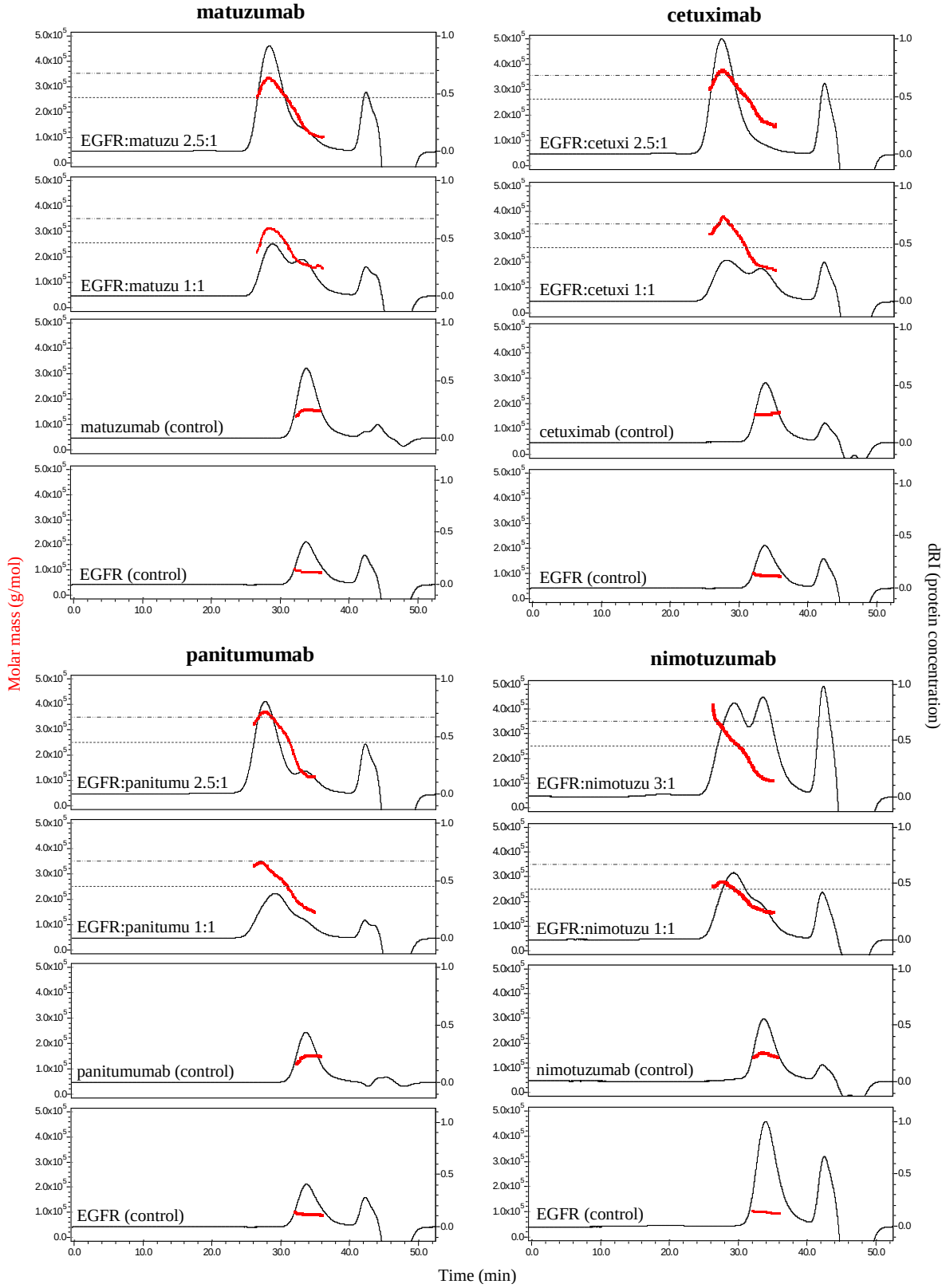

Fig. 20: Light scattering analysis of mixtures of mAb/EGFR mixtures.

Controls and mixtures were injected separately into the SEC-LS/UV/RI system. Molecular weight (red line) was determined by light scattering using peak protein concentration calculated by refractive index detection (black line). Heterodimer and heterotrimer sizes were predicted using EGFR and mAb calculated molecular weights and were marked in the chromatograms of mixtures by ·····and ·····respectively. The results are from single experiments. The results are from single experiments.

Table 6: Summary of light scattering results obtained for mAb/EGFR mixtures and controls.

Mixture	Molar ratio	Molecular weight of first eluting species (Da)
EGFR (control)	-	97,000
Matuzumab (control)	-	160,000
Cetuximab (control)	-	162,000
Panitumumab (control)	-	154,000
Nimotuzumab (control)	-	154,000
EGFR:matuzumab	1:1	315,000
	2.5:1	340,000
EGFR:cetuximab	1:1	380,000
	2.5:1	380,000
EGFR:panitumumab	1:1	350,000
	2.5:1	370,000
EGFR:nimotuzumab	0.5:1	250,000
	1:1	258,000
	2:1	310,000
	2.5:1	320,000
	3:1	340,000

Note: The results are from single experiments. However, their validity was confirmed by additional analysis of mAb/EGFR mixtures at different molar ratios and/or using a different SEC column (data not shown).

The mixtures of EGFR with mAbs all resulted in peaks eluting earlier than the mAb or EGFR controls (Fig. 20). This indicates that complexes were formed in all mixtures. The molecular weight distribution of peaks in chromatograms of mixtures is not constant over peak elution (RI detection). This is indicative of peak polydispersity caused by poor chromatographic resolution achieved with the SEC column used. Poor chromatographic resolution is also indicated by overlapping elution peaks seen from the RI detection. Nevertheless, the molecular weight maximum coincides with the maximum signal for protein elution (RI maximum). It should be kept in mind that the molecular weight detection performed delivers an average value for the molecules eluting at a given moment. In mAb/EGFR mixtures with EGFR excess, maximum average molecular weight values of 340,000, 380,000 and 370,000 Da were reached. Complex molecular sizes are consistent with the predicted sizes of heterotrimers (one mAb and two EGFR molecules), calculated using the molecular weight results of controls. Therefore, the bivalent EGFR binding of the antibodies studied is corroborated.

The average molecular weight of complexes formed in EGFR/nimotuzumab mixtures is lower in comparison with the other three mAbs. At an EGFR-to-nimotuzumab ratio of 1, the maximum of average molecular weight corresponds approximately to the predicted heterodimer size, while matuzumab, cetuximab and panitumumab correspondent mixtures

deliver average molecular weights well above this value. In the case of cetuximab and panitumumab, heterotrimer sizes are already detected. The maximal average molecular weight of EGFR/nimotuzumab complexes increases with increasing EGFR-to-mAb ratios of 2, 2.5 and 3 (Table 6). An increase in the peak polydispersity was also observed in such mixtures, as can be seen in Fig. 20 for the highest ratio studied, 3. The average molecular weight detection in this chromatogram indicates a strongly polydisperse sample; average molecular weight detection does not reach a stable (maximum) level. However, high molecular weight complexes could be observed, especially at the front of the peak where the molecular weight detection line reaches the heterotrimer size. The results indicate that heterotrimers exist in lower concentration than observed for matuzumab, cetuximab and nimotuzumab. Existing heterotrimers probably co-elute with heterodimers, free EGFR and maybe even free mAb molecules. That explains the lower average molecular weight and the polydispersity of the sample.

6.3.2 Size of complexes formed in antibody Fab fragment/EGFR mixtures

Representative chromatograms of EGFR/Fab fragments mixtures and the respective controls are shown in Fig. 21 and calculated molecular weights are summarized in Table 7. The molecular weights of the fragments were calculated as 47,000, 51,000, 47,000 and 55,000 for matuzumab, cetuximab, panitumumab and nimotuzumab Fab respectively; all are in agreement with typical Fab fragments sizes. The calculated molecular weights of EGFR and Fab molecules were used to predict the sizes of expected eluting complexes – heterodimers – represented in the chromatograms of mixtures by horizontal lines (Fig. 21). The molecular weight distribution of the first eluting peak of Fab/EGFR mixtures attained the 145,000 in the case of Fab matuzumab. As for the Fabs cetuximab, panitumumab and nimotuzumab, maximal sizes 140,000, 165,000 and 150,000 were attained. Mixtures with molar excess of Fab fragments were analyzed in order to test the hypothesis of various Fabs binding to one EGFR molecule (e.g. antibody bivalency). The results indicate that all Fab fragments form heterodimer complexes with EGFR. Trimers were not detected.

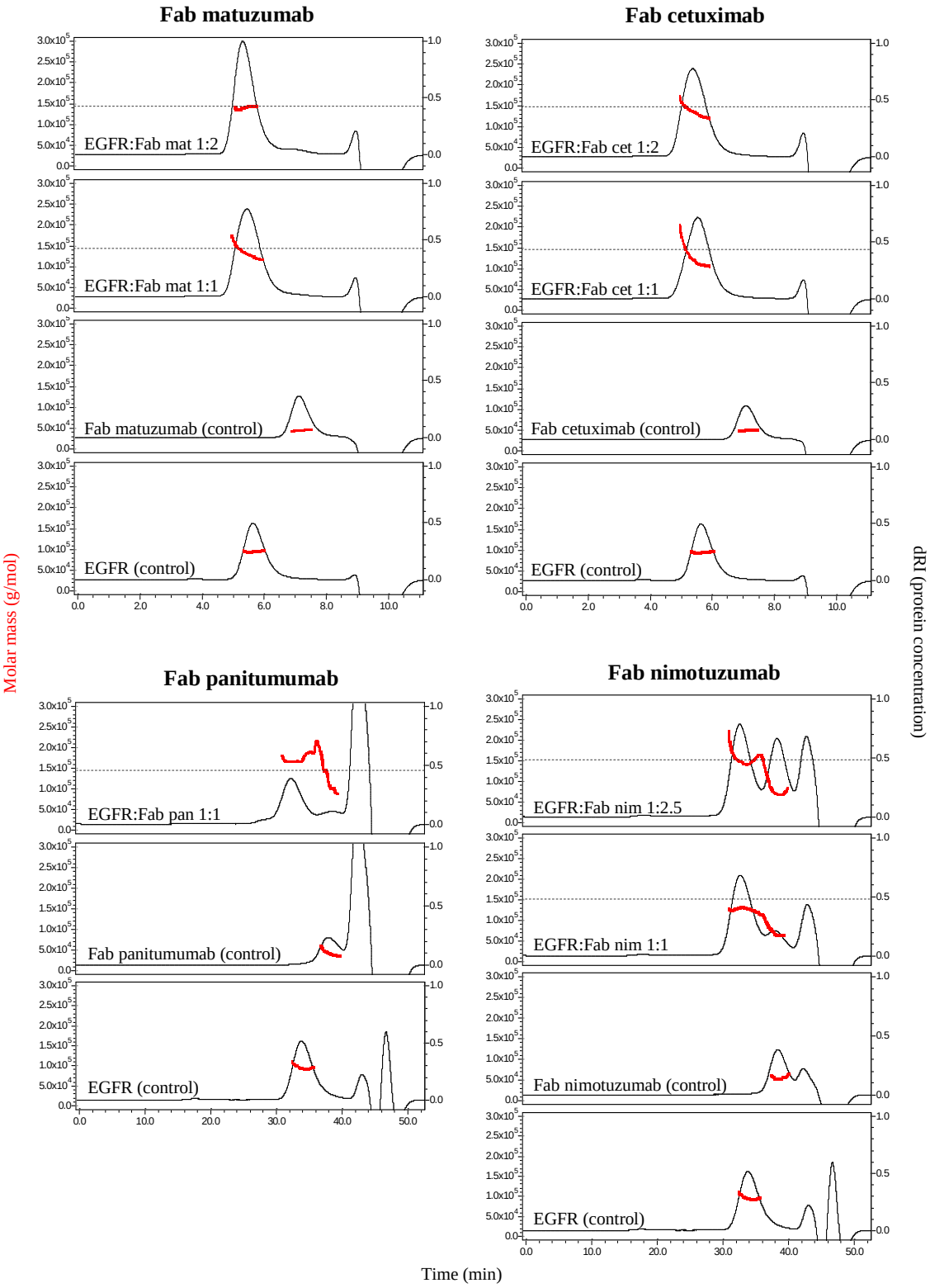

Fig. 21: Light scattering analysis of mixtures of Fab fragment/EGFR mixtures.

Controls and mixtures were injected separately into the SEC-LS/UV/RI system. Molecular weight (red line) was determined by light scattering using peak protein concentration calculated by refractive index detection (black line). Heterodimer sizes were predicted using EGFR and Fab calculated molecular weights and were marked in the chromatograms of mixtures by ·····. The results are from single experiments.

Table 7: Summary of light scattering results obtained for Fab fragment/EGFR mixtures and controls.

Mixture	Molar ratio	Molecular weight of first eluting species (Da)
EGFR (control)	-	97,000
Fab matuzumab (control)	-	47,000
Fab cetuximab (control)	-	51,000
Fab panitumumab (control)	-	47,000
Fab nimotuzumab (control)	-	55,000
EGFR:Fab matuzumab	1:1	140,000
	1:2.5	145,000
EGFR:Fab cetuximab	1:1	125,000
	1:2.5	140,000
EGFR:Fab panitumumab	1:1	165,000
EGFR:Fab nimotuzumab	1:1	130,000
	1:2.5	150,000

Note: The results are from single experiments. However, their validity was confirmed by additional analysis of mAb/EGFR mixtures at different molar ratios and/or using a different SEC column (data not shown).

6.3.3 Size of complexes formed in mixtures of EGFR with antibody combinations

Static light scattering was applied as orthogonal method to corroborate the observations of simultaneous binding of distinct antibodies to EGFR seen in Fig. 14 and Fig. 19. Samples of EGFR and mAb combinations with different molar ratios were injected into the SEC-LS/UV/RI system separately and the sizes of complexes formed in such mixtures were calculated. Representative chromatograms of EGFR/matuzumab/cetuximab and EGFR/matuzumab/nimotuzumab mixtures are shown in Fig. 22, together with the chromatograms obtained for samples with only one type of antibody. Molecular weights calculated for EGFR, matuzumab, cetuximab and nimotuzumab (Table 8) were used to predict the size of hypothetical quatromer complexes (formed by two EGFR and two different mAb molecules). Quatromer complexes are the simplest complexes consistent both with the bivalent EGFR/antibody binding and the simultaneous binding of different antibody molecules. Predicted quatromer sizes were represented in the chromatograms of heterogeneous mAb mixtures by horizontal lines (Fig. 22). The maximum average molecular weight of heterogeneous mAb mixtures corresponds to the predicted size of heterogeneous quatromers. Table 8 summarizes the SLS results of all the antibody combinations tested. Complexes formed in mixtures of EGFR with matuzumab/cetuximab and matuzumab/nimotuzumab reached maximal molecular weights of 550,000 and 500,000 respectively. Mixtures formed with EGFR and the antibody combinations

matuzumab/panitumumab, cetuximab/panitumumab and panitumumab/nimotuzumab yielded maximal average molecular weights of 370,000, 350,000 and 350,000, respectively.

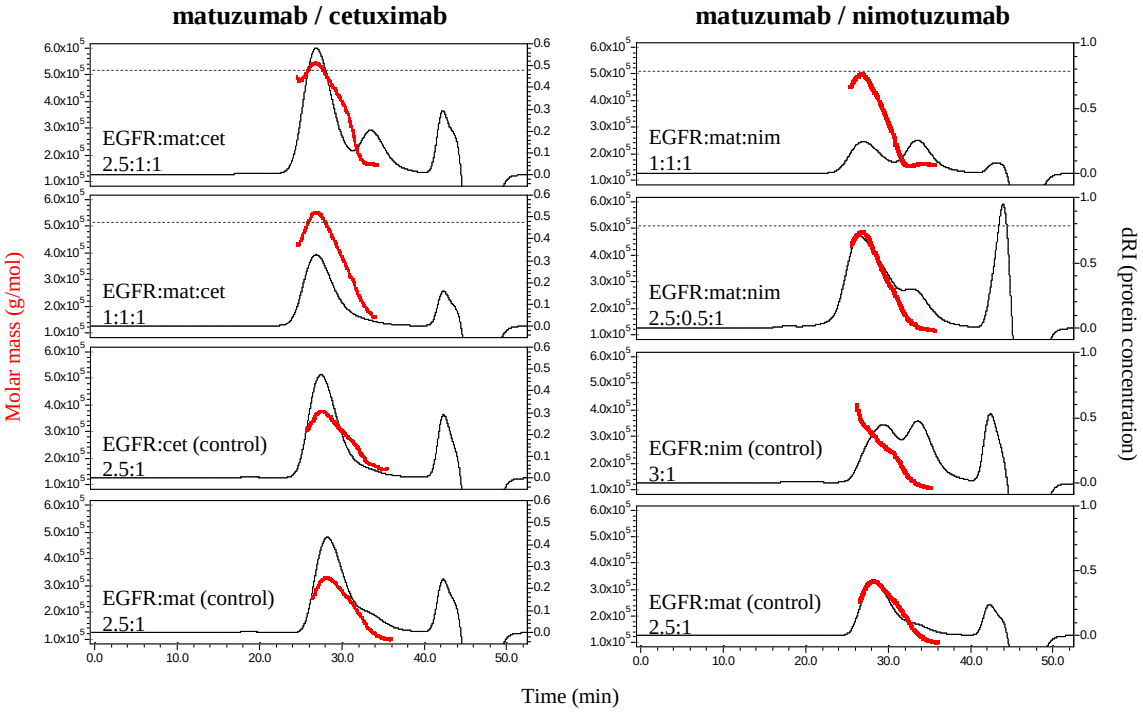

Fig. 22: Light scattering analysis of mixtures of EGFR and combinations of mAbs.

Controls and mixtures were injected separately into the SEC-LS/UV/RI system. Molecular weight (red line) was determined by static light scattering using peak protein concentration calculated by refractive index detection (black line). Sizes were predicted for heteroquatromers using EGFR and mAb calculated molecular weights (Table 1) and were marked in the chromatograms by ·····. The results are from single experiments.

Table 8: Summary of light scattering results obtained for EGFR and mAb mixtures.

Mixture	Molar ratio	Molecular weight of first eluting species (Da)
EGFR:matuzumab (control)	2.5:1	340,000
EGFR:cetuximab (control)	2.5:1	380,000
EGFR:panitumumab (control)	2.5:1	370,000
EGFR:nimotuzumab (control)	3:1	340,000
EGFR:matuzumab:cetuximab	2.5:0.5:1	500,000
	2.5:1:0.5	500,000
	1:1:1	550,000
	2.5:1:1	550,000
EGFR:matuzumab:panitumumab	2.5:0.5:1	370,000
	2.5:1:0.5	350,000
	1:1:1	360,000
	2.5:1:1	360,000
EGFR:matuzumab:nimotuzumab	2.5:0.5:1	490,000
	2.5:1:0.5	410,000
	1:1:1	500,000
EGFR:cetuximab:panitumumab	2.5:0.5:1	350,000
	2.5:1:0.5	340,000
	1:1:1	320,000
EGFR:panitumumab:nimotuzumab	2.5:0.5:1	330,000
	2.5:1:0.5	350,000
	1:1:1	350,000

Note: The results are from single experiments.

7 DISCUSSION

7.1 Antibodies bind EGFR bivalently

Antibodies are bivalent molecules; they have two identical binding sites situated in the two Fab regions. However, the binding of both antibody arms may be dependent on steric allowance. This is especially true for big antigens, such as EGFR. Two different possibilities were assumed for the stoichiometry of EGFR/mAb complexes:

- stoichiometry 1:1, corresponding to the binding of one EGFR molecule to each mAb molecule and the consequent formation of a heterodimer;
- stoichiometry 2:1, corresponding to the binding of two EGFR molecules to each mAb molecule and the consequent formation of a heterotrimer.

As for the complexes formed between EGFR and Fab fragments, a stoichiometry 1:1 was expected.

Table 9: Stoichiometry results from ITC analysis of mAb/EGFR and Fab fragment/EGFR.

mAb/Fab titrated to EGFR	Stoichiometry, N
Matuzumab	0.9 mol mAb binding sites / mol EGFR
Cetuximab	0.9 mol mAb binding sites / mol EGFR
Panitumumab	0.8 mol mAb binding sites / mol EGFR
Nimotuzumab	1.4 mol mAb binding sites / mol EGFR
Fab matuzumab	0.9 mol Fab / mol EGFR
Fab cetuximab	0.9 mol Fab / mol EGFR
Fab panitumumab	0.9 mol Fab / mol EGFR
Fab nimotuzumab	1.6 mol Fab / mol EGFR

Note: mAb results are the average of the two ITC measurements (see Fig. 16); Fab results are from single measurements (see Fig. 17), except Fab Nimotuzumab result, which is the average of the two ITC measurements.

Stoichiometric evidence obtained by ITC confirmed the bivalent binding of matuzumab, cetuximab and panitumumab (Table 9). For these mAbs, isothermal titration calorimetry analysis yielded stoichiometry values of approx. 1 mol mAb binding sites /mol EGFR, corroborating the stoichiometry EGFR:mAb 2:1. Small deviations to N=1 are usually observed with ITC as a result of errors in the concentration determination of the protein

solutions used. The total protein concentration of the solutions used for the study was determined by UV measurements at 280 nm. This method requires knowing the extinction coefficient of the molecules present in solution. The extinction coefficient can be estimated by the Edelhoch method (Edelhoch, 1967) when the primary structure of the protein is known. This was done for EGFR, matuzumab and cetuximab, whose primary structures are known. In the case of panitumumab and nimotuzumab, where primary structures have not been published, the nominal protein concentration given in the vial was assumed. For these two antibodies, a typical extinction coefficient for antibodies of the IgG type was used alternatively for protein determination. Even if estimated by the Edelhoch method, protein extinction coefficients are rarely known better than 5%, and are usually worse (Cooper, 2001). Accuracy problems in protein determination, resulting either from poor estimated extinction coefficients, or from limitations of the UV measurement technique (Cooper, 2001), are a common source of small errors in stoichiometry (N) measured by ITC. These are probably the cause for the deviations from N=1 observed for matuzumab, cetuximab and panitumumab. The stoichiometric results observed for nimotuzumab will be discussed in the next section (section 7.2).

Bivalent binding of matuzumab, cetuximab and panitumumab were confirmed by SLS studies, where mixtures of EGFR with each of the three mAbs yielded average molecular weights of complexes formed that agreed with the predicted size of heterotrimers (see Fig. 20 and Table 6). These results indicated that heterotrimers were already present when the EGFR-to-mAb molar ratio was as low as 1. Bivalent binding of matuzumab and cetuximab was also confirmed by saturation experiments of EGFR on SPR surfaces where controlled levels of matuzumab and cetuximab had been captured (see Fig. 12). These results show that the EGFR saturation level is well above the theoretical binding level expected for a monovalent interaction, almost reaching the theoretical binding level expected for a bivalent interaction.

Cetuximab and matuzumab bivalency has previously been shown by gel electrophoresis separation of crosslinked cell lysates (Fan *et al.*, 1994; Yoshida *et al.*, 2008). Bivalency of panitumumab is, to the best of my knowledge, reported in this study for the first time. Bivalency, and the consequent capacity to form antibody-mediated EGFR dimers, is believed to play a critical role in the anti-tumor efficacy of EGFR antibodies (Rehder *et al.*, 2008; Rudnick and Adams, 2009). Since antibody-antigen binding is a reversible and concentration dependent association, bivalent binding of mAb to EGFR has advantages for blockade of receptor activity. If one arm of the bivalent antibody temporarily dissociates from an EGFR,

the other arm may still adhere to another receptor on the cell surface, allowing the dissociated arm to reassociate (Fan *et al.*, 1994). This effect is known as avidity and it reduces drastically the dissociation of antibodies from the surface of tumor cells. Moreover, bivalency is responsible for a higher rate of EGFR endocytosis and consequent down-regulation (Friedman *et al.*, 2005).

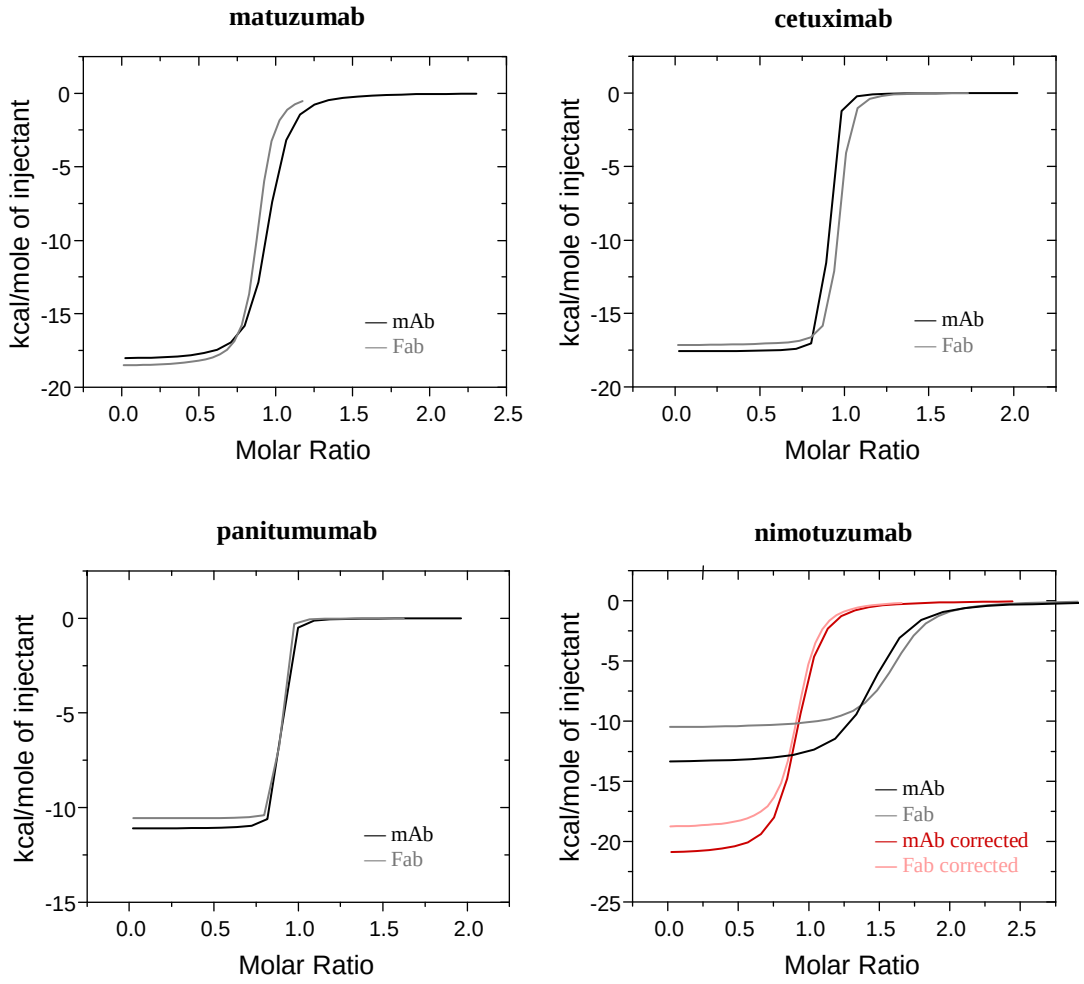

Fig. 23: Overlays of ITC mAb and Fab /EGFR isotherms.
Titration raw data were left out for simplification; the isotherms presented are the result of one-sites model fits. In reddish colour are presented the titrations of mAb and Fab nimotuzumab with corrected concentration to yield stoichiometry 1 mol mAb binding site and 1 mol Fab /EGFR (see explanation in section 7.2). mAb measurements were repeated twice (see Fig. 16); Fab results are from single measurements (see Fig. 17), except Fab Nimotuzumab result, which was repeated twice.

Despite a relatively large receptor size, the observed antibody bivalency demonstrates that there is no steric hindrance between EGFR molecules binding to both arms of the same antibody. Moreover, studies of EGFR binding to Fab fragments, indicate that the binding events occurring in both antibody arms are independent. Kinetic/affinity analysis performed with optimal configuration surface plasmon resonance assays delivered very similar results for the whole antibodies and the respective Fab fragments (see Fig. 8). Also isotherms fitting

to ITC analysis of mAb or Fab binding to EGFR are almost indistinguishable, as seen in Fig. 23 for the four antibodies in study.

7.2 Nimotuzumab is partly unfunctional

ITC-originated stoichiometry results for nimotuzumab/EGFR interaction (Table 9) apparently indicate a mixed stoichiometry of EGFR:mAb binding between 1:1 and 2:1 and a mixed stoichiometry of EGFR:Fab binding between 1:1 and 2:1. The different assembly state hypotheses and corresponding expected stoichiometry for mAb/EGFR and Fab/EGFR are shown in Fig. 24. For the interactions of matuzumab, cetuximab and panitumumab with excess EGFR, hypothesis C and E were validated (see section 7.1). The validity of the hypothesis presented and explanations for nimotuzumab atypical results are discussed in this section.

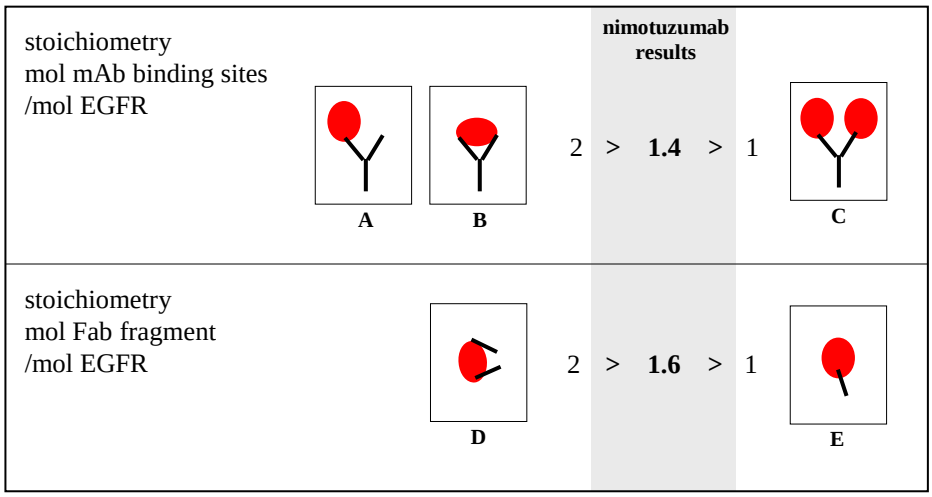

Fig. 24: Representation of the different possible assembly states for mAb/EGFR and Fab/EGFR complexes.

For mAb/EGFR interaction, three assembly states were considered as possible: **A)** Binding of only one antibody arm to one EGFR molecule, while the other arm is free – corresponding stoichiometry EGFR:mAb 1:1, or mol mAb-binding-sites /mol EGFR = 2; **B)** Binding of both antibody arms to only one EGFR molecule – corresponding stoichiometry EGFR:mAb 1:1, or mol mAb-binding-sites /mol EGFR = 2; **C)** Binding of one antibody to two EGFR molecules – corresponding stoichiometry EGFR:mAb 2:1, or mol mAb-binding-sites /mol EGFR = 1. For Fab/EGFR interaction, two assembly states were considered as possible; **D)** Binding of one Fab fragment to two EGFR molecules – corresponding stoichiometry EGFR:Fab 1:2, or mol Fab fragment /mol EGFR = 2; **E)** Binding of one Fab fragment to one EGFR molecule – corresponding stoichiometry EGFR:Fab 1:1, or mol Fab fragment /mol EGFR = 1.

Hypotheses B and D would correspond to nimotuzumab having two different binding sites, i.e., the antibody would be bi-specific. However, bispecificity is not described in the literature; on the contrary, nimotuzumab is reported as an IgG1 type humanized antibody

(Boland and Bebb, 2009). Light scattering analysis of Fab/EGFR mixtures deliver complex size agreeing with heterodimer size, thus corroborating hypothesis E and denying hypothesis D. This is consistent with published results where the bivalence of nimotuzumab/EGFR interaction has been proclaimed (Tikhomirov *et al.*, 2008). Moreover, if the two Fab regions of nimotuzumab would bind the same EGFR molecule, then these two binding events would not be independent, but rather the binding of the second arm would occur with a higher probability than the first, due to a higher chance of two molecules finding each other. However, kinetic, affinity and thermodynamic results of Fab fragments binding to EGFR agree with whole antibody results (see Fig. 8 and Fig. 23), corroborating independence of binding events taking place in both antibody arms. Thus, based on independence of antibody binding arms and on the size of complexes formed in nimotuzumab Fab fragment /EGFR mixtures, hypotheses B and D are discarded.

With hypothesis D discarded, the only possible assembly state for Fab fragment/EGFR interaction is represented by hypothesis E. As for whole antibody stoichiometry, possible assembly states for nimotuzumab/EGFR complexes are represented by hypotheses A and C, i.e. monovalency or bivalency of antibody. Light scattering analysis indicates the existence of heterotrimers in nimotuzumab/EGFR mixtures, thus corroborating assembly state hypothesis C (see Fig. 20). However, the average size of the eluting complexes in nimotuzumab/EGFR mixtures is smaller than for those formed by matuzumab, cetuximab and panitumumab mixtures. This could be caused by lower concentration of heterotrimers and co-elution of these with smaller species (heterodimers and free mAbs or EGFR). But why would nimotuzumab /EGFR mixtures yield lower heterotrimer concentration than matuzumab, cetuximab and panitumumab /EGFR mixtures?

Nimotuzumab has the weakest affinity of all studied mAbs (Fig. 8) and this could be a reason for the lower extent of complex formation. Yet, nimotuzumab /EGFR affinity is in the nanomolar range and the SLS experiments were performed in the micromolar range, so that the concentration of interactants is way above the affinity. Also, if weak affinity could explain the lower degree of complex formation in nimotuzumab /EGFR mixtures, and provided both antibody binding sites are independent, the same effect should be seen in Fab nimotuzumab studies. However, Fab nimotuzumab /EGFR mixtures deliver SLS results that are comparable to the other three Fab fragments analysed (see Fig. 20); the molecular weight of complexes formed corresponds to the expected size of heterodimers. Therefore, weaker affinity can not

be the cause – or the only cause, at least – for the lower heterotrimer concentration observed in nimotuzumab /EGFR mixtures. Other causes are further discussed.

There could be a concentration error in nimotuzumab ITC samples. However, for both panitumumab and nimotuzumab, the UV-determined protein concentration agreed well with the nominal vial concentration, thus indicating that total protein concentration is correct. Moreover, comparison of different dilutions of the four antibodies in study by SDS-PAGE (data not shown) also corroborated the nominal vial concentration of nimotuzumab, thus not supporting the hypothesis of an error in total antibody concentration. Moreover, identical quantity of nimotuzumab and other antibodies used as controls – shown by a comparable surface capture level – bound less EGFR molecules in SPR (see Fig. 12). This evidence is independent from the original nimotuzumab concentration in solution, since the same quantity was captured for each antibody, thus corroborating that the total concentration of nimotuzumab is correct.

The cause for nimotuzumab/EGFR lower heterotrimer concentration could be that a part of nimotuzumab molecules in solution are unable to build heterotrimers, i. e. they have one (or both) unfunctional arms. If part of the molecules in solution has one unfunctional arm, then nimotuzumab/EGFR mixtures would yield a mix of assembly states A and C. The independence of binding events occurring in both antibody arms has been evidenced by comparing kinetic and thermodynamic results. As a consequence of yielding identical thermodynamic profiles, the nimotuzumab populations leading to assembly states A and C would be indistinguishable by ITC. Calorimetric titration of such a mixture could explain the symmetric isotherm observed for the interaction of nimotuzumab to EGFR (Fig. 16) and the atypical “hybrid” stoichiometric results. If part of the molecules in solution has both unfunctional arms, then these molecules would not bind EGFR. The nimotuzumab solution would simply be a mix of binding-capable and binding-incapable antibodies and in this case the assembly state would be represented by hypothesis C. The binding-incapable antibodies present in solution would lead to an error in active concentration of nimotuzumab and reflect in the stoichiometry obtained from ITC. Accordingly, the generation of Fab fragments from this solution would naturally yield a mixture of binding and non-binding Fab fragments, thus also explaining the results for Fab/EGFR stoichiometry. Comparative SEC/SLS analysis of solutions of the four mAbs in study showed that the content of soluble aggregates present in the nimotuzumab solution is less than 5% (Fig. 25). Such low aggregate content could not

possibly explain the error in active concentration of nimotuzumab. Moreover, nimotuzumab molecules are captured by protein A (see Fig. 12), meaning that the protein A binding site in the Fc part of the antibody is intact.

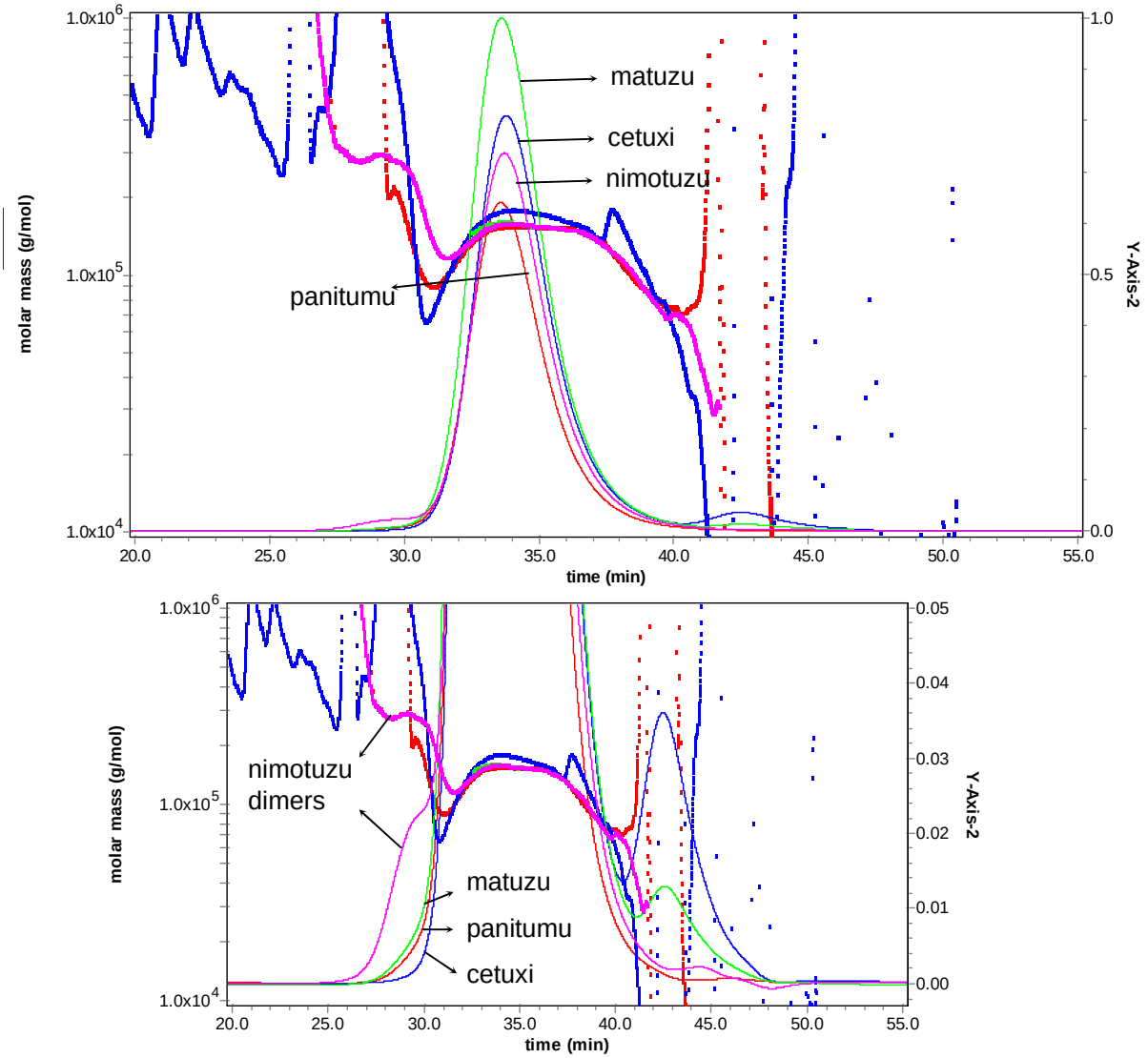

Fig. 25: SEC/SLS analysis of antibody samples.
Nimotuzumab solution shows presence of less than 5% of soluble aggregates (estimated aggregate size: dimers). In Y-Axis-2 is represented the dRI signal, indicative of protein concentration.

With the results at hand, no final conclusions can be taken regarding the reasons for nimotuzumab lower heterotrimer concentration and “hybrid” ITC stoichiometry results. The hypotheses of part of nimotuzumab molecules having one or both unfunctional binding sites remain open. ITC delivers a direct measure of stoichiometry, provided the active concentration of both interactants is accurately entered for isotherm fitting. As speculative exercise, the nimotuzumab mAb and Fab concentration values entered for fitting of ITC results were iteratively changed until stoichiometry 1 mol mAb binding site and 1 mol Fab

/EGFR were obtained (Fig. 23). The entered concentration that yielded the referred stoichiometry values was, for both mAb and Fab solutions, around 60% of the nominal concentration, meaning that around 40% of the nimotuzumab binding sites would be inactive. Speculation can be exercised about what could be the cause beneath the estimated 40 % partial or totally inactive antibody molecules present in solution. Monoclonal antibodies are, by definition, antibody molecules produced by descendents of one single clone only (therefore monoclonal). The molecules are thereby ideally all perfect copies of each other. However, achieving and proving monoclonality is a very exigent task. The presence of two binding populations in the nimotuzumab solution (namely monovalent-binders and bivalent binders) can be the result of glycosilation or post-translational modifications. Glycosylation is potentially important for the binding of the antibodies to their targets and can be variably accomplished by the producer organism machinery, being a potential source of binding heterogeneity. Post-translational modifications of the molecules can happen during production or storage and can affect the binding properties of the molecules. For example, isomerization of a single residue present in the CDR region of panitumumab has been shown to deeply affect the binding to EGFR (Rehder *et al.*, 2008). Such results suggest the importance of designing molecules with “robust” primary structures, that can be more resistant to post-translational modifications and thus yield more homogeneous protein products.

7.3 Interdependence of antibodies binding to EGFR

Motivated by reports of synergic effects of anti-EGFR mAbs (Friedman *et al.*, 2005; Dechant *et al.*, 2008; Meira *et al.*, 2009), biophysical methods were applied to test the interdependence of mAbs binding to EGFR. The results obtained with SPR, ITC and SLS are summarized on Table 10. Based on these results, the interdependence of different mAb combinations binding to EGFR could be divided in three modes:

- Simultaneous binding;
- Displacement;
- Crossblocking.

Table 10: Summary of results obtained upon analysis of mAbs interdependence with biophysical methods.

mAbs interdependence	**mAbs mixture with EGFR**	**Experimental observations**			
		SPR without crosslinking (see Fig. 14)	**SPR with crosslinking** (see Fig. 15)	**ITC** (see Fig. 19)	**SLS** (see Fig. 22)
Simultaneous binding	matuzu; cetuxi	positive binding curves	positive binding curves	strong negative enthalpy change	size of complexes corresponds to quatromer
	matuzu; nimotuzu	positive binding curves	positive binding curves	strong negative enthalpy change	size of complexes corresponds to quatromer
Displacement	matuzu; panitumu	negative binding curves	positive binding curves	positive enthalpy change	complexes size unchanged by the presence of second mAb
	nimotuzu; panitumu	negative binding curves	positive binding curves	positive enthalpy change	complexes size unchanged by the presence of second mAb
	nimotuzu; cetuxi	negative binding curves	positive binding curves	no signal	complexes size unchanged by the presence of second mAb
Crossblocking	cetuxi; panitumu	no signal	no signal	no signal	complexes size unchanged by the presence of second mAb

Simultaneous binding

The antibody pairs matuzumab/cetuximab and matuzumab/nimotuzumab are able to bind simultaneously to EGFR. The affinity of matuzumab to EGFR is actually improved by the presence of either cetuximab or nimotuzumab. According to SPR results, this is related with a slower dissociation rate of the complex when compared to the dissociation of the complex formed with free EGFR (Fig. 14). This effect can be explained by avidity. Since the antibodies bind bivalently, the less probable simultaneous dissociation of both antibody arms is needed for dissociation of complex. In the case of cetuximab and nimotuzumab, the overall affinity (avidity) of EGFR binding is not improved by the presence of a second antibody binding simultaneously to EGFR. These antibodies have slower dissociation rates from free EGFR, so that the effect of avidity is less important and the affinity to mAb-complexed or free EGFR is comparable. In thermodynamic terms (Fig. 19), although the simultaneous binding is at least as favourable as the binding of one single antibody, the calculated binding enthalpy (titration curve amplitude) of matuzumab or cetuximab titrated to bound EGFR is somewhat lower than to free EGFR. This effect may be due to steric or allosteric hindrance of individual non-covalent interactions, although as proven by the affinity results, the overall interaction is at least as strong. In general, the simultaneous binding of anti-EGFR mAbs to EGFR is enabled by non-overlapping epitopes and simultaneous absence of steric hindrance between both antibodies.

Antibody cocktails have proven increased efficacy for a number of targets (Logtenberg, 2007). Their response involves a series of direct and indirect effector mechanisms that include neutralization, phagocytosis, complement-mediated destruction and antibody-mediated cellular cytotoxicity. These are elicited by the concerted action of different species of antibodies that have multiple specificities, bind several epitopes (antigens) and act in synergy. Synergic effects of the combined use of matuzumab and cetuximab are known (Friedman *et al.*, 2005; Kamat *et al.*, 2008; Dechant *et al.*, 2008; Meira *et al.*, 2009). Moreover, the hypothesis of simultaneous binding to EGFR had already been presented as possible explanation for the synergic effects (Kamat *et al.*, 2008). This hypothesis was corroborated by the completely non-overlapping epitopes of both antibodies (Li *et al.*, 2005; Schmiedel *et al.*, 2008). The present work presents for the first time SPR and ITC evidence of the simultaneous binding of these two anti-EGFR mAbs. The simultaneous binding of matuzumab and nimotuzumab is described for the first time. A synergic effect could thus be expected from the

combined use of matuzumab and nimotuzumab in the clinic. However, such study was beyond the scope of this thesis.

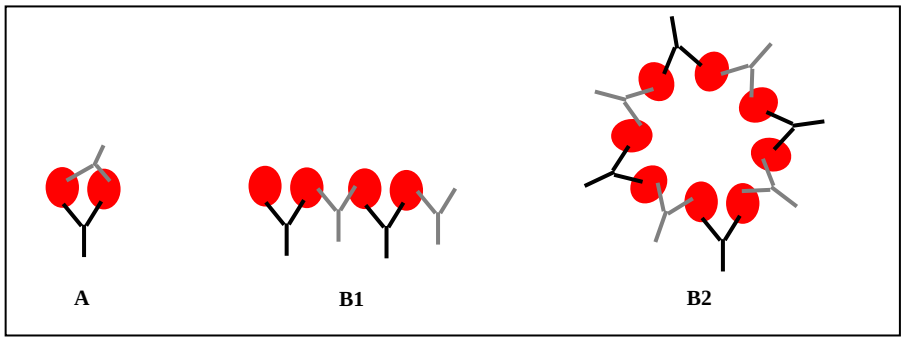

Fig. 26: Representation of the different possible assembly states for matuzumab/cetuximab and matuzumab/nimotuzumab complexes.

Possible assembly states for mAb-1/EGFR/mAb-2 complexes are: **A)** closed cycles formed of two EGFR and two different mAb molecules; **B1)** chains of intercalated mAb /EGFR molecules with variable length; **B2)** chains of intercalated mAb /EGFR molecules whose ends can eventually interact with each other.
Legend: red circle – EGFR; black y-shape – mAb-1; grey y-shape – mAb-2.

Light scattering analysis was used to further investigate such EGFR-mediated bi-antibody complexes (see Fig. 22). Results show a maximal average molecular weight of complexes formed in mixtures of EGFR with matuzumab/cetuximab or matuzumab/nimotuzumab that corresponds to the predicted size of heterogeneous quatromers (two EGFR and two different mAb molecules) – see Fig. 22. This result corroborates the simultaneous binding of these two pairs of antibodies to EGFR and indicates the formation of quatromers as preferred complex assembly state. However, the spatial arrangement of such assembly state could not be precisely determined and the question if these complexes build closed cycles (A in Fig. 26) or open chains (B in Fig. 26) remains open. The co-existence of both open and closed quatromer complexes depends on how flexible and sterically free the EGFR epitopes of both mAbs are. Moreover, the existence of larger assembly state configurations, simply pictured as variable size chains of intercalated mAb /EGFR molecules, cannot be excluded. The co-elution of larger hetero-complexes with simple one-mAb heterotrimers, heterodimers or even free monomers could explain the average molecular weight obtained. However, this possibility is not supported by the results, since the molar mass detection line of the mixtures does not indicate the presence of larger complexes. If the complexes are in the open chain configuration, then a high variability of the chain length can be envisaged and it is very probable that chains longer than quatromers exist. It is possible that such long chains would have less resistance to the sheer stress offered by the SEC column used for separation and

eventually break into smaller ones during the chromatographic process, explaining the quatromer-like size of complexes detected by light scattering analysis.

The size of EGFR-mediated bi-antibody complexes may have important implications in the clinic. It has been postulated that synergic effects of mAb combinations would be related to a higher rate of EGFR endocytosis and consequent down regulation of the receptor (Friedman *et al.*, 2005). If the rate of EGFR clearance from the cell surface is proportional to the size of EGFR-mAb lattices, then the bigger these lattices are, the faster and more efficiently EGFR can be down-regulated. Alternatively, synergic effects could be related to potent activation of complement-dependent cytotoxicity against EGFR-expressing cells (Dechant *et al.*, 2008).

Displacement

Negative concentration-dependent SPR binding curves were observed during interdependence studies for the antibody pairs matuzumab/panitumumab, nimotuzumab/cetuximab and nimotuzumab/panitumumab (see Fig. 14). These are indicative of cross-competition between these antibodies; binding of the second antibody to EGFR produces dissociation of the receptor from the first antibody, leading to the observed negative concentration-dependent curves. This hypothesis has been corroborated by ITC for the pairs matuzumab/panitumumab and nimotuzumab/panitumumab (see Fig. 19). Competitive fit to such ITC experiments yielded the same enthalpy change for panitumumab/EGFR as the one obtained from free EGFR titration, indicating that the detected heat was the difference between the heat released upon panitumumab/EGFR association and the heat uptaken upon matuzumab/EGFR or nimotuzumab/EGFR dissociation. In both SPR and ITC analysis, this interdependence mode was asymmetric. Cetuximab completely rescued EGFR from nimotuzumab while nimotuzumab itself was less efficient in binding cetuximab-bound EGFR. Panitumumab competed with both matuzumab and nimotuzumab but none of these two antibodies was as efficient in displacing panitumumab. The observed asymmetry is probably due to differences in affinity: cetuximab and panitumumab are strong binders while matuzumab and nimotuzumab bind to EGFR with lower affinity. The competition of cetuximab to nimotuzumab was not detectable by ITC, possibly due to cancellation of the enthalpic contributions from both antibodies upon EGFR binding.

Similar SPR interdependent studies, where the second antibody was titrated to EGFR that had been cross-linked to the immobilized antibody showed simultaneous binding for the pairs

referred above (see Fig. 15). This indicates that, to a certain extent, the epitopes are non-overlapping and there is steric allowance for simultaneous binding of both antibodies to EGFR. Thus, the dissociation from the first (immobilized) antibody observed in Fig. 14 could be explained by a conformational change induced by the second antibody to EGFR weakening the binding to the first antibody. The hypothesis of conformational change of EGFR upon antibody binding indicates that the interaction that takes place is not a rigid body-like interaction. The initially positive binding curves observed for matuzumab binding to panitumumab-captured EGFR are believed to be the detection of the complex matuzumab-EGFR-panitumumab and corroborate the hypothesis of short-lived simultaneous binding of both antibodies. Such complexes were not directly detectable in any other of the pairs tested. It is possible that the complex was made detectable in the special case of panitumumab/matuzumab by a coincident favourable combination of kinetic rates. Since the crosslinkage of EGFR seems to affect its binding affinity to the positive controls, considerations about the affinity of antibodies from the pairs above binding to crosslinked EGFR were not done. Controls show that affinity is affected at different degrees by crosslinking, possibly due to partial loss of complex flexibility or EGFR activity.

Crossblocking

The third mode of mAb interdependence is crossblocking, as observed for cetuximab and panitumumab. Antibodies cetuximab and panitumumab compete with each other for EGFR binding, the binding of one making the binding of the other impossible (see Fig. 14). This can be due to EGFR overlapping epitopes and/or to strong steric or allosteric hindrance. Point mutations in EGFR revealed critical for both cetuximab and panitumumab binding, indicating strong overlapping of the epitopes of both antibodies (Freeman *et al.*, 2008).

7.4 Considerations about epitope and allostery mapping

Cetuximab, panitumumab and nimotuzumab all bind to EGFRvIII (Table 3). This result is consistent with their interactions with epitopes situated in domain III of EGFR (Fan *et al.*, 1994; Li *et al.*, 2005; Freeman *et al.*, 2008; Talavera *et al.*, 2009). Moreover, kinetic analyses by SPR show that these antibodies bind EGFRvIII more tightly than the wild type receptor. The same effect was previously shown for matuzumab (Schmiedel, 2009) and is possibly due to the absence of steric hindrance from the domains I and II nearly completely missing in comparison to full length EGFR. Cetuximab, panitumumab and nimotuzumab block ligand binding to EGFR, while matuzumab is not able to completely block the binding of the soluble receptor to immobilized EGF. Instead the equilibrium SPR response plateaus at 40% of the value in the absence of antibody. EGF competition results are in agreement with published results (Yang *et al.*, 2001; Li *et al.*, 2005; Schmiedel *et al.*, 2008; Talavera *et al.*, 2009). The fact that matuzumab does not completely block EGF binding is consistent with a non overlapping epitope with the EGF binding site on domain III (Schmiedel *et al.*, 2008). One possible explanation for the observed SPR responses is that both unbound EGFR and the EGFR complex can interact with the immobilized EGF, but that the complex binds with substantially weaker affinity.

Based on the above discussion and on interdependence studies discussed in section 7.3, a map of the relative epitope positions and binding interdependence of the four anti-EGFR antibodies studied was developed (Fig. 27). In this map, the epitopes of matuzumab (M), cetuximab (C), panitumumab (P) and nimotuzumab (N) are represented by circles of different colours. They are all situated on domain III of EGFR. Cetuximab, panitumumab and nimotuzumab epitopes strongly overlap with the EGF binding site. Matuzumab, on the contrary, binds to an epitope that does not overlap with the EGF binding site. The epitopes of cetuximab and panitumumab strongly overlap and they are both able to displace nimotuzumab. However, and interestingly, only panitumumab displaces matuzumab (cetuximab binds EGFR simultaneously with matuzumab).

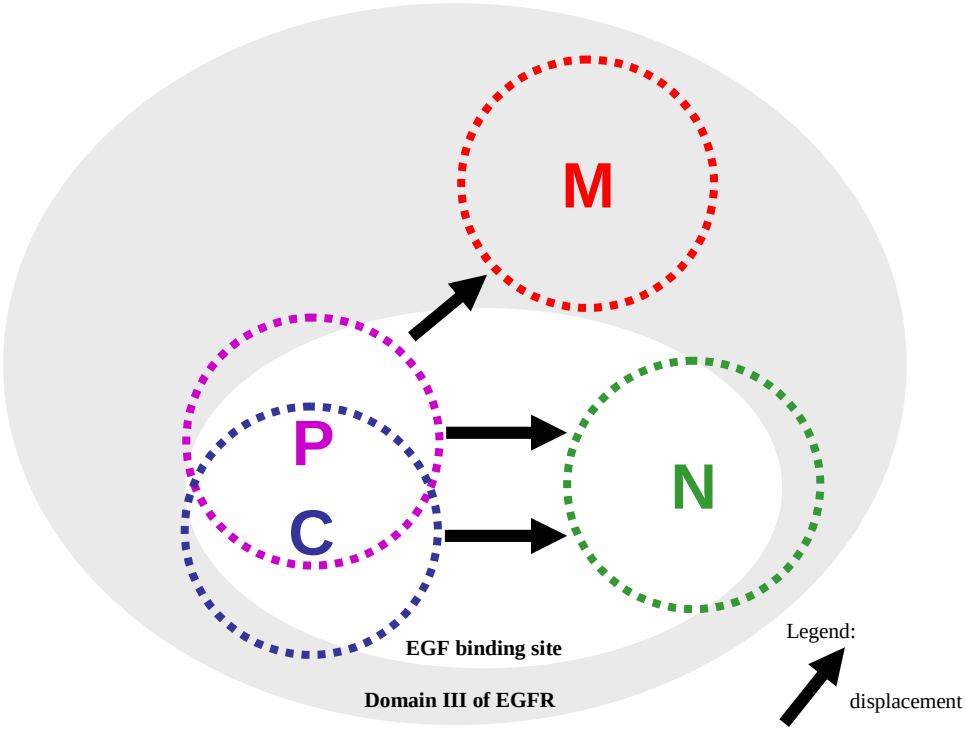

Fig. 27: Relative epitope position and allosteric displacement of anti-EGFR mAbs.
Grey area - domain III of EGFR; white area - EGF binding site within domain III; red - matuzumab epitope; blue - cetuximab epitope; purple - panitumumab epitope; green - nimotuzumab epitope.

7.5 Kinetics of antibody/EGFR binding

Cetuximab and panitumumab are the two strong affinity antibodies, although the kinetic reasons for their strong affinities are distinct (see Fig. 8). Cetuximab binding to EGFR delivered the highest association rate from all four antibodies in study. The strong affinity of panitumumab is explained by the slowest dissociation of all EGFR-mAb interactions studied. Matuzumab and nimotuzumab are the two weak affinity antibodies of the lot. Matuzumab/EGFR complexes are the less stable ones, as indicated by a high dissociation rate constant. The weak nimotuzumab affinity is due to a low association rate.

Careful SPR assay design and development is essential for obtaining good quality kinetic data and meaningful rate and equilibrium constants of binding. Therefore, some considerations about assay design will be done. The very first question in SPR assay development is which interactant to immobilize. Multivalent interactants, like antibodies, are preferably immobilized. This avoids avidity effects arising if they are passed over in solution. The anti-

EGFR mAbs in study were either directly immobilized by amine coupling or captured by protein A (Fig. 8).

Excellent overall consistency was observed between kinetic results obtained when EGFR was titrated to protein A-captured antibodies and when Fab fragments were titrated to directly immobilized EGFR. Obtaining comparable results from such distinct assays shows robustness of the kinetic determination. Moreover, both assays delivered the fastest association rate constants for all antibodies studied, and consequently lower K_D values, indicating optimal assay configuration. Optimal assay configuration has been defined as the one which produces the strongest affinity between ligand and analyte (Patel and Andrien, Jr., 2009). The direct immobilization of antibodies or Fab fragments delivered lower association rate constant values although dissociation rates are consistent with those obtained by protein A or EGFR immobilization. Since this happened for all antibodies studied, it indicates a systematic error caused by the immobilization of either mAb or Fab fragment. Direct immobilization of antibodies may result in aleatory antibody orientation at the biosensor surface, since amine coupling will use any free amine groups at the surface of the protein. Protein A specifically binds the Fc part of antibodies. Thus, the capture alternative offers an oriented immobilization where steric hindrance is minimized and all binding sites are oriented towards the flow channel and thus available for EGFR binding.

7.6 Thermodynamics of antibody/EGFR binding

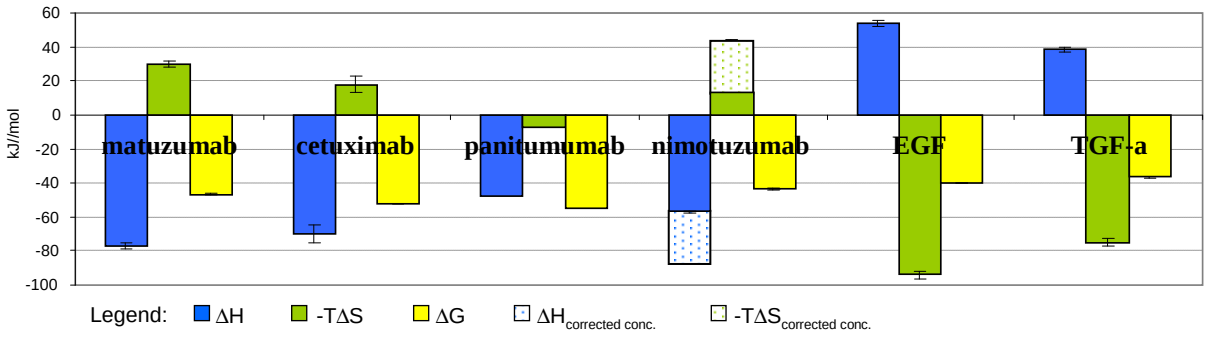

Fig. 28: Thermodynamic profiles of mAb/EGFR and ligand/EGFR interactions (ITC results).
In pointed bars are presented the mAb and Fab nimotuzumab thermodynamics obtained from treating ITC analysis with corrected concentrations to yield stoichiometry 1 mol mAb binding site and 1 mol Fab /EGFR (see section 7.2). Thermodynamic profiles shown are the average of best fits to two independent ITC measurements (see Fig. 16).

In the previous section, kinetic explanations for the different antibodies affinities were discussed. In this section, the thermodynamic reasons for the different affinities will be

highlighted. The thermodynamic profiles presented in Fig. 28 were constructed with results originated by ITC (see Fig. 16). The equilibrium constant values of cetuximab and panitumumab could not be determined accurately by simple ITC experiments due to their too steep isotherm curves, indicative of a K_D value lower than 2 nM. The K_D value of panitumumab/EGFR interaction, and consequently the Gibb's energy change, ΔG, could be quantified from the ITC analysis of panitumumab to matuzumab-saturated EGFR (Fig 19). Competitive fit of that interaction yielded ΔH of -49 kJ/mol, a value comparable to the one obtained by simple interaction (-52 kJ/mol, Fig 16) and thus indicating validity of this determination. The resulting K_D value was 0.2 nM. Similar results were obtained for the panitumumab titration to nimotuzumab-saturated EGFR: K_D 0.1 nM and ΔH -45 kJ/mol. These results were obtained when the concentration of nimotuzumab was corrected to yield a stoichiometry of 1 mol antibody binding sites / mol EGFR from the fitting of a one-sites isotherm to the nimotuzumab/EGFR titration raw data (Fig. 25). The same strategy could not be applied to calculate the affinity of cetuximab, since the cetuximab/nimotuzumab titration did not deliver measurable calorimetric detection. This was possibly due to a match of the binding enthalpies of cetuximab/EGFR and nimotuzumab/EGFR binding, that cancel each other upon competition.

Matuzumab and cetuximab have close enthalpy contributions; a lower entropic penalty seems to be the reason for cetuximab stronger affinity. Panitumumab has the smallest enthalpy contribution of all four mAbs, that is compensated in terms of binding strength by a null or even slightly favourable entropic change. Enthalpy of binding is related to the difference in electrostatic interactions (H-bonds, van der Waals) that take place in the complex and in the interactants alone. Entropy of binding is related to the desolvation of surfaces upon bonding and conformational changes. Although cetuximab and panitumumab have very similar affinities and compete with each other for EGFR binding (see section 7.3), their thermodynamic profiles are quite different. This indicates that although interacting with comparable (overlapping) epitopes at the EGFR surface, the two antibodies probably do so in rather distinct modes. This allegation could only be done in view of the thermodynamic profiles (enthalpy and entropy) of the two antibodies. A strongly negative heat capacity change was observed for matuzumab, panitumumab and nimotuzumab. Negative heat capacity change has been correlated with the burial of non-polar groups upon binding.

Binding of antibodies and ligands to EGFR yielded opposite thermodynamic profiles. While antibody interactions are enthalpy-driven and mostly entropy-penalized, ligand interactions are entropy-driven and enthalpy-penalized. Enthalpy-driven reactions are typically related to polar interactions and are usually the case for antibody-antigen interactions (Sundberg and Mariuzza, 2002). Anti-EGFR antibodies bind and stabilize a tethered conformation of the receptor (Li *et al.*, 2005; Schmiedel *et al.*, 2008). It was seen by comparison of antibody-complexed and monomeric EGFR that the binding of antibody does not seem to affect the structural conformation of EGFR extracellular domains (Li *et al.*, 2005; Schmiedel *et al.*, 2008). Entropy-driven reactions, as observed for ligand/EGFR binding, have been related to conformational or dynamic (e.g. solvation, desolvation) changes. This result is coherent with structural studies. Ligands bind preferentially to an extended form of EGFR and "trap" the receptor in the conformation that can dimerize through the exposed dimerization arm. Since the receptor exists in solutions preferentially in the tethered conformation (Ferguson *et al.*, 2003), ligand binding has to induce a quite large-scale conformational change (Burgess *et al.*, 2003).

The indirect determination of binding thermodynamics from the van't Hoff treatment of temperature dependent equilibrium constants yielded by SPR analysis will be discussed in the next section.

7.7 Comparative evaluation of SPR, ITC and SLS

The most significant characteristic of surface plasmon resonance /Biacore technology is the possibility of real time monitoring of macromolecular interactions. This enabled a wealth of information about mAb/EGFR interactions to be collected. Firstly, the calculation of binding kinetics provided a broader understanding about complex formation than equilibrium constants alone (see section 7.5). Secondly, SPR studies of different mAb combinations binding to EGFR were very helpful on clarifying the way antibodies influenced each other upon binding EGFR (see section 7.3). The advantage of SPR for this kind of study is evident in Fig. 14 and Fig. 15, where the binding of a second antibody to EGFR can be observed in real time. For this purpose, ITC could only deliver equilibrium data (Fig. 19) that would have been harder to interpret without the information collected with SPR. Moreover, since ITC relies on measurements of total heat released or absorbed in solution, false negatives can be obtained for reactions where the total heat is close to zero. That was the case for the antibody

pair cetuximab/nimotuzumab: although SPR analysis indicated that the binding of the second antibody lead to displacement of the first (Fig. 14), no signal could be measured by ITC (Fig. 19). The two antibodies may have a close enthalpy change upon EGFR binding (Fig. 28), resulting in a total heat change close to zero. Another advantage of SPR is that it can be applied to a wide range of binding affinities, enabling the determination of affinities as strong as 10^{-10} M (Schuck *et al.*, 2004). ITC applicability to study strong affinities (as often the case for antibody-antigen interactions) is limited. This was the case for cetuximab and panitumumab, whose EGFR affinity could not be accurately determined by a simple ITC experiment since the isotherm curves were too steep (see Fig. 16). However, SPR allowed affinity determinations of these two strong EGFR binders.

Good correlation is observed between the affinity results obtained by ITC and by SPR for mAb/EGFR and ligand/EGFR interactions (Fig. 29). A systematic bias is observed: SPR originated K_D values (K_D(Biacore)) were generally higher than ITC ones (K_D(ITC)), for all the interactions tested. This effect is possibly related to the immobilization of one interactant in SPR studies.

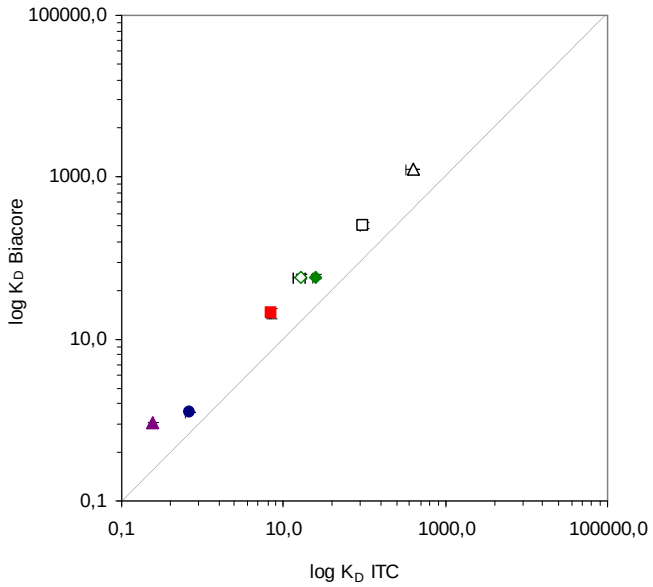

Fig. 29: Correlation of ITC and SPR-generated affinity results.
The diagonal line represents a correlation of 1. Error bars indicate the standard deviation on two independent measurements. Legend: □ EGF; Δ TGF-α; ■ matuzumab; ● cetuximab; ▲ panitumumab; ◆ nimotuzumab; ◇ nimotuzumab with corrected concentration to yield N=1.

Additionally to enabling real time monitoring of interactions, determination of binding kinetics and study of high affinity interactions, SPR also allowed for studying the

thermodynamics of antibody/EGFR. Although ITC remains the standard method for direct measurement of binding thermodynamics, the sample consumption can be very high. The relatively low material consumption makes SPR an interesting alternative for thermodynamic studies. In this study, design of SPR and ITC methods was oriented towards minimal consumption of EGFR material. ITC analysis consumed two times the material needed for thermodynamic analysis with SPR, respectively 0.4 mg and 0.2 mg. However, three days were needed to obtain thermodynamic information with SPR, while ITC results could be obtained in a couple of hours. Although good agreement of SPR-based and calorimetric thermodynamic parameters has been reported in the literature, most of these studies have been done for the interaction of small molecules or proteins with small molecules (Day *et al.*, 2002; Myszka *et al.*, 2003; Papalia *et al.*, 2008). The extrapolation of such results to complex protein-protein interactions should be done with prudence. Protein-protein interactions are very complex. They result from multiple single interactions, involve the burial of large protein surface areas – 1,400 to 2,300 $Å^2$ for antibody-antigen interactions (Sundberg and Mariuzza, 2002) – and consequent displacement of solvent molecules and may also involve quite dramatic rearrangement of domains and conformational changes.

Enthalpic and entropic changes were determined indirectly from the temperature dependence of K_D using the van't Hoff plot (see Fig. 11). Linear fitting of van't Hoff plots presumes that the enthalpy change of reaction is constant with the temperature. However, the temperature dependence of enthalpy was determined by ITC (see Fig. 18) and this was only the case for cetuximab. Matuzumab, panitumumab and nimotuzumab have negative dependencies of enthalpy with the temperature and so the correct fit to the van't Hoff plot is a quadratic function delivering ΔC_P together with ΔH and ΔS. However, observation of the plots suggests that there would be no benefit in such a fitting, since the experimental error seems to be too high covering the curvature of the experimental points. Values of ΔC_P thus determined would have very low significance. Thus, heat capacity change could not be determined by SPR due to a high results scattering in the van't Hoff plot that masked the curvature expected from interactions whose enthalpy was not constant with the temperature.

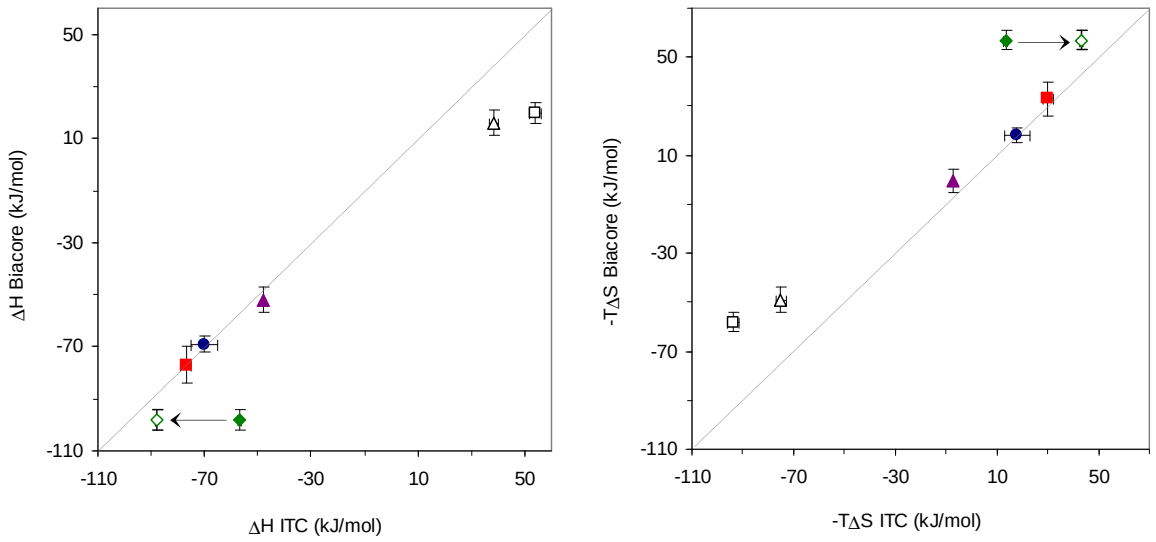

Fig. 30: Correlation of ITC and SPR-generated thermodynamic results.
The diagonal line represents a correlation of 1. Error bars indicate the standard deviation on two independent measurements. Legend: □ EGF; Δ TGF-α; ■ matuzumab; ● cetuximab; ▲ panitumumab; ◆ nimotuzumab; ◇ nimotuzumab with corrected concentration to yield N=1.

The thermodynamic contributions ΔH and -TΔS calculated by SPR and ITC analysis are compared in Fig. 30. Very good correlation is observed for results of both methods for matuzumab, cetuximab and panitumumab interactions. As for nimotuzumab, ITC delivers lower enthalpic contribution as well as lower entropic penalty in comparison to SPR values. However, after correction of nimotuzumab concentration to yield EGFR:nimotuzumab stoichiometry of 2:1, there is an increase in both thermodynamic terms (Fig. 28) and a better correlation with SPR-based results is obtained. In SPR experiments EGFR is titrated to captured mAb and the affinity results thus originated are only dependent on the EGFR concentration. Therefore, an error in nimotuzumab concentration would normally not be propagated to the affinity results calculated by SPR. For the two agonists studied, EGF and TGF-α, the correlation between SPR and ITC thermodynamic parameters is poor and this can be due to the complexity of agonist/EGFR interactions. The binding of either EGF or TGF-α to EGFR involves a dramatic EGFR conformational change and results in dimerization of the receptor. Conformational change and receptor dimerization are thus equilibria linked to ligand binding and can take place with different extents in SPR and ITC, depending on conditions like rotational and diffusional freedom and concentration effects. Such effects could not be quantified and represent a deviation from the models used to fit SPR and ITC experimental results, respectively 1:1 binding model and one-sites model. Thus, the poor correlation observed for the agonist interactions is probably due to too simplistic data modelling in both methods, rather than to the methods themselves. Moreover, heterogeneities in ligand/EGFR

interaction affinities have highlighted the complexity and interdependence of the various linked equilibria that compose this complex interaction (Macdonald and Pike, 2008; Lemmon, 2009). A poor fit of the 1:1 interaction model to SPR binding curves was actually observed, which is why affinity was calculated by steady state analysis. Other models of interaction were considered as possible ways to explain the interaction and fit the binding curves: the two state reaction model, accounting for the existence of a second reaction (EGFR conformational change and/or dimerization) linked to the first; and the heterogeneous ligand model, accounting for the existence of different immobilized interactants (different conformations – tethered, open, dimerized – of EGFR on the surface). Two-state reaction and heterogeneous ligand both yielded better fits to the raw data, but it is unclear how realistic or significant such analyses are or if the better fit is simply a result of a higher model flexibility. Since the fit of more complicated models to the SPR binding curves of agonists to EGFR could not be validated, it was decided to work with the steady state affinity results.

Surface plasmon resonance and isothermal titration calorimetry most fundamental difference is that the former is a surface-based biosensor method whilst the latter is a solution-based method. The fact that biosensors require the immobilization of one of the binding partners onto a surface has brought about speculation that the immobilization onto a surface would result in artificial change of the binding constants. The perturbation could arise from nonspecific surface binding and limitations to the transport of analyte to and from the surface. Very important features included in Biacore systems that helped overcome the limitations mentioned are the dextran layer in the surface of sensor chips and the flow cell system used. The dextran layer provides a hydrophilic fluid environment where the immobilized interactant retains most of its rotational and some diffusional freedom. The flow cell system used by Biacore provides rapid delivery of a constant supply of analyte during the association phase and for rapid washout of the surface during the dissociation phase. The overall good correlation of SPR results with ITC (Fig. 29, Fig. 30) shows that immobilization onto a surface does not affect the binding very much. Together the two techniques delivered a very complete stoichiometric, kinetic and thermodynamic profile of the anti-EGFR antibodies studied. Their combined utilities and corroborative use is in accordance with published studies (Deinum *et al.*, 2002; Myszka *et al.*, 2003).

Static light scattering provided corroborative qualitative results that confirmed the stoichiometry of binding. However, the SEC separation used did not provide sufficient

resolution to discriminate between heterotrimers and heterodimers. Nevertheless, SLS analysis delivered absolute measurements of the average size of complexes formed in mAb/EGFR solutions.

8 CONCLUSIONS

The applicability of SPR, ITC and SPR for the generation of meaningful quantitative data on binding interactions is demonstrated. Clear stoichiometric, kinetic and thermodynamic answers were obtained that together provide a deep understanding of the interactions on the molecular level. SPR provided real-time monitoring of interactions, while ITC and SLS are steady state techniques. Real-time monitoring of interactions was a highly interesting feature since it allowed determination of the binding kinetics and gave insights into the dynamic processes of the interdependence of different mAbs binding to EGFR. Affinity and thermodynamic characterization of mAb/EGFR interactions was performed both by SPR and ITC. SPR critics have argumented that the immobilization of one interactant onto a surface would result in artificial perturbation of the binding. This could explain the systematic bias observed for the affinity constants: K_D(Biacore) were generally higher than K_D(ITC), for all the interactions tested. However, a good overall correlation was obtained between the thermodynamic results of mAb/EGFR interactions from both techniques.

Discrepancies were observed between ITC and SPR results of ligands/EGFR interactions. Due to the complexity of the ligand/EGFR interactions, experimental results are difficult to model in an accurate way. More than only related with the correlation between both determination methods, these results show the limitations of biophysical methods in the study of complex interactions, with many linked equilibria (Lemmon, 2009). The data treatment involves modelling of the experimental results and the first model of choice corresponds to independent binding sites and absence of linked equilibria (1:1 interaction model in SPR; one-sites model in ITC). These models yield kinetic, affinity or thermodynamic results representing the average bulk interactions, however, physical significance of the values obtained is hardly assigned. On the other hand, the use of higher sophisticated models also implies the risk of low significance of results obtained. A model with more variables will always yield a better fit, not meaning that this model better describes the physical reality.

Multiple publications have dealt with the comparability of ITC and Biacore results (Deinum *et al.*, 2002; Day *et al.*, 2002; Myszka *et al.*, 2003). Interestingly, given that EGFR is a

membrane protein, one could think that the surface- and not the solution-based technique mimics best the in vivo situation. In principle, confirmation of results with orthogonal techniques can provide validation of those results and that is highly valuable for the experimental scientist. Beyond that, it is important to always keep in mind the conditions in which the results were produced and how they can be interpreted to yield answers to the questions asked. This study shows the combined utilities and corroborative use of SPR and ITC techniques; together they delivered a very complete stoichiometric, kinetic and thermodynamic profile of the anti-EGFR antibodies studied.

This study provided for the first time clear stoichiometric evidence for the bivalent binding of anti-EGFR antibodies. Moreover, it was shown that the binding events taking place in both antibody arms are independent from each other. Bivalent binding has been related with an increase in the stability of antibody at the surface of tumor cells, due to avidity effects (Rehder *et al.*, 2008) and the formation of antibody-mediated EGFR dimers has been related to a faster receptor internalization rate and consequently a faster down-regulation (Friedman *et al.*, 2005).

The strength of antibody/EGFR binding affinities is the result of kinetic rates and thermodynamic physical quantities. The kinetic and thermodynamic study of interactions provided for the first time a deeper understanding of the reasons behind anti-EGFR antibodies affinities. Cetuximab and panitumumab are strong binders, with affinities equal to or lower than 1 nM. Both antibodies have fast association rates and slow dissociation rates. Matuzumab's 10 times weaker affinity is mainly due to a very fast dissociation rate. Nimotuzumab's at least 20 times weaker affinity is mainly due to a very slow association rate. In thermodynamic terms, an interesting correlation was seen between large enthalpy contributions and weak affinities. For weaker affinity antibodies, such as matuzumab, the large enthalpy contribution is partially cancelled by strong entropy penalty, so that the overall resulting binding strength is moderate. Panitumumab, the antibody studied with strongest affinity, showed the smallest enthalpy contribution, however the entropy term was around zero.

The simultaneous binding of matuzumab and cetuximab to EGFR was proven with stoichiometry, kinetic and thermodynamic evidence. Indeed, *in vitro* studies had shown a synergistic effect of matuzumab and cetuximab in combination (Dechant *et al.*, 2008; Kamat

et al., 2008) and recent structure studies indicated that the simultaneous binding of the two antibodies is possible (Schmiedel *et al.*, 2008). The simultaneous binding of matuzumab and nimotuzumab is reported in this study for the first time, and stoichiometric, kinetic and thermodynamic evidence for this is as well presented. The simultaneous binding of antibody combinations to EGFR has important implications for the clinical use of therapeutic antibody combinations. The study of the combined application of matuzumab/nimotuzumab in cell-based models would be very interesting to see if synergic effects are also observed. Further investigations on the assembly states formed by EGFR complexes with antibody combinations would help understand the molecular basis for the synergic effects observed. If the rate of EGFR clearance from the cell surface is proportional to the size of EGFR-mAb lattices, then the bigger these lattices are, the faster and more efficiently EGFR can be down-regulated (Friedman *et al.*, 2005). The results of this study indicate that antibody combinations do not complex more than two EGFR molecules, the same number of molecules complexed by only one antibody type. If they are confirmed, then down regulation of EGFR is not likely to be the reason behind the synergic effects observed. Alternatively, synergic effects could be related to potent activation of complement-dependent cytotoxicity against EGFR-expressing cells (Dechant *et al.*, 2008).

The biophysical results obtained with nimotuzumab indicate that the solution studied has 40% of inactive antibody arms, what is somehow troubling having in account that the solution used was a market product and thus directed for clinical use. A comparability study indicated that the same results would be obtained by a second product vial from an independent batch and a completely independent supply route. The hypothesis of this vial being one unfortunate case was thus excluded.

9 REFERENCES

Alfthan,K. (1998). Surface plasmon resonance biosensors as a tool in antibody engineering. Biosens. Bioelectron. 13, 653-663.

Arakawa,T. and Wen,J. (2001). Size-exclusion chromatography with on-line light scattering. Curr. Protoc. Protein Sci. Chapter 20, Unit 20.6.

Berezov,A., Chen,J., Liu,Q., Zhang,H.T., Greene,M.I., and Murali,R. (2002). Disabling receptor ensembles with rationally designed interface peptidomimetics. J Biol Chem 277, 28330-28339.

Bergethon,P.R. (1998). The Physical Basis of Biochemistry: the Foundations of Molecular Biophysics, Berlin: Springer

Biacore (1998). BIAtechnology Handbook, Uppsala: Biacore AB

Biacore (2005). Biacore T100 Instrument Handbook, Uppsala: Biacore AB

Biacore (2006). Biacore T100 Software Handbook, Uppsala: Biacore AB

Biacore (2008). Sensor Surface Handbook, Uppsala: GE Healthcare Bio-Sciences AB

Biotechnology Industry Organization (2008). Guide to Biotechnology, Biotechnology Industry Organization. http://www.bio.org/speeches/pubs/er/BiotechGuide2008.pdf

Bleeker,W.K. *et al.* (2004). Dual mode of action of a human anti-epidermal growth factor receptor monoclonal antibody for cancer therapy. J. Immunol. 173, 4699-4707.

Boland,W.K. and Bebb,G. (2009). Nimotuzumab: a novel anti-EGFR monoclonal antibody that retains anti-EGFR activity while minimizing skin toxicity. Expert. Opin. Biol. Ther. 9, 1199-1206.

Burgess,A.W., Cho,H.S., Eigenbrot,C., Ferguson,K.M., Garrett,T.P.J., Leahy,D.J., Lemmon,M.A., Sliwkowski,M.X., Ward,C.W., and Yokoyama,S. (2003). An open-and-shut case? Recent insights into the activation of EGF/ErbB receptors. Mol Cell 12, 541-552.

Carter,P. (2001). Improving the efficacy of antibody-based cancer therapies. Nat. Rev. Cancer 1, 118-129.

Cohen,S., Chang,A., Boyer,H.W., and Helling,R.B. (1973). Construction of biologically functional bacterial plasmids in vitro. Proc. Nat. Acad. Sci. USA 70, 3240-3244.

Congy-Jolivet,N., Probst,A., Watier,H., and Thibault,G. (2007). Recombinant therapeutic monoclonal antibodies: mechanisms of action in relation to structural and functional duality. Crit Rev. Oncol. Hematol. 64, 226-233.

Cooper,A. ITC Notes 08/06/01. http://www.chem.gla.ac.uk/staff/alanc/itcnotes.pdf . 2001. 6-5-2010.

Dawson,J.P., Bu,Z., and Lemmon,M.A. (2007). Ligand-induced structural transitions in ErbB receptor extracellular domains. Structure 15, 942-954.

Day,Y.S., Baird,C.L., Rich,R.L., and Myszka,D.G. (2002). Direct comparison of binding equilibrium, thermodynamic, and rate constants determined by surface- and solution-based biophysical methods. Protein Sci. 11, 1017-1025.

de Haard,H.J., van Neer,N., Reurs,A., Hufton,S.E., Roovers,R.C., Henderikx,P., de Bruine,A.P., Arends,J.W., and Hoogenboom,H.R. (1999). A large non-immunized human Fab fragment phage library that permits rapid isolation and kinetic analysis of high affinity antibodies. J. Biol. Chem. 274, 18218-18230.

De Larco,J.E. and Todaro,G.J. (1978). Growth factors from murine sarcoma virus-transformed cells. Proc. Natl. Acad. Sci. U. S. A 75, 4001-4005.

De Larco,J.E. and Todaro,G.J. (1987). Epithelioid and fibroblastic rat kidney cell clones: epidermal growth factor (EGF) receptors and the effect of mouse sarcoma virus transformation. J Cell Physiol 94, 335-342.

Dechant,M. *et al.* (2008). Complement-dependent tumor cell lysis triggered by combinations of epidermal growth factor receptor antibodies. Cancer Res. 68, 4998-5003.

Deinum,J., Gustavsson,L., Gyzander,E., Kullman-Magnusson,M., Edstrom,A., and Karlsson,R. (2002). A thermodynamic characterization of the binding of thrombin inhibitors to human thrombin, combining biosensor technology, stopped-flow spectrophotometry, and microcalorimetry. Anal. Biochem. 300, 152-162.

Demeester,J., De Smedt,S., Sanders,N., and Haustraete,J. (2005). Light Scattering, In: Methods for Structural Analysis of Protein Pharmaceuticals. ed. W.Jiskoot and D.Crommelin. Arlington, VA: American Association of Pharmaceutical Sciences.

Edelhoch,H. (1967). Spectroscopic determination of tryptophan and tyrosine in proteins. Biochemistry 6, 1948-1954.

Ernst,R.E., High,K.N., Glass,T.R., and Zhao,Q. (2009). Determination of Equilibrium Dissociation Constants, In: Therapeutic Monoclonal Antibodies - from Bench to Clinic. ed. Z.An. New Jersey: John Wiley and Sons, Inc., 505-524.

Fan,Z., Lu,Y., Wu,X., and Mendelsohn,J. (1994). Antibody-induced epidermal growth factor receptor dimerization mediates inhibition of autocrine proliferation of A431 squamous carcinoma cells. J. Biol. Chem. 269, 27595-27602.

Ferguson,K.M., Berger,M.B., Mendrola,J.M., Cho,H.S., Leahy,D.J., and Lemmon,M.A. (2003). EGF activates its receptor by removing interactions that autoinhibit ectodomain dimerization. Mol Cell 11, 507-517.

Fernandez,A., Spitzer,E., Perez,R., Boehmer,F.D., Eckert,K., Zschiesche,W., and Grosse,R. (1992). A new monoclonal antibody for detection of EGF-receptors in western blots and paraffin-embedded tissue sections. J. Cell Biochem. 49, 157-165.

Freeman,D., Sun,J., Bass,R., Jung,K., Ogbagabriel,S., Elliott,G., and Radinsky,R. Panitumumab and cetuximab epitope mapping and in vitro activity. 2008 ASCO Annual Meeting. May 20 suppl, abstr 14536. 2008. *J Clin Oncol*, *26*.

Friedman,L.M., Rinon,A., Schechter,B., Lyass,L., Lavi,S., Bacus,S.S., Sela,M., and Yarden,Y. (2005). Synergistic down-regulation of receptor tyrosine kinases by combinations of mAbs: implications for cancer immunotherapy. Proc. Natl. Acad. Sci. U. S. A 102, 1915-1920.

Garrett,T.P.J. *et al.* (2002). Crystal structure of a truncated epidermal growth factor receptor extracellular domain bound to transforming growth factor α. Cell 110, 763-773.

Gill,D.S. and Damle,N.K. (2006). Biopharmaceutical drug discovery using novel protein scaffolds. Curr. Opin. Biotechnol. 17, 653-658.

Harding,S.E. and Jumel,K. (2001). Light scattering. Curr. Protoc. Protein Sci. Chapter 7, Unit.

Harris,R.C., Chung,E., and Coffey,R.J. (2003). EGF receptor ligands. Exp Cell Res 284, 2-13.

Herbst,R.S. and Shin,D.M. (2002). Monoclonal antibodies to target epidermal growth factor receptor-positive tumors: a new paradigm for cancer therapy. Cancer 94, 1593-1611.

Holbro,T. and Hynes,N.E. (2004). ErbB receptors: directing key signaling networks throughout life. Annu. Rev. Pharmacol. Toxicol. 44, 195-217.

Holdgate,G.A. (2001). Making cool drugs hot: isothermal titration calorimetry as a tool to study binding energetics. Biotechniques 31, 164-6, 168, 170.

Holdgate,G.A. and Ward,W.H. (2005). Measurements of binding thermodynamics in drug discovery. Drug Discov. Today 10, 1543-1550.

Hubbard,S.R. and Miller,W.T. (2007). Receptor tyrosine kinases: mechanisms of activation and signaling. Curr Opin Cell Biol 19, 117-123.

Huber,W. and Mueller,F. (2006). Biomolecular interaction analysis in drug discovery using surface plasmon resonance technology. Curr. Pharm. Des 12, 3999-4021.

Jelesarov,I. and Bosshard,H.R. (1999). Isothermal titration calorimetry and differential scanning calorimetry as complementary tools to investigate the energetics of biomolecular recognition. J. Mol. Recognit. 12, 3-18.

Jelesarov,I., Leder,L., and Bosshard,H.R. (1996). Probing the energetics of antigen-antibody recognition by titration microcalorimetry. Methods 9, 533-541.

Johns,T.G. *et al.* (2004). Identification of the epitope for the epidermal growth factor receptor-specific monoclonal antibody 806 reveals that it preferentially recognizes an untethered form of the receptor. J Biol Chem 279, 30375-30384.

Johnson,I.S. (1983). Human insulin from recombinant DNA technology. Science 219, 632-637.

Jones,P.T., Dear,P.H., Foote,J., Neuberger,M.S., and Winter,G. (1986). Replacing the complementarity-determining regions in a human antibody with those from a mouse. Nature 321, 522-525.

Jonsson,U. *et al.* (1991). Real-time biospecific interaction analysis using surface plasmon resonance and a sensor chip technology. Biotechniques 11, 620-627.

Kamat,V., Donaldson,J.M., Kari,C., Quadros,M.R., Lelkes,P.I., Chaiken,I., Cocklin,S., Williams,J.C., Papazoglou,E., and Rodeck,U. (2008). Enhanced EGFR inhibition and distinct epitope recognition by EGFR antagonistic mAbs C225 and 425. Cancer Biol. Ther. 7, 726-733.

Karlsson,R. and Falt,A. (1997). Experimental design for kinetic analysis of protein-protein interactions with surface plasmon resonance biosensors. J. Immunol. Methods 200, 121-133.

Karlsson,R., Roos,H., Fägerstam,L., and Persson,B. (1994). Kinetic and concentration analysis using BIA technology. Methods 6, 99-110.

Kohler,G. and Milstein,C. (2005). Continuous cultures of fused cells secreting antibody of predefined specificity (Reprinted from Nature, vol 256, 1975). Journal of Immunology 174, 2453-2455.

Kretschmann,E. (1971). Die bestimmung optischer Konstanten von Metallen durch Anregung von Oberflächenplasmaschwingungen. Zeitschrift für Physik 241, 313-324.

Kuan,C.T., Wikstrand,C.J., and Bigner,D.D. (2001). EGF mutant receptor vIII as a molecular target in cancer therapy. Endocr. Relat Cancer 8, 83-96.

Kwong,P.D. *et al.* (2002). HIV-1 evades antibody-mediated neutralization through conformational masking of receptor-binding sites. Nature 420, 678-682.

Lammerts van Bueren,J.J., Bleeker,W.K., Brannstrom,A., von,E.A., Jansson,M., Peipp,M., Schneider-Merck,T., Valerius,T., van de Winkel,J.G., and Parren,P.W. (2008). The antibody zalutumumab inhibits epidermal growth factor receptor signaling by limiting intra- and intermolecular flexibility. Proc. Natl. Acad. Sci. U. S. A 105, 6109-6114.

Leahy,D.J. (2008). A molecular view of anti-ErbB monoclonal antibody therapy. Cancer Cell 13, 291-293.

Lemmon,M.A. (2009). Ligand-induced ErbB receptor dimerization. Exp. Cell Res. 315, 638-648.

Li,S., Schmitz,K.R., Jeffrey,P.D., Wiltzius,J.J., Kussie,P., and Ferguson,K.M. (2005). Structural basis for inhibition of the epidermal growth factor receptor by cetuximab. Cancer Cell 7, 301-311.

Li,S., Kussie,P., and Ferguson,K.M. (2008). Structural basis for EGF receptor inhibition by the therapeutic antibody IMC-11F8. Structure 16, 216-227.

Liedberg,B., Nylander,C., and Lundstrom,I. (1983). Surface plasmon resonance for gas detection and biosensing. Sensors and Actuators 4, 299-304.

Liedberg,B., Nylander,C., and Lundstrom,I. (1995). Biosensing with surface plasmon resonance - how it all started. Biosensors and Bioelectronics 10, i-ix.

Logtenberg,T. (2007). Antibody cocktails: next-generation biopharmaceuticals with improved potency. Trends Biotechnol 25, 390-394.

Lonberg,N. (2005). Human antibodies from transgenic animals. Nat. Biotechnol. 23, 1117-1125.

Lu,D. *et al.* (2004). Simultaneous blockade of both the epidermal growth factor receptor and the insulin-like growth factor receptor signaling pathways in cancer cells with a fully human recombinant bispecific antibody. J. Biol. Chem. 279, 2856-2865.

Macdonald,J.L. and Pike,L.J. (2008). Heterogeneity in EGF-binding affinities arises from negative cooperativity in an aggregating system. P Natl Acad Sci USA 105, 112-117.

Mateo,C., Moreno,E., Amour,K., Lombardero,J., Harris,W., and Perez,R. (1997). Humanization of a mouse monoclonal antibody that blocks the epidermal growth factor receptor: recovery of antagonistic activity. Immunotechnology. 3, 71-81.

Meira,D.D., Nobrega,I., de,A., V, Mororo,J.S., Cardoso,A.M., Silva,R.L., Albano,R.M., and Ferreira,C.G. (2009). Different antiproliferative effects of matuzumab and cetuximab in A431 cells are associated with persistent activity of the MAPK pathway. Eur. J. Cancer 45, 1265-1273.

Mendelsohn,J. and Baselga,J. (2006). Epidermal growth factor receptor targeting in cancer. Semin. Oncol. 33, 369-385.

Mishima,K. *et al.* (2001). Growth suppression of intracranial xenografted glioblastomas overexpressing mutant epidermal growth factor receptors by systemic administration of monoclonal antibody (mAb) 806, a novel monoclonal antibody directed to the receptor. Cancer Res. 61, 5349-5354.

Morrison,S.L., Johnson,M.J., Herzenberg,L.A., and Oi,V.T. (1984). Chimeric human antibody molecules: mouse antigen-binding domains with human constant region domains. Proc. Natl. Acad. Sci. U. S. A 81, 6851-6855.

Morton,T.A. and Myszka,D.G. (1998). Kinetic analysis of macromolecular interactions using surface plasmon resonance biosensors. Methods in Enzimology 295, 268-294.

Murthy,U., Basu,A., Rodeck,U., Herlyn,M., Ross,A.H., and Das,M. (1987). Binding of an antagonistic monoclonal antibody to an intact and fragmented EGF-receptor polypeptide. Arch Biochem Biophys 252, 549-560.

Myszka,D.G. *et al.* (2003). The ABRF-MIRG'02 study: assembly state, thermodynamic, and kinetic analysis of an enzyme/inhibitor interaction. J. Biomol. Tech. 14, 247-269.

Nieri,P., Donadio,E., Rossi,S., Adinolfi,B., and Podesta,A. (2009). Antibodies for therapeutic uses and the evolution of biotechniques. Curr. Med. Chem. 16, 753-779.

Normanno,N., De,L.A., Bianco,C., Strizzi,L., Mancino,M., Maiello,M.R., Carotenuto,A., De,F.G., Caponigro,F., and Salomon,D.S. (2006). Epidermal growth factor receptor (EGFR) signaling in cancer. Gene 366, 2-16.

Oda,K., Matsuoka,Y., Funahashi,A., and Kitano,H. (2005). A comprehensive pathway map of epidermal growth factor receptor signaling. Mol Syst Biol 1.

Ogiso,H. *et al.* (2002). Crystal structure of the complex of human epidermal growth factor and receptor extracellular domains. Cell 110, 775-787.

Papalia,G.A., Giannetti,A.M., Arora,N., and Myszka,D.G. (2008). Thermodynamic characterization of pyrazole and azaindole derivatives binding to p38 mitogen-activated protein kinase using Biacore T100 technology and van't Hoff analysis. Anal. Biochem. 383, 255-264.

Park,B.H. and Vogelstein,B. (2003). Tumor-Suppressor Genes, In: Holland-Frei Cancer Medicine 6. ed. R.E.Pollock, R.R.Weichselbaum, R.C.Bast, D.W.Kufe, and T.S.Gansler. B.C. Decker.

Patel,R. and Andrien,B.A., Jr. (2009). Kinetic analysis of a monoclonal therapeutic antibody and its single-chain homolog by surface plasmon resonance. Anal. Biochem.

Peipp,M., Dechant,M., and Valerius,T. (2008). Effector mechanisms of therapeutic antibodies against ErbB receptors. Curr. Opin. Immunol. 20, 436-443.

Perozzo,R., Folkers,G., and Scapozza,L. (2004). Thermodynamics of protein-ligand interactions: history, presence, and future aspects. J. Recept. Signal. Transduct. Res. 24, 1-52.

Pierce,M.M., Raman,C.S., and Nall,B.T. (1999). Isothermal titration calorimetry of protein-protein interactions. Methods 19, 213-221.

Pierotti,M.A., Sozzi,G., and Croce,C.M. (2003). Oncogenes, In: Holland-Frei Cancer Medicine 6. ed. R.E.Pollock, R.R.Weichselbaum, R.C.Bast, D.W.Kufe, and T.S.Gansler. B.C. Decker.

Projan,S.J., Gill,D., Lu,Z., and Herrmann,S.H. (2004). Small molecules for small minds? The case for biologic pharmaceuticals. Expert. Opin. Biol. Ther. 4, 1345-1350.

Qian,R.L., Mhatre,R., and Krull,I.S. (1997). Characterization of antigen-antibody complexes by size-exclusion chromatography coupled with low-angle light-scattering photometry and viscometry. J. Chromatogr. A 787, 101-109.

Rehder,D.S. *et al.* (2008). Isomerization of a single aspartyl residue of anti-epidermal growth factor receptor immunoglobulin gamma2 antibody highlights the role avidity plays in antibody activity. Biochemistry 47, 2518-2530.

Rich,R.L. and Myszka,D.G. (2006). Survey of the year 2005 commercial optical biosensor literature. J. Mol. Recognit. 19, 478-534.

Rich,R.L. and Myszka,D.G. (2007a). Higher-throughput, label-free, real-time molecular interaction analysis. Anal. Biochem. 361, 1-6.

Rich,R.L. and Myszka,D.G. (2007b). Survey of the year 2006 commercial optical biosensor literature. J. Mol. Recognit. 20, 300-366.

Rich,R.L. and Myszka,D.G. (2008). Survey of the year 2007 commercial optical biosensor literature. J. Mol. Recognit. 21, 355-400.

Rowinsky,E.K., Youssoufian,H., Tonra,J.R., Solomon,P., Burtrum,D., and Ludwig,D.L. (2007). IMC-A12, a human IgG1 monoclonal antibody to the insulin-like growth factor I receptor. Clin Cancer Res 13, 5549s-55555.

Rudnick,S.I. and Adams,G.P. (2009). Affinity and avidity in antibody-based tumor targeting. Cancer Biother. Radiopharm. 24, 155-161.

Sato,J.D., Kawamoto,T., Le,A.D., Mendelsohn,J., Polikoff,J., and Sato,G.H. (1983). Biological effects in vitro of monoclonal antibodies to human epidermal growth factor receptors. Mol. Biol. Med. 1, 511-529.

Schlessinger,J. (2000). Cell signaling by receptor tyrosine kinases. Cell 103, 211-225.

Schmiedel,J. Struktur und molekulare Interaktionsanalyse von monoklonalen Antikörpern in Komplex mit Rezeptor-Tyrosinkinasen. 2009. Frankfurt-am-Main, Johann Wolfgang Goethe-Universität.

Schmiedel,J., Blaukat,A., Li,S., Knochel,T., and Ferguson,K.M. (2008). Matuzumab binding to EGFR prevents the conformational rearrangement required for dimerization. Cancer Cell 13, 365-373.

Schmitz,K.R. and Ferguson,K.M. (2009). Interaction of antibodies with ErbB receptor extracellular regions. Exp. Cell Res. 315, 659-670.

Schuck,P., Boyd,L.F., and Andersen,P.S. (2004). Measuring protein interactions by optical biosensors. Curr. Protoc. Cell Biol. Chapter 17, Unit 17.6.

Sivasubramanian,A., Chao,G., Pressler,H.M., Wittrup,K.D., and Gray,J.J. (2006). Structural model of the mAb 806-EGFR complex using computational docking followed by computational and experimental mutagenesis. Structure. 14, 401-414.

Sjolander,S. and Urbaniczky,C. (1991). Integrated fluid handling system for biomolecular interaction analysis. Anal. Chem. 63, 2338-2345.

Sporn,M.B. and Roberts,A.B. (1985). Autocrine growth factors and cancer. Nature 313, 745-747.

Stanfield,R.L. and Wilson,I.A. (2009). Antibody Molecular Structure, In: Therapeutic Monoclonal Antibodies - from Bench to Clinic. ed. Z.An. New Jersey: John Wiley and Sons, Inc., 51-66.

Stenberg,E., Persson,B., Roos,H., and Urbaniczky,C. (1991). Quantitative determination of surface concentration of protein with surface plasmon resonance using radiolabeled proteins. Journal of Colloid and Interface Science 143, 513-526.

Stroop,C.J., Weber,W., Gerwig,G.J., Nimtz,M., Kamerling,J.P., and Vliegenthart,J.F. (2000). Characterization of the carbohydrate chains of the secreted form of the human epidermal growth factor receptor. Glycobiology 10, 901-917.

Sun,M. (1980). Insulin wars: new advances may throw market into turbulence. Science 210, 1225-1228.

Sundberg,E.J. and Mariuzza,R.A. (2002). Molecular recognition in antibody-antigen complexes. Adv Protein Chem 61, 119-160.

Talavera,A. *et al.* (2009). Nimotuzumab, an antitumor antibody that targets the epidermal growth factor receptor, blocks ligand binding while permitting the active receptor conformation. Cancer Res. 69, 5851-5859.

Tikhomirov,I.A., Garrido,G., Yang,E., Sherman,I., and Pérez,R. (2008). Bivalent binding properties of epidermal growth factor receptor (EGFR) targeted monoclonal antibodies: factors contributing to differences in observed clinical profiles. AACR Cancer Clinical Trials and Personalized Medicine 2008 Abstract A36.

Ullrich,A. *et al.* (1984). Human epidermal growth factor receptor cDNA sequence and aberrant expression of the amplified gene in A431 epidermoid carcinoma cells. Nature 309, 418-425.

Velazquez-Campoy,A., Kiso,Y., and Freire,E. (2001). The binding energetics of first- and second-generation HIV-1 protease inhibitors: implications for drug design. Arch. Biochem. Biophys. 390, 169-175.

Waldmann,T.A. (2003). Immunotherapy: past, present and future. Nat. Med. 9, 269-277.

Ward,W.H. and Holdgate,G.A. (2001). Isothermal titration calorimetry in drug discovery. Prog. Med. Chem. 38, 309-376.

Weber,W., Gill,G.N., and Spiess,J. (1984). Production of an epidermal growth factor receptor-related protein. Science 224, 294-297.

West,C.M., Joseph,L., and Bhana,S. (2008). Epidermal growth factor receptor-targeted therapy. Br. J. Radiol. 81 Spec No 1, S36-S44.

Williams,D.H., Stephens,E., O'Brien,D.P., and Zhou,M. (2004). Understanding noncovalent interactions: ligand binding energy and catalytic efficiency from ligand-induced reductions in motion within receptors and enzymes. Angew. Chem. Int. Ed Engl. 43, 6596-6616.

Wofsy,C., Goldstein,B., Lund,K., and Wiley,H.S. (1992). Implications of epidermal growth factor (EGF) induced EGF receptor aggregation. Biophys J 63, 98-110.

Wu-Pong,S. and Rojanasakul,Y. (2008). Biopharmaceutical Drug Design and Development, Humana Press

Wyatt,P. (1993). Light scattering and the absolute characterization of macromolecules. Analytica Chimica Acta 272, 1-40.

Yang,X.D., Jia,X.C., Corvalan,J.R., Wang,P., and Davis,C.G. (2001). Development of ABX-EGF, a fully human anti-EGF receptor monoclonal antibody, for cancer therapy. Crit Rev. Oncol. Hematol. 38, 17-23.

Yarden,Y. and Sliwkowski,M.X. (2001). Untangling the ErbB signalling network. Nat Rev Mol Cell Biol 2, 127-137.

Yoshida,T., Okamoto,I., Okabe,T., Iwasa,T., Satoh,T., Nishio,K., Fukuoka,M., and Nakagawa,K. (2008). Matuzumab and cetuximab activate the epidermal growth factor receptor but fail to trigger downstream signaling by Akt or Erk. Int. J. Cancer 122, 1530-1538.

Zhang,H., Berezov,A., Wang,Q., Zhang,G., Drebin,J.A., Murali,R., and Greene,M.I. (2007a). ErbB receptors: from oncogenes to targeted cancer therapies. J Clin Invest 117, 2051-2058.

Zhang,Q., Chen,G., Liu,X., and Qian,Q. (2007b). Monoclonal antibodies as therapeutic agents in oncology and antibody gene therapy. Cell Res. 17, 89-99.

Zhang,X., Gureasko,J., Shen,K., Cole,P.A., and Kuriyan,J. (2006). An allosteric mechanism for activation of the kinase domain of epidermal growth factor receptor. Cell 125, 1137-1149.